



The Effect of Nitrate and Nitrite Supplementation on the Biocorrosion of Mild Steel Coupons in a Loam Soil System

By

Rishaad Ballim

Submitted in fulfilment of the academic requirements for the degree of Masters in Microbiology in the College of Agriculture, Science and Engineering, University of KwaZulu-Natal, Durban

Supervisor: Prof J Lin

May 2015

Preface

The experimental work described in this dissertation was carried out in the Discipline of Microbiology of the School of Life Sciences, College of Agriculture, Engineering and Science, University of KwaZulu-Natal (Westville campus), from March 2013 to May 2015 under the supervision of Professor Johnson Lin.

The experimental findings represent original work by the author and have not otherwise been submitted in any form for any degree or diploma to any University. Where use has been made of the work of others, it is duly acknowledged in the text.

Signed

Date

.....
Rishaad Ballim (209502981)

.....

Signed

Date

.....
Prof Johnson Lin (Supervisor)

.....

Declaration – Plagiarism

I, **Mr Rishaad Ballim**, declare that:

1. The research reported in this dissertation, except where otherwise indicated, is my original research.
2. This dissertation has not been submitted for any degree or examination at any other university.
3. This dissertation does not contain other scientists' data, pictures, graphs or other information, unless specifically acknowledged as being sourced from other scientists.
4. This dissertation does not contain other scientists' writing, unless specifically acknowledged as being sourced from other scientists. Where other written sources have been quoted, then their words have been re-written but the general information attributed to them has been referenced.
5. This dissertation does not contain text, graphics or tables taken from the internet, unless specifically acknowledged, and the source being detailed in the dissertation and in the reference section.

Signed

.....
Rishaad Ballim (209502981)

Declaration Plagiarism 22/05/08 FHDR Approved

Acknowledgements

The author gratefully acknowledges the following, without which the completion of this project would not have been possible:

Prof. Johnson Lin, for his guidance, extreme patience and support during the course of this work,

The National Research Foundation of South Africa for financial support,

The Staff and students in the Discipline of Microbiology,

Ashmita Arjoon, for your invaluable assistance during DGGE analysis

My family (Feroza, Tony, Nadia and Denise) for their encouragement, patience, love and support, and friends (Tom, Veronna, Ridwaan and Zohra) for making this a truly memorable experience,

And Lishavia, I thank you for your endless love, support, patience and motivation, you make everything possible.

Abstract

Microbially influenced corrosion is the participation of microorganisms in the corrosion process. This study determined the effect of nutrients, viz., nitrate and nitrite supplementation on the microbial corrosion of mild steel in loam soil. The optimal concentration of nitrate and nitrite needed to sufficiently inhibit biocorrosion was determined by incubating mild steel coupons in loam soil supplemented with increasing concentrations of nitrate and nitrite (5, 10, 20 and 40 mM respectively). Coupons were removed every 4 weeks and used to determine the extent of corrosion based on the weight loss method. The surface of the coupon was analysed using Scanning Electron Microscopy (SEM) and Electron Dispersive X-ray (EDX) analysis. The biofilm formed on the coupon surface was studied by determining the protein and carbohydrate content as well as the species diversity within the biofilm using Denaturing Gradient Gel Electrophoresis (DGGE). Optimal nitrate and nitrite concentration were used in an *in situ* study to determine the efficacy in the external environment. Individual aerobic species were isolated from the coupons supplemented with nitrite and used to determine their potential to inhibit corrosion in a corrosive saltwater environment.

Nitrate supplementation was found to increase the extent of corrosion and biofilm formation significantly, with greater concentrations leading to higher corrosion rates, when compared to the non-supplemented coupons. SEM observations confirmed the presence of extensive corrosion product and biofilm formation. EDX analysis determined the main components of the corrosion products to be iron and oxygen. Maximum corrosion rate was determined at 40 mM at week 20 (123.85 mg/cm²). The *in situ* study revealed similar results in which 20 mM nitrate supplementation increased corrosion rate significantly.

Nitrite supplementation led to a decrease in corrosion rates as well as biofilm formation, with no corrosion or biofilm formation detected at 20 mM nitrite supplementation. SEM observations determined no corrosion or biofilm formation at 20 mM. The *in situ* results using 20 mM nitrite showed a decrease in corrosion rate. However this was not significant when compared to the unsupplemented controls.

Sequence data in the laboratory experiments revealed phylotypes belonging to 2 major distinct phylogenetic groups, the Firmicutes and α -Proteobacteria. *In situ* experiments showed bacterial diversity exhibited phylotypes belonging to the Firmicutes, α -Proteobacteria, and γ -Proteobacteria. The community was found to differ between the non-autoclaved and nitrate-

treated systems, with a higher bacterial diversity observed in the nitrate treated systems, however, the dominant microorganisms were found to be *Bacillus* species. This group of microorganisms are iron-oxidizing bacteria that could also promote the corrosion process.

Nitrate addition, in this study, was found to increase corrosion rate of mild steel in loam soil, however, nitrite addition was found to significantly reduce corrosion rates as well as decrease biofilm formation. Furthermore, aerobic microorganisms were observed to play a role in the corrosion process in mild steel. Further studies would require a multidiscipline approach into the various soil factors involved and their interplay in the corrosion reaction to determine the viability of nitrite in the long term control of mild steel corrosion in loam soil.

Contents

Acknowledgements.....	iii
Abstract.....	iv
List of Tables	ix
List of Figures	x
Chapter 1: Introduction and Literature Review	1
1.1 Introduction	1
1.2 Literature Review	3
1.2.1 Metal Corrosion	3
1.2.2 Biocorrosion	5
1.2.3 Microorganisms in Biocorrosion	9
1.2.4 EPS and Biocorrosion	16
1.2.5 Methods Used to Study Biocorrosion	18
1.2.6 Metal Corrosion in Soil.....	20
1.2.7 Prevention of corrosion	22
1.4 Aims:	27
1.4.1 Objectives:	27
Chapter 2: The Effect of Nitrite and Nitrate Supplementation on the Biocorrosion of Mild Steel Coupons in a Loam Soil System	28
2.1 Introduction	28
2.2 Materials and Methods.....	29
2.2.1 Soil Sample Collection and Preparation.....	29
2.2.2 Mild Steel Coupon Preparation.....	29
2.2.3 Laboratory Experiment: Construction of loam soil system supplemented with nitrate and nitrite.....	30
2.2.4 Carbohydrate and protein content of biofilm from coupon surface.....	31
2.2.5 Scanning electron microscopy (SEM) and electron dispersive X-ray (EDX) analyses of the coupons.....	31
2.2.6 Microbial Population analysis of biofilm on corroded mild steel coupons using Denaturing Gradient Gel Electrophoresis (DGGE)	31
2.2.7 Statistical Analysis.....	33
2.3 Results.....	34
2.3.1 Physical characterisation of loam soil.....	34
2.3.2 Weight loss measurements of mild steel coupons in a stimulated loam soil system	34

2.3.3: Protein and carbohydrate content of the biofilm on the surface of the mild steel coupon	36
2.3.4 Scanning electron microscopy and electron dispersive x-ray analyses of corroded mild steel coupons in a loam soil system.....	38
2.3.5 DGGE analysis of biofilm communities on corroded mild steel coupons and phylogenetic affiliation of dominant bacteria	44
2.4 Discussion.....	53
Chapter 3: The Effect of Nitrite and Nitrate Supplementation on the Corrosion of Mild Steel Coupons in a Loam Soil System: An <i>in situ</i> Study.....	59
3.1 Introduction	59
3.2 Materials and Methods.....	60
3.2.1 Soil Sample Collection and Preparation of Mild Steel Coupons	60
3.2.2 <i>In situ</i> Experiment: Construction of Loam Soil System Supplemented with Nitrate and Nitrite	61
3.2.3 Carbohydrate and Protein Analysis from Biofilms of Coupon Surface	61
3.2.4 Scanning Electron Microscopy (SEM) and Electron Dispersive X-Ray (EDX) Analysis of the Coupon Surface	61
3.2.5 Microbial Population Analysis of Biofilm on Corroded Mild Steel Coupons Using Denaturing Gradient Gel Electrophoresis (DGGE)	62
3.3 Results	62
3.3.1 Physical characterisation of loam soil.....	62
3.3.2 Weight loss measurements of mild steel coupons in a loam soil system.....	63
3.3.3: Protein and carbohydrate content of the biofilm on the surface of the mild steel coupon	66
3.3.4 Scanning Electron Microscopy and Electron Dispersive X-ray analysis of Corroded mild steel coupons in an <i>in situ</i> loam soil system	68
3.3.5 DGGE analysis of biofilm communities on corroded mild steel coupons and phylogenetic affiliation of dominant bacteria	74
3.4 Discussion.....	82
Chapter 4: Biocorrosion by bacterial species isolated from corroded mild steel coupons: The effect of nitrite supplementation.....	88
4.1 Introduction	88
4.2 Materials and Methods.....	89
4.2.1 Experimental Set-Up	89
4.2.2 The isolation of the cultivatable fraction of bacterial isolates within the biofilm formed on the surface of the mild steel coupons	90
4.2.3 Preparation of the inoculum and mild steel coupons	90

4.2.4 Determination of the corrosion activities of the bacterial isolates isolated from bacterial biofilms formed on corroding mild steel surfaces	90
4.2.5 DNA Extraction	90
4.2.6 Amplification of 16 S rDNA and Sequencing	91
4.2.7 Database Searches and Phylogenetic Analysis	91
4.2.8 Statistical Analysis	91
4.3 Results	92
4.3.1 Identification of bacterial isolates	92
4.3.2 Weight loss measurements of mild steel coupons in the presence of bacterial isolates supplemented with nitrite	92
4.3.3 pH changes over the incubation period	95
4.4 Discussion	95
Chapter 5: Concluding Remarks	99
Appendix I: Raw weight loss data and corrosion rate calculations	114
Appendix II: EDX Spectra	124
Appendix III: Bacterial population analysis: PCR Gels	126
Appendix IV: pH measurements	130

List of Tables

Table 2.1: Physical characteristics of soil used in study.....	34
Table 2.2: Total protein concentration (mg/ml) in biofilm samples extracted from mild steel coupons in loam soil over a period of 24 weeks.....	37
Table 2.3: Total carbohydrate concentration (mg/ml) of biofilm samples extracted from mild steel coupons in loam soil over a period of 24 weeks.....	38
Table 2.4: Elemental composition of different corrosion products formed on the surface of the treated and untreated mild steel coupons analysed by EDX analysis.....	43
Table 2.5: Partial 16S rDNA sequence similarity of the excised bands on DGGE profiles over the 24 week period.....	50
Table 3.1: Physical characteristics of soil used in <i>in situ</i> study.....	63
Table 3.2: Total protein concentration (mg/ml) in biofilm samples extracted from mild steel coupons in loam soil over a period of 24 weeks.....	66
Table 3.3: Total carbohydrate concentration (mg/ml) in biofilm samples extracted from mild steel coupons in loam soil over a period of 24 weeks.....	67
Table 3.4: Elemental composition of different corrosion products formed on the surface of the treated and untreated mild steel coupons analysed by EDX analysis.....	73
Table 3.5: Partial 16S rDNA sequence similarity of the excised bands on DGGE profiles over the 24 week period.....	76
Table 4.1: Putative identities of bacteria isolated from the surface of nitrite treated mild steel coupons.....	92

List of Figures

Figure 1.1: Differential aeration cell created by tubercle formation (Coetser and Cloete, 2005).....	8
Figure 1.2: The function of hydrogenase enzymes in anaerobic biocorrosion (Bryant and Laishley; 1989).....	10
Figure 1.3: Hypothetical mechanisms by which metal oxidising bacteria participate in biocorrosion (Olesen <i>et al.</i> , 2000).....	14
Figure 1.4: Corrosion of a ferrous metal facilitated by metal binding by microbial EPS (Beech and Sunner, 2004).....	17
Figure 2.1: Figure 2.1: Weight loss of mild steel coupons conditions over a period of 24 weeks. Coupons were incubated at 25°C in a 3-L catering jar containing loam soil, and increasing concentrations of nitrate and nitrite.....	35
Figure 2.2: Some typical examples of SEM images of the surface of mild steel coupons in a stimulated loam soil system after 4 weeks of incubation. (A1, A2, A3) – Autoclaved system after 4, 8 and 20 weeks respectively; (NA1, NA2, NA3) – Non-autoclaved system after 4, 8 and 20 weeks respectively; (SN1, SN2, SN3) – 20 mM nitrite supplemented systems after 4, 8 and 20 weeks respectively; (AN1, AN2, AN3) – 10 mM nitrate supplemented system after 4, 8 and 20 weeks respectively.....	40
Figure 2.3: Corrosion products investigated using EDX analysis. CP1- Corrosion product 1 (5 mM nitrate supplemented system- week 8), CP2- Corrosion product 2 (Non-autoclaved system- week 12), CP3- Corrosion product 3 (Non-autoclaved system- week 4), CP4- Corrosion product 4 (5 mM nitrite supplemented system- week 12).....	42
Figure 2.4: PCR amplification of the 16S rDNA of biofilm samples after 16 weeks incubation in loam soil. Lane 1: GeneRuler DNA Ladder Mix (ThermoScientific); 2: positive control (<i>Bacillus subtilis</i>); 3: autoclaved control; 4: non-autoclaved control; 5: 5 mM nitrate; 6: 10 mM nitrate; 7: 20 mM nitrate; 8: 40 mM nitrate;.....	44
Figure 2.5: PCR amplification with DGGE primers after 16 weeks incubation in loam soil. Lane 1: GeneRuler DNA Ladder Mix (ThermoScientific); 2: positive control (<i>Bacillus subtilis</i>); 3:	

autoclaved control; 4: non-autoclaved control; 5: 5 mM nitrate; 6: 10 mM nitrate; 7: 20 mM nitrate; 8: 40 mM nitrate.....45

Figure 2.6: PCR amplification of DGGE bands after DGGE analysis at 16 weeks incubation in loam soil. Lane 1: GeneRuler DNA Ladder Mix (ThermoScientific); 2: positive control (*Bacillus subtilis*); 3: autoclaved control; 4: non-autoclaved control; 5: 5 mM nitrate; 6: 10 mM nitrate; 7: 20 mM nitrate; 8: 40 mM nitrate.....46

Figure 2.7: DGGE profile of biofilm samples after 4, 8, 12, 16, 20 and 24 weeks incubation in loam soil (Lanes - M: DGGE markers; A: autoclaved control; NA: non-autoclaved control; A5: 5 mM nitrate; A10: 10 mM nitrate; A20: 20 mM nitrate; A40: 40 mM nitrate. The labelled bands indicate gel portions that were sequenced, and identified.....48-49

Figure 2.8: The phylogenetic tree inferred using the Neighbour-Joining method for the non-autoclaved sample. The bootstrap consensus tree inferred from 500 replicates is taken to represent the evolutionary history of the taxa analysed. The tree is drawn to scale, with branch lengths in the same units as those of the evolutionary distances used to infer the phylogenetic tree. The evolutionary distances were computed using the Maximum Composite Likelihood method and are in the units of the number of base substitutions per site. Codon positions included were 1st+2nd+3rd+Noncoding. Phylogenetic analyses were conducted in MEGA 6.....51

Figure 2.9: The phylogenetic tree inferred using the Neighbour-Joining method for the nitrate samples. The bootstrap consensus tree inferred from 500 replicates is taken to represent the evolutionary history of the taxa analysed. The tree is drawn to scale, with branch lengths in the same units as those of the evolutionary distances used to infer the phylogenetic tree. The evolutionary distances were computed using the Maximum Composite Likelihood method and are in the units of the number of base substitutions per site. Codon positions included were 1st+2nd+3rd+Noncoding. Phylogenetic analyses were conducted in MEGA 6.....52

Figure 3.1: Weight loss of mild steel coupons conditions over a period of 24 weeks. Coupons were incubated *in situ* in loam soil containing 20 mM of nitrate and nitrite.....65

Figure 3.2: Some typical examples of SEM images of the surface of mild steel coupons in a stimulated loam soil system after various weeks of incubation. (A1, A2, A3) – Autoclaved

system after 4, 8 and 20 weeks respectively; (NA1, NA2, NA3) – Non-autoclaved system after 4, 8 and 20 weeks respectively.....69

Figure 3.3: Some typical examples of SEM images of the surface of mild steel coupons in a stimulated loam soil system after various weeks of incubation. (ASN1, ASN2, ASN3) – Autoclaved system supplemented with 20 mM nitrite after 4, 8 and 20 weeks respectively; (NSN1, NSN2, NSN3) – Non-autoclaved system supplemented with nitrite after 4, 8 and 20 weeks respectively.....70

Figure 3.4: Some typical examples of SEM images of the surface of mild steel coupons in a stimulated loam soil system after various weeks of incubation. (AN1, AN2, AN3) – Autoclaved system supplemented with 20 mM nitrate after 4, 8 and 20 weeks, respectively; (NN1, NN2, NN3) – Non-autoclaved system supplemented with 20 mM nitrate after 4, 8 and 20 weeks, respectively70

Figure 3.5: Corrosion products investigated using EDX analysis. IC1) Corrosion product 1 (Autoclaved nitrate supplemented system), IC2) corrosion product 2 (Non-autoclaved system), IC3) corrosion product 3 (Non-autoclaved system), IC4) corrosion product 4 (Autoclaved system).....72

Figure 3.6: DGGE profile of biofilm samples after 4, 8 and 12 weeks incubation in loam soil (Lanes 1, 14: DGGE markers; 2: non-autoclaved (week 4); 3: autoclaved control (week 4); 4: non-autoclaved supplemented with nitrate (week 4); 5: autoclaved supplemented with nitrate (week 4); 6: non-autoclaved (week 8); 7: autoclaved control (week 8); 8: non-autoclaved supplemented with nitrate (week 8); 9: autoclaved supplemented with nitrate (week 8); 10: non-autoclaved (week 12); 11: autoclaved control (week 12); 12: non-autoclaved supplemented with nitrate (week 12); 13: autoclaved supplemented with nitrate (week 12); The numbers indicate gel portions that were sequenced and identified.....77

Figure 3.7: DGGE profile of biofilm samples after 16, 20 and 24 weeks incubation in loam soil (Lanes 1: DGGE markers; 2: non-autoclaved (week 16); 3: autoclaved control (week 16); 4: non-autoclaved supplemented with nitrate (week 16); 5: autoclaved supplemented with nitrate (week 16); 6: non-autoclaved (week 20); 7: autoclaved control (week 20); 8: non-autoclaved supplemented with nitrate (week 20); 9: autoclaved supplemented with nitrate (week 20); 10: non-autoclaved (week 24); 11: autoclaved control (week 24); 12: non-autoclaved supplemented

with nitrate (week 24); 13: autoclaved supplemented with nitrate (week 24); The numbers indicate gel portions that were sequenced and identified.....78

Figure 3.8: The phylogenetic tree inferred using the Neighbour-Joining method for the autoclaved samples. The bootstrap consensus tree inferred from 500 replicates is taken to represent the evolutionary history of the taxa analysed. The tree is drawn to scale, with branch lengths in the same units as those of the evolutionary distances used to infer the phylogenetic tree. The evolutionary distances were computed using the Maximum Composite Likelihood method, and are in the units of the number of base substitutions per site. Codon positions included were 1st+2nd+3rd+Noncoding. Phylogenetic analyses were conducted in MEGA6.....79

Figure 3.9: The phylogenetic tree inferred using the Neighbour-Joining method for the non-autoclaved samples. The bootstrap consensus tree inferred from 500 replicates is taken to represent the evolutionary history of the taxa analysed. The tree is drawn to scale, with branch lengths in the same units as those of the evolutionary distances used to infer the phylogenetic tree. The evolutionary distances were computed using the Maximum Composite Likelihood method, and are in the units of the number of base substitutions per site. Codon positions included were 1st+2nd+3rd+Noncoding. Phylogenetic analyses was conducted in MEGA6.....80

Figure 3.10: The phylogenetic tree inferred using the Neighbour-Joining method for the autoclaved sample supplemented with nitrate. The bootstrap consensus tree inferred from 500 replicates is taken to represent the evolutionary history of the taxa analysed. The tree is drawn to scale, with branch lengths in the same units as those of the evolutionary distances used to infer the phylogenetic tree. The evolutionary distances were computed using the Maximum Composite Likelihood, method and are in the units of the number of base substitutions per site. Codon positions included were 1st+2nd+3rd+Noncoding. Phylogenetic analyses was conducted in MEGA6.....81

Figure 3.11: The phylogenetic tree inferred using the Neighbour-Joining method for the non-autoclaved sample supplemented with nitrate. The bootstrap consensus tree inferred from 500 replicates is taken to represent the evolutionary history of the taxa analysed.. The tree is drawn to scale, with branch lengths in the same units as those of the evolutionary distances used to infer the phylogenetic tree. The evolutionary distances were computed using the Maximum Composite Likelihood method and are in the units of the number of base substitutions per site. Codon

positions included were 1st+2nd+3rd+Noncoding. Phylogenetic analyses was conducted in MEGA6..... **82**

Figure 4.1: Weight loss of mild steel coupons by various isolates under different concentrations of nitrite..... **94**

Figure 4.2: pH changes of isolate 2 under various nitrite concentrations..... **95**

Chapter 1: Introduction and Literature Review

1.1 Introduction

Corrosion is a spontaneous electrochemical reaction between a metal and its environment that involves the transfer of electrons from the metal to an external electron acceptor, resulting in the release of metal ions and the deterioration of the metal (Beech and Sunner, 2004). It occurs on most metals and results in a significant impairment in the function of the metal (Garcia *et al.*, 2012). Corrosion occurs in almost all industries and constitutes an ancient and fundamental industrial problem which results in substantial repair and prevention costs.

Microbially influenced corrosion (MIC), alternatively known as biocorrosion, is the initiation, facilitation or acceleration of the corrosion reaction due to the activities of microorganisms without a change in its electrochemical nature (Beech and Sunner, 2004). It results due to coupled biotic and abiotic redox reactions. Microorganisms are ubiquitous in nature and can affect the corrosion of all known types of metal corrosion (Shi *et al.*, 2011). MIC is, therefore, a serious problem to all types of common engineering materials and structures and accounts for approximately 20 percent of the total cost of all corrosion damage (Shi *et al.*, 2011).

The main types of microorganisms implicated in the deterioration of metals in both aquatic and terrestrial environments are the sulphate reducing/oxidising bacteria, metal reducing/oxidising bacteria, extracellular polymeric substance (EPS) producers and acid producers (Bachmann and Edyvean, 2006). Due to its considerable economic and environmental impact, numerous studies into MIC have been performed over the last few decades and several mechanisms have been proposed (Beech and Sunner, 2004).

The first stage in the biocorrosion process is the formation of a biofilm on the metal surface. Many different microorganisms with varying physiological abilities typically coexist within mature biofilms and form complex consortia, using a wide range of energy sources for their growth (Beech and Sunner, 2004). It is these physiological abilities that result in a marked change in the environmental conditions at the interface between the biofilm and the metal surface, resulting in MIC. Due to their relatively minute size, microorganisms are able to attach and colonise relatively inaccessible areas in a system, resulting in localised corrosion

(Shi *et al.*, 2011). Due to the immense diversity and physiological capabilities of microbes, the mechanisms governing MIC are not well understood. A variety of factors govern microbial involvement in metal corrosion, such as species, type of metal, surface characteristics and environmental conditions (Shi *et al.*, 2011). Furthermore, MIC in nature is rarely ever attributed to a single species or mechanism.

Traditional measures for MIC prevention involve proper selection of materials, protective coatings, cathodic protection and biocides (Lin and Ballim, 2012). Biocides used for biocorrosion control include oxidising agents such as chlorine, ozone and chloramines, enzyme poisons, protein denaturants such as heavy metal salts and aldehydes, and surface active agents such as quaternary ammonium compounds (Shi *et al.*, 2011). However, most biocidal agents are not environmentally friendly and there are health concerns over their use. Furthermore, the presence of spores or biofilm forming bacteria, as well as the development of resistance limits the effectiveness of these chemicals, necessitating the use of higher concentrations of biocides.

Some studies have observed the protective abilities on metal surfaces of microbial biofilms (Bano and Qazi, 2011; Chongdar *et al.*, 2005; Garcia, *et al.*, 2012; Jayaraman *et al.*, 1997). Mechanisms by which biofilms may protect metals from corrosion include neutralising corrosive substances, forming a protective barrier or stabilising an already present barrier on metal surface, inducing a decrease in solution corrosivity, or producing antibiotics that prevent the growth of corrosive bacteria (Juzeliunas *et al.*, 2006).

Biocompetitive exclusion (BE) strategies are becoming increasingly popular in the control of biocorrosion by sulphate reducing bacteria (SRB) (Tabari *et al.*, 2011). This strategy has been shown to be successful at the laboratory and field scale and has been used in the oil industry (Videla and Herrera, 2005). BE involves the use of nutrients that stimulate the growth of competitive bacteria such as nitrate reducing bacteria (NRB) and nitrite reducing bacteria that are able to displace the (SRB) from the community. The addition of nitrate and nitrite has been promising and has been shown to shift the dominant bacterial populations from the sulphate reducing bacteria to nitrate reducing bacteria, which therefore prevents the production of hydrogen sulphide and SRB growth (Tabari *et al.*, 2011). In most cases, the inoculation of NRB into the site is not necessary as the addition of nitrate stimulates the growth of indigenous NRB (Videla and Herrera, 2005). In some cases the addition of nitrate was even shown to encourage the SRB to shift from sulphate metabolism to the nitrate reduction pathway (Beech and Sunner,

2004). Biocompetitive exclusion strategies offer many advantages over traditional methods. These include: simplicity and sustainable results, reduction and removal of hydrogen sulphide and iron sulphide deposits that can lead to significant corrosion and health concerns, reduced cost compared to corrosion inhibitors and biocide use, reduced corrosion and increased life of production equipment (Gevertz *et al.*, 2000).

Metal corrosion is a significant problem to many industries worldwide. The metabolic activities of microorganisms in particular have been shown to have a great impact on the corrosion of metals. Despite the large amount of research into MIC, this phenomenon is still not very well understood and there are many issues that still need to be addressed. This study focusses on the effect of nitrate and nitrite supplementation on the biocorrosion of mild steel in a loam soil system.

1.2 Literature Review

1.2.1 Metal Corrosion

Corrosion is the disintegration of any substance due to a chemical reaction with its environment (Herbert *et al.*, 2002). With the exception of certain noble metals, metals in nature are generally found in their oxidized state. However, metals used in most man-made structures of today are found in their high energy, elemental state, and easily become oxidized in the presence of a suitable electron acceptor (Coetser and Cloete, 2005). Corrosion of metals is electrochemical in nature. This phenomenon occurs when an electrical potential difference of two adjacent areas on a metal surface occurs within a conductive medium, so that one becomes anodic and the other cathodic (Enning *et al.*, 2012). Due to the ability of metals to allow the free flow of electrons throughout the metallic matrix, it is not necessary for anodic and cathodic areas to occur at the same locality (Enning *et al.*, 2012). Corrosion is not unique to iron but can occur in all base metals when exposed to an aqueous environment (De Bruyn, 1992).

Metals susceptible to corrosion can be placed into two groups: the active metals including iron, and the passive metals such as stainless steel (Lewandowski and Beyenal, 2008). The rates at which various types of metals corrode are dependent upon the environment, such as oxygen availability as well as the biotic and abiotic factors (Herbert *et al.*, 2002). Abiotic corrosion is thermodynamically favoured, but is often a relatively slow process.

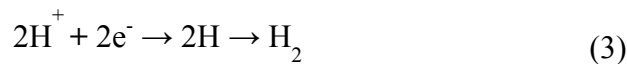
Corrosion of metals occurs immediately upon dispersion of the metal into a hostile aqueous medium, and involves two reactions, an anodic and a cathodic reaction. The anodic reaction would involve the release of electrons which are transferred to the electron acceptor in the cathodic reaction (Juzeliunas *et al.*, 2006). Metal dissolution occurs at the anode, shown as follows (Hamilton 1985; Barton 1997):



Electrons are transferred to and accepted at cathodic sites. The most common electron acceptor is oxygen. The cathodic reduction of oxygen occurs in neutral and alkaline pH values, according to the following reaction:



Under acidic conditions though, protons act as the cathodic reactant (Coetser and Cloete, 2005):



this forms first atomic, then molecular hydrogen (Hamilton 1985)

Mild steel is the most commonly used engineering material and is used in various industries such as nuclear and fossil fuel power plants, transportation, chemical processing, petroleum production and refining, pipelines, mining, construction as well as metal processing equipment (Nik *et al.*, 2011). It is cheap, malleable and versatile. However, it has a relatively low tensile strength. Mild steel requires approximately 0.05-0.15% carbon (Adeosun and Sanni, 2013). Mild steel though, has a low corrosion resistance.

The following reactions may describe the corrosion of mild steel or iron (Morcillo *et al.*, 2014):

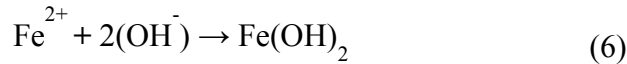
Anode:



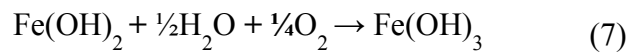
At the cathode in the presence of oxygen:



The products of the anodic and cathodic reactions then react leading to corrosion products (Coetser and Cloete, 2005):

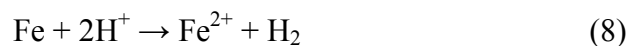


This ferrous hydroxide then reacts with additional oxygen to yield hydrous ferric oxide (Coetser and Cloete, 2005):



Eventually the rust deposited on the steel surface is composed of three layers of iron oxides at the different stages of oxidation (Lee *et al.*, 1995). The innermost layer is composed of the greenish ferrous hydroxide $\text{Fe}(\text{OH})_2$, the intermediate layer of black magnetite Fe_3O_4 , and the outermost layer of orange ferric hydroxide $\text{Fe}(\text{OH})_3$.

In the absence of oxygen, however, the most common electron acceptor are protons formed by dissociated water molecules, as shown in the previous reaction. Here the overall reaction for the corrosion of iron is as formula 8 (Enning *et al.*, 2012):



The corrosion products form a slightly adhesive, thin protective film over the surface of the steel which decreases the rate of corrosion (De Bruyn, 1992). Anodic and cathodic reactions must remain in equilibrium and remain functional over long periods of time for corrosion to proceed to any significant degree (Morcillo *et al.*, 2014).

1.2.2 Biocorrosion

The overall chemical corrosion reaction is energetically favoured, therefore bacterial interaction is not needed. However, due to the opportunistic nature of microorganisms, the corrosion reaction represents a perfect site to harvest the energy available (Kan *et al.*, 2011). Microbially

Influenced Corrosion (MIC), or biocorrosion, is the result of the interactions that occur between the metal surface, abiotic corrosion products, the microbial cells as well as metabolic products (Beech and Sunner, 2004).

Microbially Influenced Corrosion affects a wide range of industries, especially the oil and gas industries, and causes significant economic losses (Brenda and Lee, 2009). Studies in the United Kingdom, Japan, Australia, and Germany estimate the total cost of corrosion to be 1-5% of gross national product, with biocorrosion accounting for approximately 20% of this total (Little and Lee, 2007). Due to its considerable economic importance, MIC has been the subject of widespread studies over the last few decades, with many different mechanisms of biocorrosion being proposed. Biocorrosion can occur in terrestrial as well as aquatic habitats that differ in temperature, nutrient content, pH as well as pressure (Beech and Sunner, 2004).

The first stage in MIC is the formation of a biofilm on the metallic surface. Within minutes of exposure of the metal surface to the environment, the adsorption of organic molecules such as exopolymers, humic acids or glycoproteins and other inorganic macromolecules produced by microbes or already present in the environment occurs. This conditioning film alters the properties of the metal surface such as surface tension, wettability and surface energy that allows the subsequent adhesion of bacteria (Compere and Le Bozec, 1997). The bacterial cells themselves can be thought of as charged colloidal particles (Marshall and Blainey, 1991). Their surfaces are generally negatively charged and their attraction towards a surface occurs by chemotaxis or by physical forces (Sreekumari *et al.*, 2001). Bacterial settlement is also reported to be influenced by surface roughness, surface energy and geometry (Walsh *et al.*, 1994). Bacterial cells have also been shown to settle at the grain boundaries of a metal surface, this preference probably due to the elemental segregation occurring at the grain boundaries as well as the presence of specific elements (Sreekumari *et al.*, 2001).

This first attachment step to the metal surface is reversible and occurs by species such as *Pseudomonas*, known as the primary colonisers (Pillay and Lin, 2013). The second step of attachment involves the secretion of extracellular polymeric substances that develop a polymeric bridging between the cell and the substrate (Compere and Le Bozec, 1997). Considerable amounts of EPS are excreted such that in young biofilms, less than 10 percent of its dry weight consists of cells (Coetser and Cloete, 2005). Once this attachment occurs and if the environmental conditions are adequate, the bacteria start to grow on the surface as microcolonies.

Young biofilms contain only a few pioneer species, however, a gradient starts to develop across the biofilm, due to the exchange of substances such as metabolic products, nutrients and gases (Pillay and Lin, 2012). Respiration occurs at the surface of the biofilm, and fermentation in the middle layer (Pfennig, 1984). Once the thickness of the biofilm reaches 10-25 μm , conditions at the base are anaerobic, allowing the growth of anaerobic organisms (Coetser and Cloete, 2005). The biofilm now has a high species diversity and stability and is approaching maturity. Bacteria normally coexist in biofilms as highly structured consortia, with the individual species benefitting in many ways. Protection from antibiotics and predators, enhanced access to nutrients as well as proximity to mutualistic or synergistic bacterial species are just some of the benefits of biofilm formation (Coetser and Cloete, 2005).

The biofilm promotes physicochemical reactions at the interface between the metal and the biofilm, which would not normally occur abiotically, such as in low chloride environments, leading to corrosion rates that can be quite high (Brenda and Lee, 2009; Beech and Sunner, 2004). Spectacularly rapid corrosion failures have been observed in soil due to microbial action and it is becoming increasingly apparent that most metallic alloys are susceptible to some form of MIC (Ismail and El-Shamy, 2009). The corrosion process promoted by biofilms is not a new mechanism of corrosion, as corrosion in non-sterile as well as sterile environments involves the same electrochemical reactions (Dzieriewicz *et al.*, 1997). Rather biocorrosion involves the activity of microorganisms during the normal corrosion reactions (Al-Judaibi and Al-Moubaraki, 2013).

The main microorganisms involved in MIC are bacteria, however, other microbes such as fungi may also participate in the process (Al-Judaibi and Al-Moubaraki, 2013). The most studied microbes involved in biocorrosion are the anaerobic sulphate SRB (Ismail and El-Shamy, 2009). These organisms typically occur in the deeper underlying soil layers due to their anaerobic nature. SRB catalyse the reduction of sulphate ions (SO_4^-) to sulphide (S^-). The production of sulphide leads to the oxidation of the metal, as it is highly corrosive (Ismail and El-Shamy, 2009). Additional microorganisms that can participate in biocorrosion are: (a) Bacteria capable of oxidising iron or manganese; (b) EPS producing microbes; (c) Acid producing microorganisms and methanogens (Gu, 2012); and/or (d) Fungi that degrade protective coatings (Coetser and Cloete, 2005).

As stated by Coetser and Cloete (2005), microorganisms contribute to the corrosion process via the following mechanisms: (a) The creation of differential aeration cells. Respiration by aerobic microbes results in the absence of oxygen below the biofilm. This leads to anodic areas due to the localized difference in aeration and the creation of localized corrosion cells; (b) The consumption of hydrogen leading to cathodic depolarization and metal loss at the anode; (c) Degradation of protective passive layers on the metal surface and the degradation of corrosion inhibitors added to the system; (d) Production of corrosive metabolic end products such as organic and inorganic acids and extracellular polymeric material that are able to bind and precipitate metal ions.

The formation of differential aeration cells leads to a process known as tuberculation (Lee *et al.*, 1995). Oxygen utilization occurs around the tubercle base and anodic metal dissolution occurs at the base of the tubercle. Positively charged metal ions then migrate outwards through the overlying material resulting in an anion flux into the tubercle in the opposite direction. Anions such as chloride enter the tubercle and lower its pH (Coetser and Cloete, 2005). Corrosion by differential aeration leads to the formation of deep pits, shown in the following Figure 1.1:

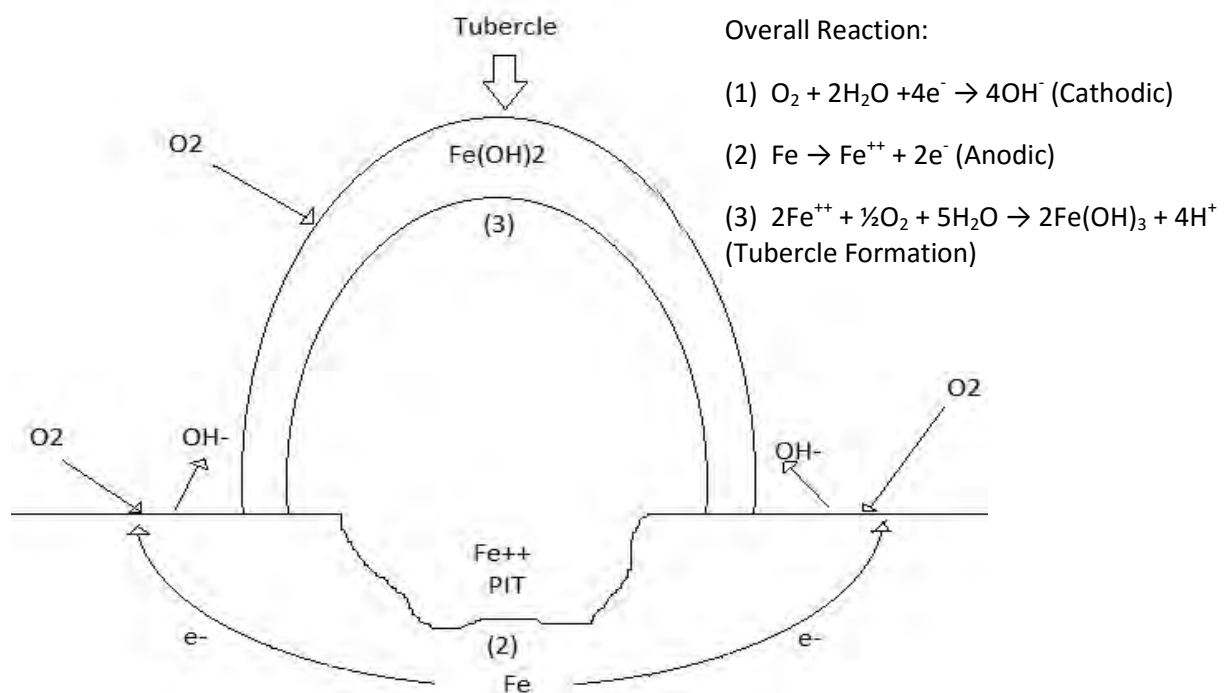


Figure 1.1: Differential aeration cell created by tubercle formation (Coetser and Cloete, 2005)

Metal reducing bacteria and metal oxidizing bacteria are able to facilitate the biomineralisation of the metal (Rajaseker *et al.*, 2010). Metal reducing bacteria are also able to remove protective

metal oxide films present on the metal surface. Acid producing bacteria (APB) are able to cause rapid cathodic depolarization and enhance corrosion, whereas SRB and Sulphur Oxidising Bacteria (SOB) are able to participate in a synergistic sulphur cycle, and produce metabolic products such as hydrogen sulphide and sulphuric acids (Kan *et al.*, 2011).

Our knowledge on the detailed mechanisms of biocorrosion is still however, lacking. In nature, microorganisms typically coexist as mixed communities or consortia. When a material is exposed to a uniform, pure group of microorganism, it becomes much easier to detail and explain the mechanisms of corrosion occurring, however, in mixed consortia, many different mechanisms may occur that may even be synergistic in nature. The rates of corrosion obtained during studies using mixed consortia of microbes are considerably higher than with pure cultures (Beech and Sunner, 2004). The identified mechanisms of biocorrosion explained reflect the diverse array of physiological capabilities of microorganisms that can be found within biofilms, with the mechanisms of corrosion dependent on the species of microorganism present as well as the chemistry of the colonised metal surface (Rajaseker *et al.*, 2010). It has been found that species metabolic specificity within biofilms can have a significant effect on biocorrosion (Beech and Sunner, 2004). Species within the same genus can differ significantly in their metal degrading capability. It is these differences within species that may explain findings that experiments conducted under the same environmental conditions and system can vary widely with regards to the corrosion rate (Beech and Sunner, 2004).

1.2.3 Microorganisms in Biocorrosion

1.2.3.1 Sulphate Reducing Bacteria (SRB)

Due to their role in the corrosion of metallic structures, most studies into MIC under anaerobic conditions have focused on the Sulphate Reducing Bacteria (Eduardo *et al.*, 2003). The SRB are a group of anaerobic bacteria that are capable of conducting dissimilatory sulphate reduction (Dzieriewicz *et al.*, 1997), gaining energy by the reduction of sulphates to sulphide using electrons from the degradation of organic matter or molecular hydrogen, a common product of fermentation in anoxic environments (Enning *et al.*, 2012). Alternatively sulphites, tetrathionate or lactate can be used as a final electron acceptor (Widdel, 1988; Barrett and Clark, 1987). SRB are commonly linked to corrosion in anoxic environments due to three main recurrent observations. Firstly, anaerobic environments rich in sulphates are highly corrosive. Secondly, ferrous sulphide, a characteristic corrosion product of SRB is ubiquitously associated with

anaerobic corrosion and thirdly, laboratory grown cultures produce corrosion rates higher than any other physiological groups (Enning and Garrelfs, 2014).

Due to their relative ease of isolation and purification, the genus *Desulfovibrio* is best studied with regards to biocorrosion. *Desulfovibrio* is able to utilise gaseous hydrogen as an electron donor during the reduction of sulphate (Dzieriewicz *et al.*, 1997). SRB metabolism of sulphate is demonstrated in the following reactions (Malucknov, 2012):



The initial step in the dissimilatory sulphate reduction pathway is the activation of the sulphate ion by its conversion to adenosine phosphosulphate (APS). APS-reductase then reduces APS to sulphite and adenosine monophosphate (AMP). Sulphite then enters the catalytic sulphite reductase system and is reduced to sulphide. Hydrogenases are involved in the reversible oxidation of hydrogen (Dzieriewicz *et al.*, 1997). The activity of the enzymes involved in hydrogen and sulphur metabolism as shown in Figure 1.2 is one of the major factors governing the activity of SRB (Dzieriewicz *et al.*, 1997). It has been found that the specific activity of the enzyme is directly proportional to the level of hydrogen sulphide production (Malucknov, 2012).

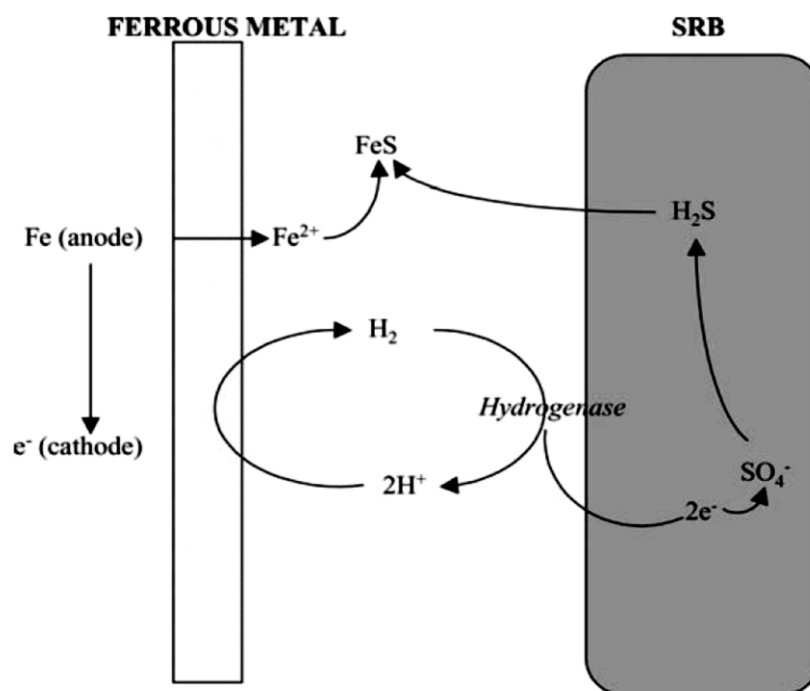


Figure 1.2: The function of hydrogenase enzymes in anaerobic biocorrosion (Bryant and Laishley, 1989)

The first theory put forward to explain corrosion caused by SRB is known as the cathodic depolarisation theory (Eduardo *et al.*, 2003). Cathodic depolarization is a dominant mechanism under conditions of sulphate excess and lack of electron donor (Hubert *et al.*, 2005). The theory is explained as follows: Under anaerobic conditions, due to the lack of gaseous oxygen available for the cathodic reaction, cathodic areas on the metal surface become polarised with molecular hydrogen (Javaherdashti, 2009). The hydrogen then forms a passive film that prevents further proton reduction, resulting in passivation of the metal (Eduardo *et al.*, 2003). Activity by the SRB results in the consumption of this hydrogen and the balance is broken (Eduardo *et al.*, 2003). This also results in the dissociation of water molecules which become involved in the cathodic reaction with hydrogen ions produced on the metal surface and utilised by the hydrogenase enzyme (Javaherdashti, 2009). Sulphide produced by the SRB may also be involved, as it reacts with iron ions to form ferrous sulphide, which forms an adhesive film (Eduardo *et al.*, 2003). Ferrous sulphide may act as a cathode for the evolution of hydrogen, but it may also have a protective effect (Eduardo *et al.*, 2003).

Although most studies have focused on the production of sulphide by the reduction of sulphate, other microbial processes such as the reduction of thiosulphate or sulphite can lead to the production of significant amounts of sulphide (Magot *et al.*, 1997), resulting in metal corrosion. Hydrogen sulphide has also been shown to slow down the combination of hydrogen atoms to molecular hydrogen on the metal surface (Elboujdaini, 2011). This leads to diffusion of these hydrogen atoms into the metal matrix and its subsequent combination into hydrogen gas within the matrix, leading to hydrogen-embrittlement of the metal.

Most research into MIC has focused on a more indirect role of SRB on the corrosion process, i.e., the production of corrosive hydrogen sulphide. This is known as Chemical Microbially Influenced Corrosion (CMIC) (Enning and Garrelfs, 2014). However, there is growing evidence that some species of SRB are able to remove electrons directly from the metal surface, a process known as Electrical Microbially Influenced Corrosion (EMIC). This process is fundamentally different to CMIC and can result in significant corrosion rates (Enning and Garrelfs, 2014). EMIC circumvents the slow abiotic formation of cathodic hydrogen and allows for the efficient utilization of iron as an electron donor by its direct uptake by iron oxidation. Although all SRB are able to influence corrosion due to the production of hydrogen sulphide, direct uptake of electron from the metal surface has only been observed in few corrosive SRB species. All are members of the Deltaproteobacteria, namely *Desulfovibrionaceae* and *Desulfobulbaceae* (Enning

et al., 2012). However, many of the commonly studied SRB do not show this capability (Enning and Garrelfs, 2014).

The mechanism of direct electron uptake from the metal surface is currently unknown, however, it is assumed that it involves the utilization of outer membrane redox proteins such as c type cytochromes (Enning *et al.*, 2012). These are found in other microorganisms that interact with extracellular electron donors.

The main products that form on the surface of iron in the presence of SRB are iron sulphides (Al-Judaibi and Al-Moubaraki, 2013). Iron sulphides can act as a semiconductor, forming a galvanic couple with the steel surface and allowing for the transportation of electrons, thus increasing the rate of the anodic reaction (Al-Judaibi and Al-Moubaraki, 2013). The presence of iron sulphide may also lead to corrosion reduction by forming a tightly adherent film on the metal surface by direct reaction of the metal surface with produce sulphide (Newman *et al.*, 1992). This film prevents to dissolution of ferrous ions into the environment, a process known as anodic polarization (Enning *et al.*, 2012).

Corrosion by SRB occurs in anaerobic environments in the presence of water (Coetser and Cloete, 2005). Tubercles on the metals surface harbour and provide perfect spots for SRB activity (Coetser and Cloete, 2005). Characteristics of MIC caused by SRB include: the pitting of the metal rather than general corrosion, with the rate of pitting increasing with time; and the presence of carbon residue at the corrosion site, leading to the graphitization of the metal (Coetser and Cloete, 2005).

Biofilms have been shown to develop oxygen gradients, and it has been demonstrated that biofilms can develop anaerobic niches even in fully oxygenated environments (Beech and Sunner, 2004). SRB have been shown to adapt to extreme environments, and are commonly isolated from within biofilms found in aerobic environments (Dzieriewicz *et al.*, 1997). Oxygen resistant proteins have actually been demonstrated to exist within certain species of SRB. Genome analysis of *D. vulgaris* demonstrated the presence of genes that code for oxidases, oxidoreductases, plasmid encoded catalases and superoxide dismutase (Beech and Sunner, 2004). However, it is still not known whether these enzymes participate in oxygen reduction on the metal surface.

The differences in the species present in the biofilm can lead to vastly different metabolic activities within the biofilm. This can explain why corrosion rates may vary in two systems under the same environmental conditions. This emphasizes the importance in considering species diversity when investigating the corrosion of metals.

1.2.3.2 Manganese Oxidising Bacteria (MOB)

Metal oxidising oxidizing bacteria are microorganisms capable of depositing iron and manganese hydroxides at a rate hundreds of times greater than occurs abiotically (Moradi *et al.*, 2011). They are, therefore extremely dangerous with regards to controlling corrosion. Due to their ability to oxidise metal ions these bacteria are able to interfere with and induce changes in the passive layer on the metal surface and induce local corrosion cells by depassivation of the metal surface (Moradi *et al.*, 2011).

Many studies have established a relationship between the deposition of manganese oxides/hydroxides and the corrosion of stainless steels in natural waters (Landoulsi *et al.*, 2008). The deposition of these manganese accumulations were attributed to the presence of Mn oxidising chemolithotrophic bacteria, such as *Leptothrix* and *Siderocapsa*.

Manganese oxidisers are categorised into three groups (Rajaseker *et al.*, 2007b):

- a. Those that are involved in the oxidation of dissolved Mn^{2+} ;
- b. Those that are involved in the oxidation of Mn^{2+} bound to solids, and
- c. Those that are involved in the oxidation of dissolved Mn^{2+} by the metabolic H_2O_2 using catalase.

All known manganese oxidising bacteria are aerobes which form manganese oxides within the cell envelope or extracellularly. Lewandowski and Beyenal (2008), suggested a mechanism by which MOB catalyse biocorrosion. Divalent manganese ions (Mn^{2+}), are oxidised to manganese oxyhydroxide ($MnOOH$), which is, thereafter, deposited onto the metal surface. The $MnOOH$ is then oxidised to manganese dioxide (MnO_2), which are also deposited onto the metal surface. These oxides on the metal surface are then reduced back to Mn^{2+} using electrons released at anodic sites. However, the ennoblement process does not terminate there, as the soluble Mn^{2+} is then reoxidised to by the MOB in a continuous cycle, producing renewable reactants such as

MnOOH and MnO₂ that act as cathodic reactants (Lewandowski and Beyenal, 2008). The above mechanism results in pitting corrosion as summarised below in Figure 1.3:

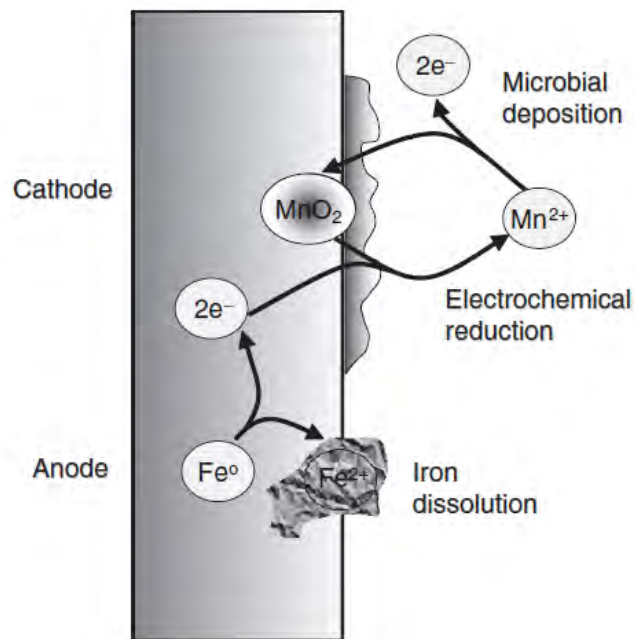


Figure 1.3: Hypothetical mechanisms by which metal oxidising bacteria participate in biocorrosion (Olesen *et al.*, 2000)

The corrosion process catalysed by MOB requires direct contact between the Mn oxides and hydroxides and the metal surface (Hamilton, 2003). After oxygen, manganese oxides are some of the most powerful natural oxidising agents and they take part in various redox reactions as well as in bacterial respiration. Fungi are also known to cause biocorrosion due to the oxidation of manganese (Gadd, 2010). These organisms oxidise dissolved Mn²⁺ to form enriched mineral encrustations. Manganese oxide depositions can form on many submerged substances such as metal, plastic, glass and stone in environments with manganese concentrations as low as 10-20 ppb (Lewandowski and Beyenal, 2008). However, it has been shown that on non-passivating metals such as mild steel, where the oxides are reduced as rapidly as they are deposited, an increase in corrosion rate may occur without evidence of microbial activity.

Species such as *Bacillus* have been found in water pipelines and galvanised steel and have been shown to be capable of manganese and iron oxidation as well as acid production (Kan *et al.*, 2011). *Bacillus* spp. are able to oxidise manganous ions to manganic ions onto the metal surface resulting in the deposition of manganese dioxides on the metal surface which subsequently promotes corrosion (Rajaseker *et al.*, 2007a).

1.2.3.3 Acid Producing Bacteria (APB)

Acid producing bacteria are a group of heterotrophic bacteria that are able to produce organic acids as metabolic products when grown under reductive environmental conditions (Wilkie, 2005). Acids are produced during the fermentation of organic materials. These bacteria have been shown to cause a drop in pH from neutral to pH values as low as 3.5 to 5.5 (Wilkie, 2005). These acidic conditions are aggressive enough to affect the integrity of any metal materials, causing corrosion. Conditions that would suggest the presence of APB in biocorrosion sites include the creation of highly reductive conditions, growth on the surface of the site as well as the presence of organic matter that may be broken down into fatty acids. Both SRB as well as APB are known to propagate in reductive conditions, although SRB thrive in the presence of high sulphate concentrations whereas APB tend to thrive in conditions which are rich in organic matter (Gu, 2012).

Thiobacilli are aerobic, chemolithotrophic and autotrophic bacteria that are able to catalyse the oxidation of a number of compounds such as sulphur, hydrogen sulphide or other sulphur compounds to sulphuric acids (Cloete & Flemming 1997). Acid producing bacteria grow in the absence of oxygen, therefore it is generally considered that these bacteria may be partners to the SRB in the biocorrosion process, especially in the oil and gas industries (Setareh and Javaherdashti, 2003). They can be found in close relationships with SRB and, in stressing the role of SRB in anaerobic corrosion, their role in biocorrosion could well be overlooked (Coetser and Cloete, 2005). Due to these findings, biocorrosion management commonly involves the assessment of both SRB and APB activity (Setareh and Javaherdashti, 2003). Species such as *Thiobacillus thiooxidans* and *T. concretivorus* can grow at pH values of less than 0.7 (Borenstein, 1994). *T. ferrooxidans* is particularly interesting as it has been shown to oxidise sulphur and iron compounds (Borenstein, 1994).

It is widely recognised that APB are in fact significant contributors to biocorrosion, causing a gradual dissolution of the metals colonised due to the acidic conditions created by the bacteria (Soracco *et al.*, 1988). Acid producing bacteria are normally found within biofilms, tubercles, nodules or encrustations under reductive conditions and are generally found at the metal biomass interface (Thomas, 2002). The corrosion caused by APB can be characterised as shallow depressions, which differs from the corrosion caused by SRB, which normally cause deep pitting attacks (Thomas, 2002). APB are known to produce organic acids that cause a drop in pH below

2.0. These bacteria generally increase corrosion rate due to rapid depolarisation of the cathode (Thomas, 2002).

1.2.4 EPS and Biocorrosion

Bacterial extracellular polymeric substances play an important role in the attachment of cells to surfaces. In nutrient-deficient environments, nutrients would adsorb to solid surfaces. It would therefore be highly advantageous to microbial cells to attach to these surfaces and form a biofilm (Beech, 2004). The EPS consists of polysaccharides, proteins, nucleic acids and lipids, of which the content varies according to species and growth conditions (Sutherland, 1985; Beech and Gaylarde, 1999). The EPS is highly adhesive in nature and forms a stable structural network that allows for biofilm development, but may also serve as a nutrient reserve under conditions of famine, and as a protective barrier to toxic substances by delaying or limiting the diffusion of these toxins into the biofilm (Hubert *et al.*, 2005). Bacterial EPS does not always have to be associated with the cell and can be released into the bulk media and attach to surfaces, thus competing with bacterial cells for binding sites on the metal surface (Paradies *et al.*, 1992). Bacterial EPS not only contributes to the corrosion of metals by allowing for the attachment of cells to the metal surface, but may also be directly involved by their ability to bind metal species, thus leading to the formation of metal concentration cells (Beech and Cheung, 1995).

All microorganisms require metal ions to survive, and the availability and the type of these ions will have an effect on the colonisation of a metal surface (Beech and Sunner, 2004). Metal surface chemistry can affect the colonisation of microorganisms either positively, by facilitating the attachment of the cells through EPS-metal binding, or negatively, due to the toxicity of certain metal ions to microbes (Beech, 2004). Studies into EPS produced by SRB have shown that the composition of the EPS released into the bulk phase and produced within the biofilm differs according to the type of metal surface (Zinkevich *et al.*, 1996).

Microbial EPS has the ability to form complexes with metal ions, which depends on the microbial species as well as the metal ion (Beech, 2004; Beech and Sunner, 2004). This is due to the acidic and metal binding nature of the EPS (Hubert *et al.*, 2005). Many bacterial exopolymers act as polyanions under natural conditions which allow for interaction with counterions, such as metal cations (Beech, 2004). This interaction occurs with the anionic functional groups present on the carbohydrate and protein components of the EPS such as carboxyl, phosphate, sulphate, glycerate, pyruvate and succinate groups (Beech and Sunner, 2004). The affinity of these ligands

for ions such as Fe^{3+} , Mg^{2+} , Ca^{2+} and Cu^{2+} can be quite high (Beech, 2004; Beech and Sunner, 2004). Bacterial exopolymers show great specificity in their ability to bind metal ions (Beech, 2004). This could result in the formation of ion concentration cells, thus further accelerating corrosion (Hubert *et al.*, 2005). There is however, some controversy as which component of the EPS, be it carbohydrate or protein, plays a larger role in the binding of metal ions.

Figure 1.4 shows the facilitation of corrosion of a ferrous metal by microbial EPS. Significant shifts in the standard reduction potentials can occur due to the presence of metal ions in different oxidation states within the biofilm EPS matrix. When metal ions bind to the EPS, this can result in the addition of novel redox reaction pathways, such as the direct transfer of electrons from the metal surface (Figure 1.4(a)) or from a biomineral (Figure 1.4(b)) (Beech and Sunner, 2004). When a suitable cathodic reactant is present, such as oxygen in aerobic environments or sulphate or nitrate in anaerobic environments, cathodic depolarisation may occur leading to corrosion acceleration.

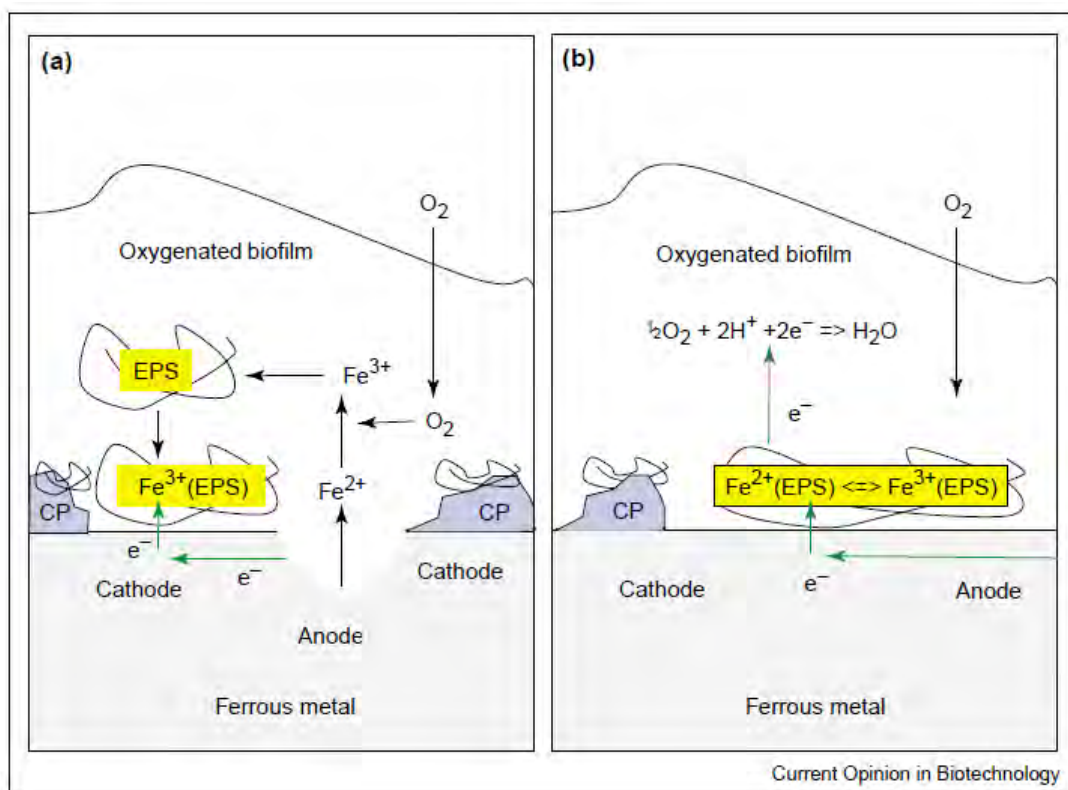


Figure 1.4: Corrosion of a ferrous metal facilitated by metal binding by microbial EPS (Beech and Sunner, 2004)

Very little is known about the synthesis and chemical structure of microbial EPS formed on metal surfaces, as well as the types of anionic functional groups that are responsible with interaction with the metal ions (Beech, 2004). More research, however, is focusing on this significant area of interest, so as to gain greater insight into this phenomenon.

1.2.5 Methods Used to Study Biocorrosion

The type of corrosion can be determined using microscopic techniques, however, this gives only a qualitative approach (Garcia *et al.*, 2012). For a quantitative analysis, the corrosion rate is calculated, usually in terms of the average depth of penetration per year (Uhlig, 2000). Recent advances in microbial genomics and molecular ecology, along with advances in imaging and surface analytical techniques, have allowed for a greater understanding of the community structure within biofilms (Beech and Sunner, 2004). This understanding is critical to explain the spatial and temporal distributions of abiotic and biotic reactions occurring within biofilms on the metal surface and how this affects the electrochemical reactions occurring (Beech and Sunner, 2004).

With regards to corrosion rate, many different techniques have been used across literature to study the corrosion process. Weight loss measurements involve the determination of the amount of material lost during incubation and are typically performed using metal coupons at different depths, soil particle sizes and humidity conditions (de Freitas *et al.*, 2012; Aung and Tan, 2004). However, weight loss measurements have certain limitations, as it requires the removal of the sample at periodic intervals, which could disturb the surrounding medium and interrupt the corrosion process (Aung and Tan, 2004). Electrochemical and ultrasonic techniques have also been used to study the rate of corrosion. Measurement of the corrosion current and voltage allows for the determination of the rate, type and initiation point of corrosion in real time (Kelly *et al.*, 2007). This is done by measuring the fluctuations in potential and current observed on a pair of electrically connected corroding specimens, known as electrochemical noise (EN) (Garcia *et al.*, 2012). Ultrasonic techniques involve the use of long range, low frequency guided ultrasonic waves. However, this technique makes it difficult to determine instantaneous rates of corrosion and has difficulties in accessing certain areas of a buried structure (Aung and Tan, 2004). The use of electrochemical techniques and aqueous solutions is well documented (de Freitas *et al.*, 2012). Linear polarisation resistance measurements and electrochemical impedance spectroscopy have been used to study the corrosion of buried electrodes, however,

these techniques are often difficult to perform and present difficulties in determining corrosion patterns (Aung and Tan, 2004).

Microscopy can be used to determine the structure of corrosion products, as well as study the shapes of microbial colonies and biofilms, the presence of EPS as well as their distribution upon the metal surface. Biofilms formed in different environments have been extensively studied at different stages of their development using a wide range of microscopy techniques (Malucknov, 2012). To some extent, microscopy can be used to determine the type of corrosion that has occurred, such as pitting, by determining the microstructure of the metal surface after removal of the biofilm and corrosion products (Beech, 2004). Microscopy techniques such as Scanning Electron Microscopy (SEM), Transmission Electron Microscopy (TEM) and Epifluorescence Microscopy (OEM) can provide data about the two dimensional surface of an object, however these techniques either do not have sufficient resolution or require extensive sample preparation, thereby preventing use on site (Bachmann and Edyvian, 2006). Environmental Scanning Electron Microscopy (ESEM), Atomic Force Microscopy (AFM) and Confocal Laser Scanning Microscopy (CLSM) allow for the observation of biofilms in real time in their fully hydrated form, without changing the structure of the sample. CLSM and AFM provide high quality three dimensional images of the biofilm (Malucknov, 2012).

Data on the type of microorganisms obtained using microscopy, combined with the chemical and electrochemical analysis of the metal surface can be used to obtain information on the extent of corrosion as well as the composition of corrosion products (Malucknov, 2012). Information on the chemical structure of corrosion products and deposits can be used to determine corrosive reactions occurring in the corrosive process. Popular instruments are the X-ray Diffraction (XRD) and Energy Dispersive X-ray analysis (EDX) techniques, which have been used to gain insight into the elemental composition of the corrosion products (Marquis, 1989). However, XRD does not possess the high spatial resolution to detect localised attack (Beech, 2004). EDX does possess this high spatial resolution at sampling depths of approximately 1 nm, and may not only provide elemental composition data on the corrosion product, but also on the underlying bulk metal. Techniques such as Atomic Absorption Spectrometry, Polarography and Inductively Coupled Plasma Spectrometry (ICP) can be used, however, they require large amounts of sample, in the milligram range, to determine minute levels of metals, in the parts the billion range. More recent techniques such as Time of Flight Secondary Ionization Mass Spectrometry (TOF-SIMS) and X-ray Photoelectron Spectroscopy (XPS) are able to detect metals at much lower sample sizes, in the nanogram range (Muddlman *et al.*, 1994).

Research into the microbial species involved in biocorrosion have traditionally relied upon the growth of bacterial cultures in the laboratory isolated from corroded samples. Laboratory growth media cannot accurately reflect the true conditions within the environment, as, due to the highly selective nature of culture media, it is estimated that more than 99 percent of microbe present in the environment cannot be successfully cultivated (Amann *et al.*, 1992; Dunbar *et al.*, 1999; Kan *et al.*, 2011). Thus microbial communities would be underestimated using culture-dependent approaches (Mansouri *et al.*, 2012). Culture independent techniques, using genetic material have shown to be much more successful in covering a broader spectrum of the diversity of microorganisms and allow for the identification and quantification of the population of microorganisms in environmental samples (Kan *et al.*, 2011). Newer molecular techniques such as Denaturing Gradient Gel Electrophoresis (DGGE), Fluorescent *in situ* Hybridization (FISH) and single strand conformation polymorphism allow for the identification of dominant bacteria in a given environmental system without the limitations of standard techniques; allow for the calculation of the ratio of MIC-contributing bacteria in the total population; the identification of bacteria that are susceptible or resistant to antimicrobials; the assessment of the changes in populations caused either by the of biocides or nutrient modifications; and also allow for more reliable sampling that is not affected by time or transport factors (Videla and Herrera, 2005).

Molecular techniques usually involve the extraction of DNA, amplification of the gene of interest using PCR, examination of the products using a community fingerprint technique, and the cloning and sequencing of a particular gene which is then compared to a database (Videla and Herrera, 2005). Due to the progress of microbial ecology a large database of microbial 16S rDNA sequence data is currently available (<http://www.ncbi.nlm.nih.gov>).

1.2.6 Metal Corrosion in Soil

Structures buried underground are usually expected to have a working life of approximately 50 to 100 years. However, the main cause of the deterioration of underground metal structures is corrosion. These structures can include natural gas and crude oil pipelines as well as water mains (Ismail and El-Shamy, 2009). Soil can be thought of as a porous, heterogeneous environment with colloidal characteristics containing a mineral or organic soil phase, a gas phase and a liquid water phase (Córdoba *et al.*, 2011; Adeosun and Sanni, 2013). The corrosiveness of soil varies according to the composition of the soil. Therefore, corrosivity tests on a particular location are

only applicable to that location. When exposed to soil, structures composed of pure metals as well as their alloys would begin to corrode immediately (Al-Judaibi and Al-Moubaraki, 2013).

The corrosiveness of soil can be defined as its capacity to cause corrosion. Corrosion in soil can be studied by electrochemical techniques as it is defined as an electrolyte (Córdoba *et al.*, 2011). When compared to other environments such as air or water, it is much more difficult to assess its corrosivity due to its complexity (Córdoba *et al.*, 2011). The aggressiveness of soil to cause corrosion is dependent on many factors, which include temperature, moisture and oxygen content, pH, permeability, redox potential, resistivity, soluble salts and microbial activity (Wan *et al.*, 2013, de Freitas *et al.*, 2012). Many of these factors affect electrical resistance which is a good measure of corrosiveness (Adeosun and Sanni, 2013). Dry soils with high resistance will generally not be very corrosive.

One of the basic methods of classifying soils with regards to corrosion is based on soil resistivity. Sandy soils are considered less corrosive and are therefore much higher on the resistivity scale. Clay soils are considered much more corrosive (de Freitas *et al.*, 2012). Corrosion of mild steel was found to be affected by grain size, swelling, shrinkage and clay mineral content (Adeosun and Sanni, 2013). Many of the corrosion problems related to soils are due to the interaction between soil and water, with the presence of water being a vital prerequisite for the development of corrosion cells (Al-Judaibi and Al-Moubaraki, 2013). A study by Wan *et al.* (2013) determined the average corrosion rate of Q235 steel under different moisture contents at different times in loam soil. The study showed a relationship between moisture content in soil and corrosion rate, with corrosion rates increasing up to 33% moisture content. A great increase in corrosion rate occurred between 19 to 26% moisture content, with this rate decreasing from 26 to 33% moisture content. Due to the prerequisite of water in the corrosion reaction, the position of the buried structure in relation to the groundwater table, which can vary in different areas, is of utmost importance. However, even in soil located above the groundwater table, there is still water held by capillaries and pores, with finer soil particles holding more water (Ismail and El-Shamy, 2009).

Oxygen is involved in the cathodic reaction and is in most cases a prerequisite for the corrosion reaction in soil. In neutral and alkaline soils, degree of aeration is significant in corrosion (Ismail and El-Shamy, 2009). It has been shown that the mass transfer of dissolved oxygen is essential in the kinetics of the corrosion reaction, and that the entire corrosion reaction is limited by both activation and diffusion control (Wan *et al.*, 2013). The oxygen supply decreases with increasing

depth, with aeration much higher above the groundwater table, and much less below it (Ismail and El-Shamy, 2009). The type of soil also affects aeration, with sandy soils having much greater oxygen content than clay. Disturbed soil would also have greater aeration than undisturbed soil (Adeosun and Sanni, 2013). These different aeration characteristics can lead to major corrosion problems due to the development of oxygen concentration cells (Ismail and El-Shamy, 2009).

Soils with low pH would most likely pose a significant risk with regards to corrosion of metal structures. Generally soils will not have a pH lower than 5, with most soils falling within the range of 5-8. At this range, pH is not considered a major variable in corrosion rate as, according to the pH-potential diagram for iron, the hydroxides and oxides formed at higher pH values tend to have a passivating effect (Cordoba *et al.*, 2011). The pH of soil can be affected by different activities, with lower pH caused by the decomposition of acidic plants, mineral leaching and acid rain, and higher pH caused by high sodium, magnesium, calcium and potassium contents (Ismail and El-Shamy, 2009).

Chloride ions can play a role in the anodic dissolution of metallic structures and their presence in soils is generally considered harmful. Chlorides can be found naturally in soils due to the presence of brackish groundwater or historical sea beds, and will vary as the soil conditions alternate between wet and dry (Ismail and El-Shamy, 2009). The presence of chloride ions in soil could prevent the passivation of steel surfaces due to the formation of soluble compounds, even at high pH values (Cordoba *et al.*, 2011). When compared to chlorides though, sulphates are in most cases considered much more corrosive with regards to metallic structures (Ismail and El-Shamy, 2009).

Much research into soil corrosion has been performed. However, due to the complexity and heterogeneous nature of soil, a comprehensive and thorough model of the corrosion process as well as methods to assess corrosion in soils is lacking (Wan *et al.*, 2013).

1.2.7 Prevention of corrosion

It is possible that biocorrosion actually occurs as a result of, and is not a cause of corrosion. For this reason the conventional methods of controlling chemical corrosion still applies (Javaherdashti, 2009). The principle methods used to prevent corrosion include: selecting proper materials of construction able to resist corrosion, the use of protective coatings such as paints, preventing or controlling microbial growth and cathodic protection (Lin and Ballim, 2012).

One of the classic concepts used to prevent corrosion or reduce its harmful effects in an industrial system is to keep the system clean (Videla and Herrera, 2005). Many different strategies have been used to achieve this task, and they can be grouped into physical, chemical and biological methods (Lin and Ballim, 2012).

Physical methods include the use of flushing (the simplest) and coatings. Flushing has limited efficacy. Though, for increased effectiveness, flushing can be supported by the use of cleaners or chemical agents that encourage biofilm detachment (Lin and Ballim, 2012; Videla and Herrera, 2005). Abrasive and non-abrasive sponge-balls have been used in industry, although abrasive sponge-balls may cause damage to protective coatings and non-abrasive sponge-balls may be ineffective against thicker biofilms (Videla and Herrera, 2005). The application of coatings is a general methods used to protect against corrosion, with various organic coatings being studied in regards to protection (Shimura and Aramaki, 2008; Avci and Abanoz, 2004; Chou *et al.*, 2002).

Chemical control strategies involve the use of biocides, which is the most common method used in biocorrosion control (Videla and Herrera, 2005). Biocides are any chemical agent that is able to kill living organisms (Lin and Ballim, 2012), therefore, they are mostly used in closed systems. Biocides can be classified into both oxidising and non-oxidising groups and can be used in conjunction with other substances to aid with dispersion or biofilm penetration that could increase their efficacy (Lin and Ballim, 2012; Saravia *et al.*, 2003). Common oxidising agents are chlorine, bromine, and ozone whereas formaldehyde, glutaraldehyde and quaternary ammonium compounds include examples of non-oxidising biocides (Videla and Herrera, 2005). Non-oxidising biocides are reported to be more effective than oxidising compounds in the control of fungi, algae and bacteria, due to their greater persistence in the environment, as well as their pH independence (Lin and Ballim, 2012). Often, combinations of both oxidising and non-oxidising agents are used in industry to optimise microbial control (Videla and Herrera, 2005). Rajaseker *et al.* (2010), noted the widespread use of toxic biocides led to the growth and dominance of *Bacillus* species in a petroleum plant due to their ability to form highly resistant spores. *Bacillus* species have also been reported to be able to degrade some of these chemical agents (Russell, 2003). For this reason, the use of higher concentrations of these expensive biocides is necessary. The increase in legislative requirements for greater environmentally friendly control agents have led to the need for development of new biocides or carefully selected blends of already existing biocides (Videla and Herrera, 2005).

Cathodic protection is a highly effective and widely used method of corrosion protection (Saravia *et al.*, 2003). It involves coupling the metal to be protected with a more easily corroded sacrificial metal, or to an external power source supplying electrons (Orfei *et al.*, 2006). This forces the metal to be protected to act as the cathode, preventing its dissolution (Orfei *et al.*, 2006). If properly designed, cathodic protection can be used to halt corrosion rate to a negligible level (Lin and Ballim, 2012). Cathodic protection is well suited for corrosion prevention of steel structures in underground or marine environments (Orfei *et al.*, 2006). When used in conjunction with coating, cathodic protection has been reported to be successful in the prevention of biocorrosion (Zuo *et al.*, 2004). There are two types of cathodic protection systems commonly used, the impressed current and galvanic/sacrificial anode methods (Lin and Ballim, 2012). The galvanic/sacrificial method is relatively inexpensive and simple, and involves the use of a more easily corroded sacrificial metal, commonly alloys of zinc, magnesium or aluminium (Lin and Ballim, 2012). This method requires little maintenance, however, the current released may be quite low. If a larger current is required to provide adequate protection of metal, such as with larger structures, then the impressed current method can be used. This involves the use of relatively inert anodes, commonly silicon, mixed metal oxide, platinum, cast iron, nonium coated wire and graphite, which are connected to an external DC power source (Lin and Ballim, 2012).

Biological control strategies involve the use of microorganisms to control biocorrosion, though there is hardly any research on this topic (Zuo *et al.*, 2004; Videla and Herrera. 2005). When compared to chemical and physical control methods, biological control methods are much cheaper, more environmentally friendly, as well as have the potential to be more efficient (Lin and Ballim, 2012). Mechanisms by which microorganisms can inhibit corrosion include decreasing medium corrosiveness, stabilising an already present protective coating and neutralising corrosive substances in the environment (Videla and Herrera. 2005). However, microbial inhibition of corrosion is rarely, if ever, linked to a single species or mechanism.

Biocompetitive exclusion is becoming increasingly popular, especially in the petroleum industry, to prevent reservoir souring and biocorrosion due to SRB mediated hydrogen sulphide production. It has been proven in both laboratory and field studies (Videla and Herrera. 2005). Biocompetitive exclusion involves the addition of nutrients, such as nitrate, to the system which stimulates to growth of competing bacterial populations such as the nitrate reducing bacteria, due to the greater energy output generated from nitrate reduction over sulphate reduction, which are

then able to displace the sulphate reducing bacteria as the dominant bacterial populations in the system (Videla and Herrera, 2005). This shift then halts the growth of SRB and thus hydrogen sulphide production. The actual microbiological basis is not very well understood, and it is still not known whether autotrophic or heterotrophic Nitrate Reducing Bacteria (NRB) have the most significant role. However, an inoculum of NRB is unnecessary (Videla and Herrera, 2007). It has been shown, though, that the addition of nitrate into the system inhibits SRB growth due to an increase in redox potential, as well as the production of toxic by products such as nitrite (Lin and Ballim, 2012). In some cases, the addition of nitrate was even shown to encourage the SRB to shift from sulphate metabolism to the nitrate reduction pathway (Beech and Sunner, 2004; Lin and Ballim, 2012).

The addition of nitrite has also been shown to inhibit biocorrosion, acting in a similar manner to nitrate. Nitrate- or nitrite-reducing sulfide-oxidizing bacteria (NR-SOB) are able to reoxidise sulphide to elemental sulphur or sulphate, using nitrate or nitrite. This results in the net removal of sulphide from the system when there are insufficient organic electron donors available to allow for reduction of all available nitrate or nitrite. Nitrite itself has actually been shown to inhibit the enzyme dissimilatory sulphite reductase, which is responsible for the final enzymatic step in the sulphate reduction pathway. However, many SRB have the enzyme nitrite reductase that prevents this inhibition (Hubert *et al.*, 2005).

Hubert *et al.* (2005) has shown that in batch culture treated with nitrite concentrations of 1-2 mM, SRB were able to overcome nitrite mediated inhibition, and were thus not inhibited at this concentration. However, at higher concentrations of 20 mM, SRB activity decreased, coupled with a decrease in corrosion rate. It was noted, though, that nitrite itself causes corrosion at low concentrations below 3.5 mM, however, it prevents corrosion at higher concentrations of 10-20 mM. Therefore, nitrite treatment would require a dose high enough to prevent nitrite mediated corrosion, as well as inhibit SRB activity. Hubert *et al.* (2005) concluded that although nitrate was favourable in the stimulation of NRB populations due to its higher oxidative power, continuous addition of a high nitrite dose was preferable as it prevents souring and corrosion problems (Hubert *et al.*, 2005).

Pillay and Lin (2013) observed that the addition of nitrate to a simulated seawater/sediment system actually increased the weight loss of mild steel coupons when compared to the controls. The authors stated that this could have been due to an increase in the metabolic activities of

corrosive bacteria due to the supplementation of nitrate, or that the concentration used (5 mM) was too low to stimulate the inhibition of corrosion. The study also observed, however, that nitrate addition stimulated corrosion inhibition by individual bacterial isolates isolated in the study.

Biocompetitive exclusion strategies have been shown to be a stable and long term strategy of SRB mediated biocorrosion, when compared to biocide use. Nitrate injection does have its drawbacks, such as an increase in localised corrosion caused by the production of polysulfide and thiosulphate due to the simultaneous oxidation of sulphide and reduction of nitrate (Lin and Ballim, 2012).

1.3 Motivation for Study

The study of soils and their microbial populations as a corrosive medium is important due to the large number of buried structures and pipelines, whose deterioration could pose significant safety, economic and environmental problems (Córdoba *et al.*, 2011). MIC occurs in many different environments and habitats that differ in many properties such as nutrients, temperature, pH, oxygen levels and pressure. MIC also depends on the physiological properties of the organisms involved and present in the biofilm (Beech and Sunner, 2004). The many mechanisms discovered to be involved in biocorrosion reflect the wide variety of physiological abilities of microorganisms present. These mechanisms are dependent on the species of microorganism, as well as the chemistry at the metal-bulk solution interface (Beech and Sunner, 2004). The microorganisms and mechanisms discussed above do not reflect all the possible mechanisms of MIC, rather they reflect the most well understood mechanisms (Lewandoski and Beyenal, 2008).

Despite the large amount of research being conducted into MIC, our understanding of this process is still severely lacking. Not much is known on the role of microbial ecology on corrosion of metals, as well as the effect of the biofilm EPS matrix and its effect on the electrochemical behaviour of metals (Beech and Sunner, 2004). Research aiding our understanding of the microbial species involved in MIC and their interactions with metal as well as with other microorganisms, especially with regards to BE strategies, would provide a foundation for the development of novel approaches for detection, monitoring and control of biocorrosion (Mansouri *et al.*, 2012).

One of the most promising methods used for the control of biocorrosion is the addition of nutrients such as nitrates and nitrites that stimulate the activities of nitrate and nitrite reducing bacteria which outcompete SRB populations and result in lower sulphide concentrations (Gervertz *et al.*, 2000).

Therefore, this study focuses on the effects of different concentrations of nitrates and nitrites on the rate of corrosion of mild steel coupons in a loam soil system. The effect on biofilm formation and bacterial population dynamics will also be examined.

1.4 Aims:

The aim of this study was to investigate the microbiologically-influenced corrosion activities of mild steel supplemented with different concentrations of nitrates and nitrites in a loam soil system.

1.4.1 Objectives:

- 1.4.1.1 To investigate the effect of different concentrations of nitrate/nitrite on mild steel corrosion in a loam soil system under laboratory conditions.
- 1.4.1.2 To measure the property changes induced by bacterial populations on mild steel coupons under various nitrate/nitrite concentrations.
- 1.4.1.3 To verify the effect of the nitrate/nitrite concentration that is optimal for corrosion inhibition on microbiologically influenced corrosion *in situ*.
- 1.4.1.4 To determine the effect of individual isolated bacteria on corrosion of mild steel in a corrosive medium.

Chapter 2: The Effect of Nitrite and Nitrate Supplementation on the Biocorrosion of Mild Steel Coupons in a Loam Soil System

2.1 Introduction

Due to the large number of buried structures, which include natural gas and crude oil pipelines and water mains, the study of soils as a corrosive environment is crucial. Structures buried underground are usually expected to have a working life of approximately 50 to 100 years, a value significantly affected by corrosion. Soils constitute the most complex environment with regards to corrosion of metals, ranging from rapid metal loss to negligible effects. Adeosun and Sanni (2013) stated that soil can be thought of as a porous heterogeneous environment with colloidal characteristics, with its corrosiveness highly dependent on its composition. Factors affecting soil corrosivity can include temperature, moisture and oxygen content, pH, permeability, redox potential, resistivity, soluble salts and microbial activity (Wan *et al.*, 2013, de Freitas *et al.*, 2012). Generally, the most significant component of soil with regards to corrosion is moisture content, with soils with a higher moisture content being more corrosive (Al-Judaibi and Al-Moubaraki, 2013).

Microorganisms are known to influence the corrosion of metals by affecting the electrochemical reactions occurring at the metal surface and can either accelerate or inhibit corrosion (Videla and Herrera, 2005). This phenomenon has been observed in the corrosion of petroleum product pipelines, storage tanks, and various other industries (Rajaseker *et al.*, 2011). The most studied microorganisms known to affect corrosion are the anaerobic sulphate reducing bacteria (SRB); however, many other aerobic as well as anaerobic microorganisms may contribute to the process. The SRB are anaerobic in nature, and are capable of performing dissimilatory sulphate reduction, reducing sulphate to the highly corrosive and toxic sulphide (Dzieriewicz *et al.*, 1997; Enning *et al.*, 2012). Warm conditions, low oxygen level and high sulphate concentrate are known to facilitate the proliferation of SRB (Korenblum *et al.*, 2010).

Traditionally, biocides have been used to mitigate corrosion caused by SRB, however, in recent decades, nitrate addition has been introduced as a more effective and environmentally safe method (Bodtker *et al.*, 2008). This method involves the addition of nutrients, normally nitrates or nitrites, to a system to encourage the growth of a beneficial competitive microbial population to inhibit SRB growth. Several mechanisms can be attributed to the prevention of corrosion due to nitrite or nitrite addition (Pillay and Lin, 2013). Firstly, competition between nitrate or nitrite reducing bacteria and SRB results in the competitive exclusion of the SRB. Some SRB may even

switch their metabolism from sulphate reduction to nitrate reduction due to the higher energy yield. Secondly, nitrate reducing-sulphide oxidising bacteria (NR-SOB) use nitrate to oxidise produced sulphide to elemental sulphur and sulphate, resulting in a net sulphide removal from the system (Eckford and Fedorak, 2002). Thirdly, nitrite is a specific inhibitor of the enzyme dissimilatory sulphite reductase, the enzyme responsible for the terminal step in the sulphate reduction process (Pillay and Lin, 2013).

Previous studies, Bodtker *et al.* (2008) showed that the continuous addition of nitrate in an oil well water injection system led to a rapid decrease in corrosion rate of up to 40 %, with SRB activity decreasing in the process. Pillay and Lin, (2013), however, reported that the addition of 5 mM of nitrate to a loam soil system, resulted in a net increase in the corrosion rate of mild steel coupons. The observed outcomes could have been due to the low concentration of nitrate used, which was insufficient to induce a decrease in corrosion rate. Hubert *et al.* (2005) observed that treatment with 1-2 mM nitrite in a batch culture was unable to inhibit SRB growth. However, at higher concentrations of 20 mM of nitrite, SRB activity was found to decrease, coupled with a decrease in corrosion. The authors noted that nitrite itself causes corrosion at low concentrations below 3.5 mM, however, corrosion was prevented at higher concentrations of 10-20 mM.

The use of nitrite and nitrate based strategies for corrosion control is not well understood and has potential for further development so that simple dosing guidelines can be developed (Pillay and Lin, 2013). This chapter focuses on the efficacy of different concentrations of nitrate and nitrite on the corrosion of mild steel coupons in a loam soil environment. The effect on corrosion rate, as well as bacterial populations on the mild steel surface, was investigated.

2.2 Materials and Methods

2.2.1 Soil Sample Collection and Preparation

Loam soil was collected from a depth of 1m in Glenwood (KwaZulu-Natal), air-dried and homogenized. The soil was passed through a 7.5 mm (porous aperture) Madison Test Sieve. Moisture content and pH of the soil was measured according to McCauley *et al.* (2003). Moisture content was determined by measuring the weight of the soil before and after drying, with the difference used to calculate the amount of moisture.

2.2.2 Mild Steel Coupon Preparation

The mild steel coupons used in this study were obtained from the Academic Instrumentation Unit (University of KwaZulu-Natal, Westville), with dimensions of 25×25×1.2 mm and a 2 mm

drilled mounting hole. The coupons were polished with grade 100 sandpaper, rinsed with distilled water and then degreased with acetone. The coupons were air-dried and weighed to a sensitivity level of 0.01 g using an analytical balance (Sartorius Basic).

2.2.3 Laboratory Experiment: Construction of loam soil system supplemented with nitrate and nitrite

Ten 3-L catering jars were filled with 2 kg of loam soil and subjected to different nutrient conditions. One jar contained autoclaved loam soil and was employed as the control. A second jar was filled with non-autoclaved loam soil. The final 8 jars contained increasing concentrations of ammonium nitrate or sodium nitrite (20 ml with a final concentration of 5 mM, 10 mM, 20 mM and 40 mM) as the nitrate or nitrite source, respectively, in an attempt to inhibit or reduce the rate of corrosion of the steel.

The coupons were suspended into the jars within the soil in a vertical position at a depth of 3 cm. An additional 20 ml of distilled water was supplemented at each sampling time to maintain the moisture content (Aung and Tan, 2004). Jars were incubated for a total of 24 weeks under standard laboratory conditions (25°C, 1 atm). Sampling occurred every 4 weeks. At each sampling time, the corrosion products on the surface of the metal coupons (triplicate) were removed by complete immersion for 90 s in 20% hydrochloric acid under constant agitation by hand. Coupons were rinsed in distilled water and air dried (Ryhl-Svendsen, 2008). Thereafter, coupons were scrubbed vigorously with a rubber stopper. After cleaning, metal coupons were wiped with a paper towel and dried in an oven at 80°C for 10 min. The coupons were cooled and the mass loss (mg) was measured (Zuo *et al.*, 2004). The weight loss was calculated using the following formula:

$$\text{Corrosion rate (mg/cm}^2\text{)} = \frac{W_i - W_f}{A}$$

W_i : Initial weight

W_f : Final weight

A : Total surface area of coupon

2.2.4 Carbohydrate and protein content of biofilm from coupon surface

At each sampling time, the biofilm developed on the coupon surface was scraped off using a sterile surgical blade, and was suspended in 2 ml of distilled water. The resulting suspension was used for carbohydrate and protein analysis.

For the carbohydrate analysis, the suspension was vortexed at maximum speed, and 100 μ l was analysed using the DNS assay for total reducing sugars (Beech *et al.*, 2000). The absorbance was measured at an optical density of 540 nm against a reagent blank. The carbohydrate content was calculated based on the OD₅₄₀ reading against standard D-glucose curves.

Protein analysis was performed using the Bradford assay (1976). Two millilitres of Bradford reagent was added to 100 μ l of the above-mentioned biofilm suspension. The solution was vortexed and incubated at room temperature for 15 min to 1 h before being measured at an optical density of 595 nm. Protein content was calculated by comparing the OD₅₉₅ reading against a standard bovine serum albumin curve (Beech *et al.*, 2000).

2.2.5 Scanning electron microscopy (SEM) and electron dispersive X-ray (EDX) analyses of the coupons

The mild steel coupons were fixed by immersion in methanol for 10 min, thereafter air-dried. The surface of the coupon was analysed using the Zeiss FEG-SEM Ultraplus in the Microscopy and Microanalysis Unit (MMU) in the University of KwaZulu Natal, Westville. Mild steel coupons were also examined using Energy-Dispersive X-Ray analysis using the FEG-SEM equipped with a Bruker EDX detector.

2.2.6 Microbial Population analysis of biofilm on corroded mild steel coupons using Denaturing Gradient Gel Electrophoresis (DGGE)

2.2.6.1 DNA extraction and amplification of 16S rDNA

The biofilm sample was scraped off the coupon surface using a sterile surgical blade and DNA extracted directly using the MoBio Soil DNA Extraction kit, according to the manufacturer's instructions. The 16S rDNA was amplified by PCR (Zhu *et al.*, 2003). The reaction mixture (25 μ l) for PCR amplification contained 1 μ l each of forward and reverse primers (10 μ l each,

Inqaba Biotech), 12.5 µl of 2× ReadyMix Taq PCR Reaction Mix (Fermentas Life Sciences), 7.5 µl nuclease-free water and 2 µl of template DNA. One microlitre of Bovine Serum Albumin (10 mg/ml) was added to the reaction mixture at the expense of 1 µl of nuclease-free water, when PCR-amplifying DNA from biofilm samples (Kjeldsen *et al.*, 2007). The primers used in the reaction were forward primer 63F (5'-CAG GCC TAA CAC ATG CAA GTC-3') and reverse primer 907R (Marchesi *et al.*, 1998). PCR was conducted using the ThermoHybrid PCR Express Thermal Cycler under the following cycling parameters: 25 cycles of initial denaturation at 95°C for 1 min, 55°C for 1 min and 72°C for 1.5 min, followed by the final elongation step at 72°C for 5 min (Sambrook *et al.*, 1989). The PCR products were confirmed by electrophoresis on a 1% (wt/vol) agarose gel at 100 V for 30 min in 1× Tris-Acetate – EDTA running buffer, stained with ethidium bromide and visualized with the Chemi Genius2 BIO Imaging System and Gene Snap software (Syngene, UK). PCR product size was determined using GeneRuler DNA Ladder Mix (Thermo Scientific).

2.2.6.2 Denaturing Gradient Gel Electrophoresis Analysis

After amplification of the 16S rDNA was confirmed, touch-down PCR was performed (Gillan *et al.*, 1998) with the primers 357F with a 45 bp GC clamp at the 5' end (5'-CGC CCG CCG CGC GCG GCG GGC GGG GCG GGG GCA CGG GGG GCC TAC GGG AGG CAG CAG -3') and the universal primer 518R (5'-ATT ACC GCG GCT GCT GG-3'). The cycling parameters included: initial denaturation at 95°C for 5 min, followed by 20 cycles: 94°C for 30 s, 65°C for 30 s (decreasing 0.5°C every cycle) and 72°C for 1 min followed by 10 cycles of PCR: 94°C for 30 s, 55°C for 30 s and 72°C for 1 min with a final extension step at 72°C for 5 min (O' Sullivan *et al.*, 2008). DGGE was performed using the Dcode™ Universal Mutation Detection System (Bio-Rad) with the following reagents and conditions: 1× TAE, 8% 1.5 mm thick gels, supplemented with 2% glycerol and a denaturant gradient containing 30% to 55% urea-formamide at 60°C, at 60 V constantly for 16 h. The DGGE gels were stained with ethidium bromide and visualized with the Chemi Genius2 BIO Imaging System and Gene Snap software (Syngene, UK).

2.2.6.3 DNA Sequencing and Phylogenetic Analysis of DGGE Bands

Selected DGGE bands were excised using a sterile surgical blade and subjected to PCR amplification according to Ye *et al.* (2009). Excised bands were eluted in 100 µl of Millipore water and incubated overnight at 4°C. Thereafter, the bands were spun down at 10000 rpm for 5

min. The upper layer was extracted and used as the template. PCR amplification of the excised bands was carried out with primers 357F (without a GC clamp) and 518R. The cycling parameters were as follows: initial denaturation at 95°C for 5 min, followed by 30 cycles: 94°C for 30 s, 58°C for 1 min and 72°C for 1 min followed by a final extension step at 72°C for 5 min. Amplified products were sequenced with the 357F and 518R primer by Inqaba Biotech (South Africa). The Blastn search tool (Altschul *et al.*, 1990; 1997) was used to determine the most similar sequences in the GenBank database. Most similar sequences obtained by the BLAST search were used to construct multiple alignments using the Mega 6 (Tamura *et al.*, 2007). The phylogenetic relationships were determined using the neighbour-joining method and the Tamura-Nei distance analysis model, with 1000 bootstrap replications assessed to support internal branches using the Mega 6 software (Tamura *et al.*, 2007).

2.2.7 Statistical Analysis

Data were analysed using GraphPad InStat for windows (version 3.10). A one-way ANOVA was used to test mean differences in weight losses of the metal coupons over time. A p-value of <0.05 was considered statistically significant.

2.3 Results

2.3.1 Physical characterisation of loam soil

Table 2.1 shows the physical characteristics of loam soil. The loam soil used in this study was slightly acidic (pH 6.38) and had a moisture content of 15.38%.

Table 2.1: Physical characteristics of soil used in study

	Loam soil
pH	6,38
Percentage water content	15,38%
Percentage dry mass	84,62%

2.3.2 Weight loss measurements of mild steel coupons in a stimulated loam soil system

Upon removal of the metal coupons, reddish brown as well as black depositions were observed on the surface. The black layer may be attributed to Fe_3O_4 and the orange layer to $\text{Fe}(\text{OH})_3$. The weight loss measurements of mild steel coupons immersed in a stimulated loam soil system are shown in Figure 2.1 (Raw data in Appendix I). Corrosion was seen to increase with time in all cases. The autoclaved control demonstrated a lower corrosion rate when compared to the non-autoclaved control, however the difference was not significant ($p > 0.05$). The nitrate-treated systems demonstrated a significantly greater weight loss when compared to the autoclaved and non-autoclaved systems. An increase in concentration of ammonium nitrate in the jar led to an increase in weight loss of mild steel coupons, with the highest weight loss of $123,85 \text{ mg/cm}^2$ being observed at week 20 with 40 mM nitrate supplementation. A significant difference was observed between the corrosion rate of the systems treated with 5 mM and 10 mM and those treated with 20 mM and 40 mM nitrate ($p < 0.05$), however, no significant difference was observed between 10 mM and 20 mM nitrate supplementation. Supplementation with 5 mM of nitrite led to no significant decrease in corrosion when compared to the autoclaved and non-autoclaved systems, however, at concentrations 10, 20 and 40 mM of nitrite, significant decreases ($p < 0.05$) in the corrosion rate compared to the autoclaved, non-autoclaved and nitrate-treated systems, were observed. No observable corrosion was detected at 20 mM and 40 mM nitrite over the 24 week incubation period.

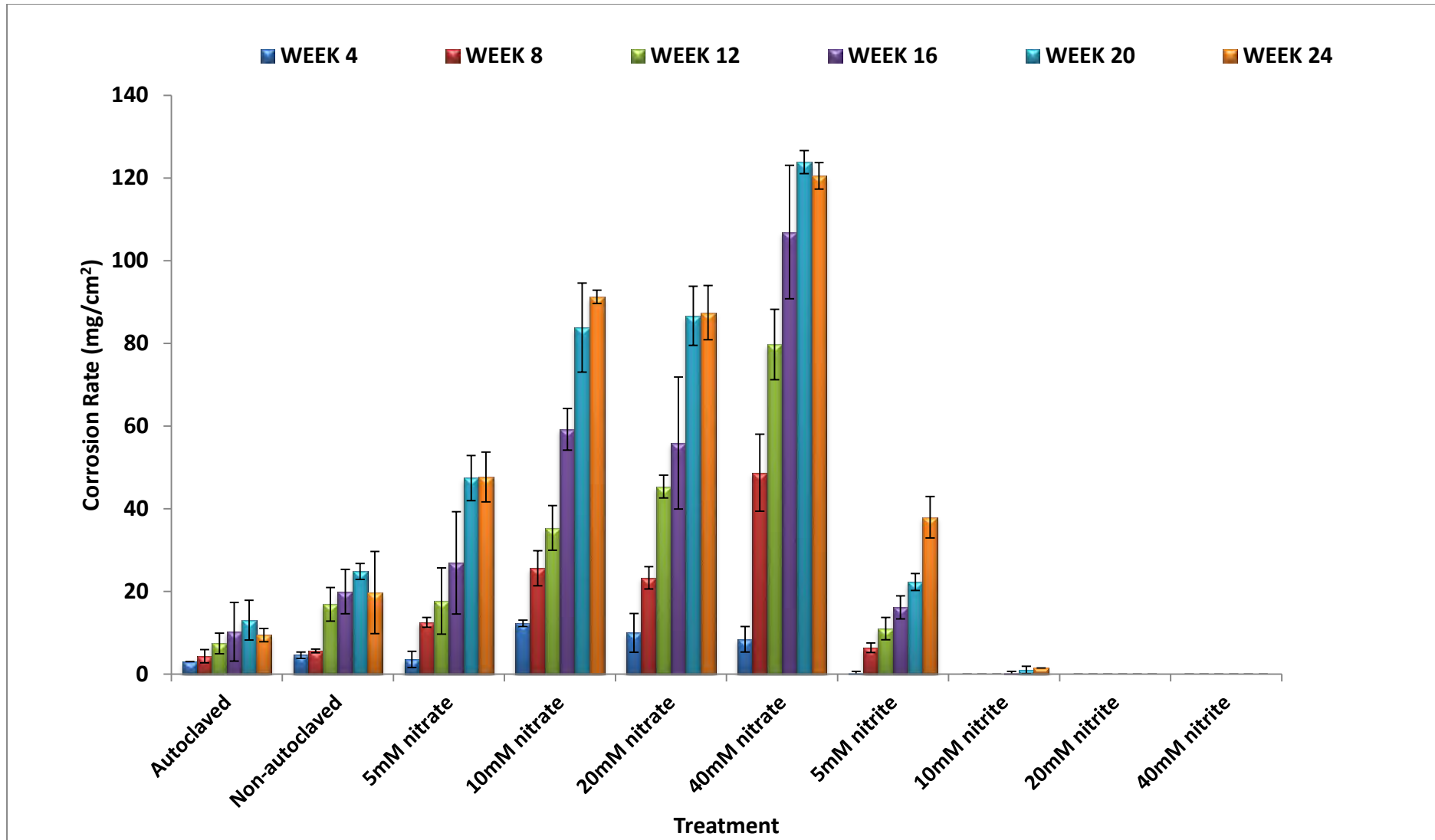


Figure 2.1: Weight loss of mild steel coupons conditions over a period of 24 weeks. Coupons were incubated at 25°C in a 3-L catering jar containing loam soil, and increasing concentrations of nitrate and nitrite.

2.3.3: Protein and carbohydrate content of the biofilm on the surface of the mild steel coupon

The protein content of the biofilm formed on the surface of the mild steel coupons immersed in the stimulated loam soil system is shown in Table 2.2. In almost all cases, a trend emerged. Protein content was observed to increase until week 12, with a subsequent decrease thereafter. The autoclaved control showed a concentration of 0.48 mg/ml at week 4, which increased to 0.9 mg/ml at week 12. The protein content subsequently decreased to 0.39 mg/ml at week 24. The protein content in the biofilm formed on the mild steel coupons incubated in the non-autoclaved system demonstrated significantly greater protein content when compared to the autoclaved control. A maximum protein concentration of 3.89 mg/ml at week 12 was observed, which subsequently decreased at week 20 to 1.66 mg/ml, before a rise to 3.82 mg/ml at week 24. The nitrate treated systems showed significantly higher protein concentrations when compared to the autoclaved control and the non-autoclaved control from weeks 12 onwards. The highest protein concentration was observed at week 20 (30.38 mg/ml) in the 40 mM nitrate treated system. In the 5 mM nitrite treated system, a non-significant difference was observed when compared to the autoclaved systems, however, lower concentrations were detected when compared to the non-autoclaved and nitrate treated systems. A maximum concentration of 1.49 mg/ml at week 12 was observed, with a subsequent decrease to 0.75 at week 24. A negative correlation ($r = -0.82$; $p < 0.05$) was observed between the protein content and the corrosion rate in the 5 mM nitrite treated system, as well as a positive correlation in the 10 mM nitrate system ($r = 0.82$; $p < 0.05$), however, no significant correlation was observed in the remaining systems. No protein was observed on the mild steel coupons incubated in the 10, 20 and 40 mM nitrite systems.

Table 2.2: Total protein concentration (mg/ml) in biofilm samples extracted from mild steel coupons incubated in loam soil over a period of 24 weeks

		Total protein content (mg/ml) of the biofilm					
		Week 4	Week 8	Week 12	Week 16	Week 20	Week 24
Autoclaved		0.48	0.75	0.9	0.85	0.73	0.39
Non-autoclaved		3.65	3.71	3.89	2.5	1.66	3.82
Nitrate	5mM	1.62	1.68	24.08	7.68	8.92	6.25
	10mM	1.69	0.94	7.79	5.69	8.27	8.63
	20mM	1.99	2.05	18.88	6.87	5.37	9.64
	40mM	2.44	0.9	30.38	9.37	10.28	5.46
Nitrite	5mM	1.34	1.4	1.49	1.48	0.95	0.75
	>10mM	ud	ud	ud	ud	ud	ud

ud: undetectable

The carbohydrate concentrations of the biofilm formed on the surface of the mild steel coupons immersed in the stimulated loam soil system are shown in Table 2.3. At weeks 4 and 8 (11.25 mg/ml and 24.8 mg/ml, respectively), carbohydrate concentration in the autoclaved sample were significantly higher than in the non-autoclaved sample. A decrease was observed from week 8 (24.8 mg/ml) to 12 (4.77 mg/ml) in the autoclaved sample, however, the concentration remained relatively constant thereafter, reaching 7.18 mg/ml at week 24. Carbohydrate contents of the non-autoclaved sample show a gradual increase over the 24 weeks, reaching a maximum concentration of 10.58 mg/ml at week 24. The nitrate treated systems showed a similar trend to that observed in the protein content, with maximum carbohydrate content observed at week 12, and a subsequent decrease thereafter. The nitrate treated systems showed a significantly higher carbohydrate content when compared to the non-autoclaved control, with the maximum carbohydrate observed at week 12 (48.27 mg/ml) at 40 mM nitrate. Thereafter, a general decrease in carbohydrate content was observed till week 24. In the 5 mM nitrite treated system, a significant decrease in carbohydrate content was observed when compared to the autoclaved, non-autoclaved and nitrate systems. Maximum concentration was observed at week 12 (4.62 mg/ml), thereafter decreasing to 1.27 mg/ml at week 24. A positive correlation ($r=0.95$; $p<0.05$) was determined between the carbohydrate content in the non-autoclaved system and the corrosion rate, however, no correlation was determined in the remaining systems. No observable carbohydrates were observed on the coupons treated with 10, 20 and 40 mM nitrite.

Table 2.3: Total carbohydrate concentration (mg/ml) of biofilm samples extracted from mild steel coupons in loam soil over a period of 24 weeks

		Total carbohydrate content (mg/ml) of biofilm					
		Week 4	Week 8	Week 12	Week 16	Week 20	Week 24
Autoclaved		11.25	24.8	4.77	6.87	8.94	7.18
Non-Autoclaved		2.36	4.88	7.78	8.64	10.48	10.58
Nitrate	5 mM	8.78	10.69	11.75	4.58	8.9	10.12
	10 mM	10.89	13.82	23.26	13.45	11.76	11.58
	20 mM	10.89	22.92	18	15.15	18.69	11.47
	40 mM	8.29	7.55	48.27	16.89	11.58	16.45
Nitrite	5 mM	1	1.94	4.62	1.56	1.28	1.27
	>10 mM	nd	nd	nd	nd	nd	nd

nd: undetectable

2.3.4 Scanning electron microscopy and electron dispersive X-ray analyses of corroded mild steel coupons in a loam soil system

2.3.4.1 Scanning Electron Microscopy

Observations of the mild steel coupons immersed in the loam soil system over a 24 week period were conducted using SEM. Figure 2.2 shows the surface of the mild steel coupons from the various experiments at 4, 8 and 20 weeks. Figure 2.2A shows the autoclaved samples over the incubation period. Light corrosion product formation was observed at weeks 4 and 8. By week 20, an adhesive heterogeneous corrosion product layer had formed over the surface of the coupon. No biofilm formation was observed.

Figure 2.2NA shows the non-autoclaved samples over the incubation period. The non-autoclaved system showed greater corrosion product formation when compared to the autoclaved system. Figure 2.2NA1 shows the formation of deep pits by week 4. By week 8 (Figure 2.2NA2), the formation of nodules, which have the appearance of being burst open, were observed. Microbial growth was observed within the nodules, surrounded by a layer of corrosion products. By week 20 (Figure 2.2NA3), the size of the nodules were observed to have increased significantly.

Figure 2.2SN show the 20 mM nitrite treated coupons at weeks 4, 8 and 20, respectively. Neither microbial growth nor corrosion product formation was observed over the entire incubation period. Similar results were obtained for the 10 mM and 40 mM treated mild steel coupons.

Figure 2.2AN shows the 10 mM nitrate treated coupons at weeks 4, 8 and 20, respectively. Significantly greater biofilm development, as well as corrosion product formation, occurred when compared to the autoclaved, non-autoclaved and nitrite treated systems. By week 4 (Figure 2.2AN1), extensive microbial growth, as signified by the presence of cocci shaped bacteria was observed. Corrosion products were seen interspersed within the microbial cells. Figure 2.2AN2 shows the formation of deep cracks and pits that formed over the coupon surface, showing extensive corrosion and metal loss. By week 20 (Figure 2.2AN3), a thick, heterogeneous biofilm was observed to have formed over the mild steel surface. Similar results were observed for the 5 mM, 20 mM and 40 mM treated samples over the 24 week period.

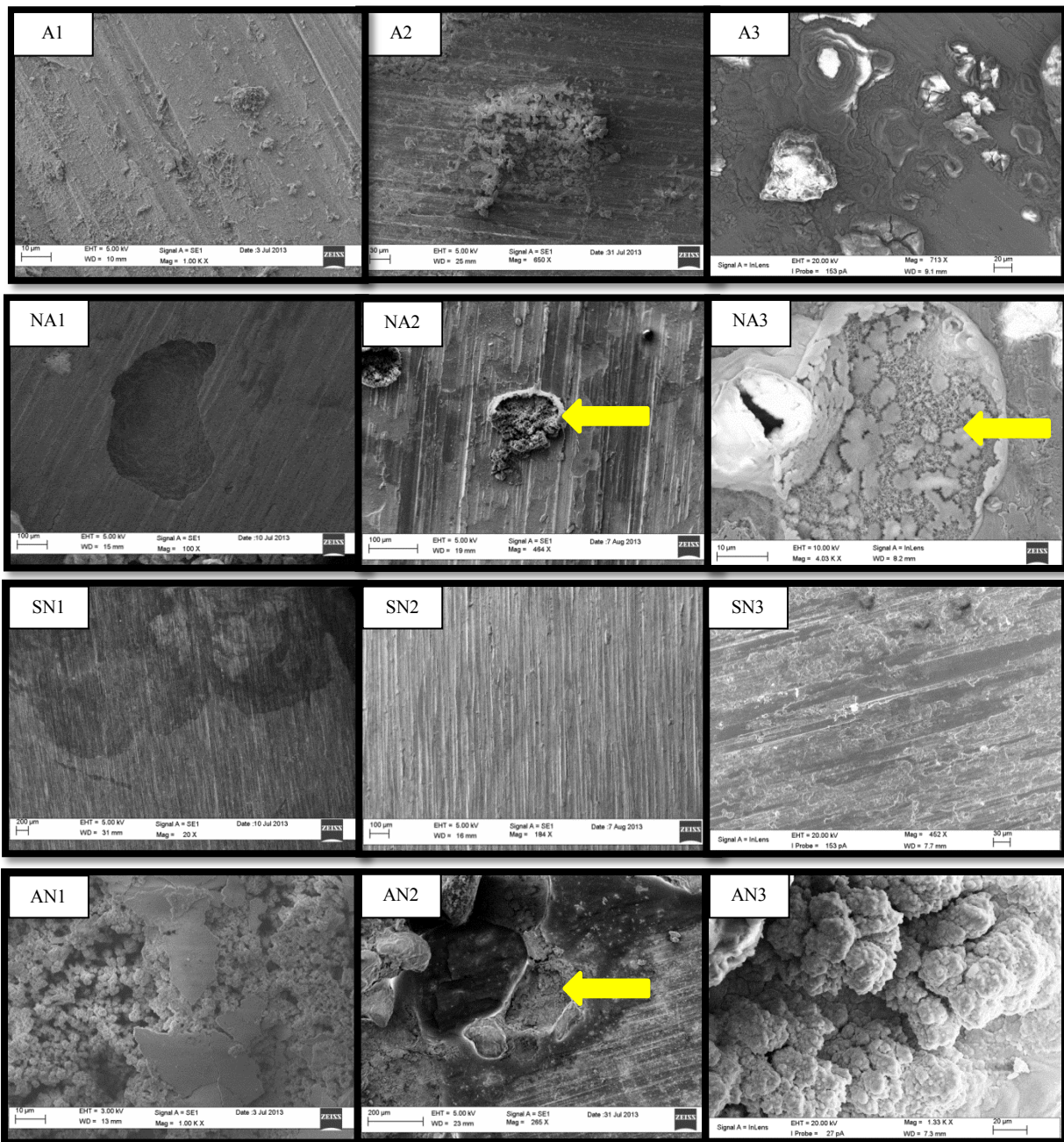


Figure 2.2: Some typical examples of SEM images of the surface of mild steel coupons in a stimulated loam soil system after 4 weeks of incubation. (A1, A2, A3) – Autoclaved system after 4, 8 and 20 weeks, respectively; (NA1, NA2, NA3) – Non-autoclaved system after 4, 8 and 20 weeks respectively; (SN1, SN2, SN3) – 20 mM nitrite supplemented systems after 4, 8 and 20 weeks, respectively; (AN1, AN2, AN3) – 10 mM nitrate supplemented system after 4, 8 and 20 weeks, respectively.

2.3.4.2 Energy Dispersive X-ray analysis of mild steel coupons

The different corrosion products formed on the surface of both the untreated and treated mild steel coupons were examined using EDX analysis for their elemental composition. Only four morphologically different corrosion products were identified throughout the study (Figure 2.3). The elemental compositions of the different corrosion products are shown in Table 2.4 (EDX Spectra in Appendix II). The untreated mild steel coupon (Table 2.4), was composed mainly of iron (88.22 %), carbon (4.87 %), and oxygen (3.53 %), with trace amounts of manganese, fluorine, aluminium, and silicon (0.2%, 1.78%, 0.4% and 1.01%, respectively) also present.

All corrosion products were composed mainly of iron and oxygen, indicating the occurrence of iron oxidation. Corrosion product 1 (CP1) was detected in the 5 mM nitrate treated coupon, and contained the highest oxygen content (32.48%) when compared to the other corrosion products investigated. An increase in manganese content (0.27%) was observed in CP1 indicating the possible activities of manganese utilising bacteria. Phosphorous (0.06%), present in ATP, and also a possible indicator of the presence of microorganisms was also observed. The presence of calcium (0.91%) could indicate the formation of calcium carbonate. CP2 and CP3, detected in the non-autoclaved system contained lower oxygen and carbon content when compared to CP1. Phosphorous was not detected in either CP2 or CP3, however, sulphur was observed in CP2, possibly indicating the activities of SRB. Trace amounts of chlorine, which could accelerate the corrosion process were detected in CP2, but was absent in the other corrosion products. CP4, observed on the surface of the 5 mM nitrite treated coupon contained the lowest oxygen content (22.94%) when compared to the other corrosion products studied, indicating lower iron oxidation. A high amount of manganese (0.47%) was observed when compared to the untreated coupon (0.2%), which could indicate the activities of manganese utilising bacteria. Trace amounts of nickel, not observed in the other corrosion products were also observed.

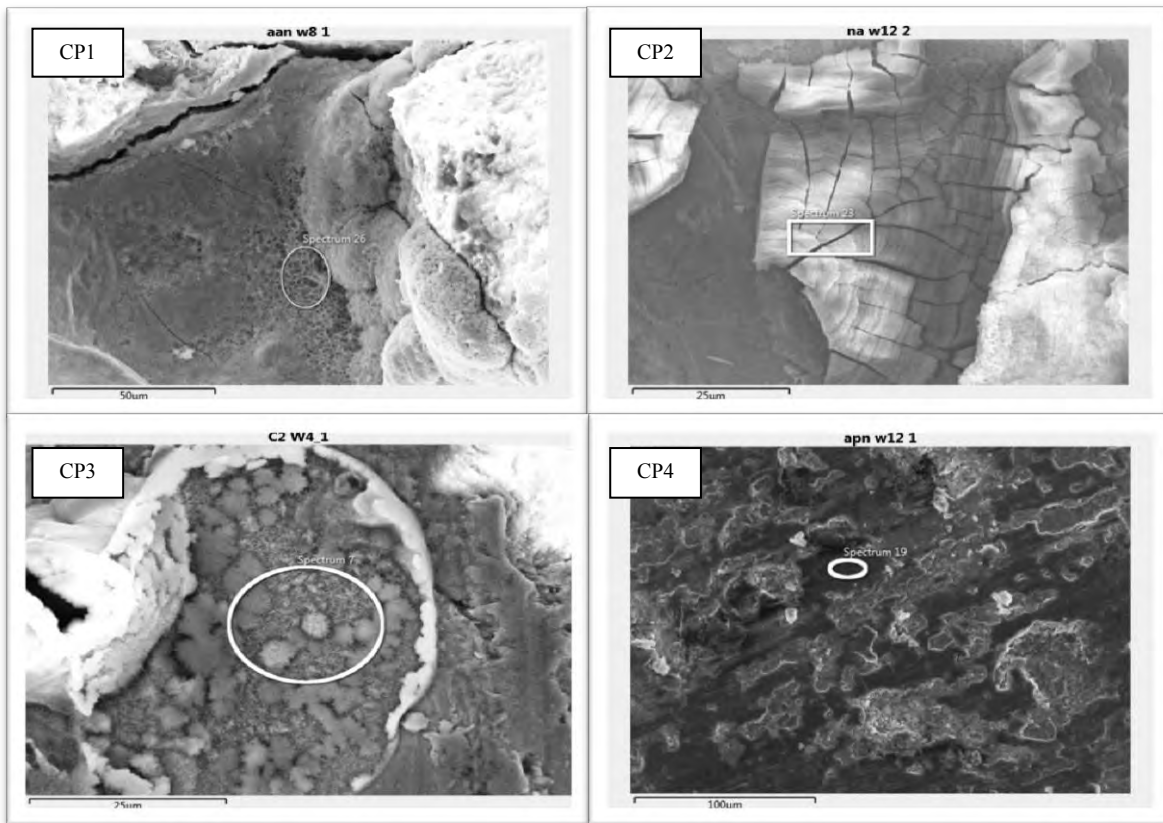


Figure 2.3: Corrosion products investigated using EDX analysis. CP1- Corrosion product 1 (5 mM nitrate supplemented system- week 8), CP2- Corrosion product 2 (Non-autoclaved system- week 12), CP3- Corrosion product 3 (Non-autoclaved system- week 4), CP4- Corrosion product 4 (5 mM nitrite supplemented system- week 12).

Table 2.4: Elemental composition of different corrosion products formed on the surface of the treated and untreated mild steel coupons analysed by EDX analysis

Element	Sample				
	Untreated Coupon	Corrosion product 1	Corrosion product 2	Corrosion product 3	Corrosion product 4
	Wt%				
Fe	88.22	61.40	62.5	72.96	72.46
O	3.53	32.48	31.98	26.58	22.94
C	4.87	4.04	3.14	-	3.38
Mn	0.2	0.27	0.2	0.06	0.47
F	1.78	-	-	-	-
Al	0.4	-	-	-	0.41
Si	1.01	0.37	0.1	0.17	-
K	-	0.07	-	0.12	-
Ca	-	0.91	0.1	-	-
Ti	-	0.11	-	-	-
Cr	-	0.10	0.05	-	-
Co	-	0.07	0.85	-	0.24
Cu	-	0.16	-	-	-
Mg	-	0.15	0.15	-	-
P	-	0.06	-	-	-
S	-	-	0.06	-	-
Cl	-	-	0.07	-	-
Ni	-	-	-	-	0.1

Samples: Corrosion product 1- (5 mM nitrate supplemented system- week 8), Corrosion product 2- (Non-autoclaved system- week 12), CP3- Corrosion product 3- (Non-autoclaved system- week 4), Corrosion product 4- (5 mM nitrite supplemented system- week 12).

2.3.5 DGGE analysis of biofilm communities on corroded mild steel coupons and phylogenetic affiliation of dominant bacteria

The biofilms formed on the mild steel coupons were scraped off the surface and the DNA extracted. No detectable biofilm was formed on the surface of the nitrite treated coupons so they were excluded from this study. The extracted DNA was then amplified using a primer pair 63F and 907R. The amplified DNA at week 16 is shown in Figure 2.4. The product size was estimated to be 844 bp. After confirmation of amplification, a further round of amplification was performed with the DGGE primer pair of 357F-GC and 518R, with the product size estimated to be 211 bp, shown in Figure 2.5. The PCR amplicons were then subjected to DGGE analysis. Individual bands of interest were removed and reamplified using the primer pair 357F without a GC clamp and 518R, with the expected amplicon size of 161 bp, shown in Figure 2.6.

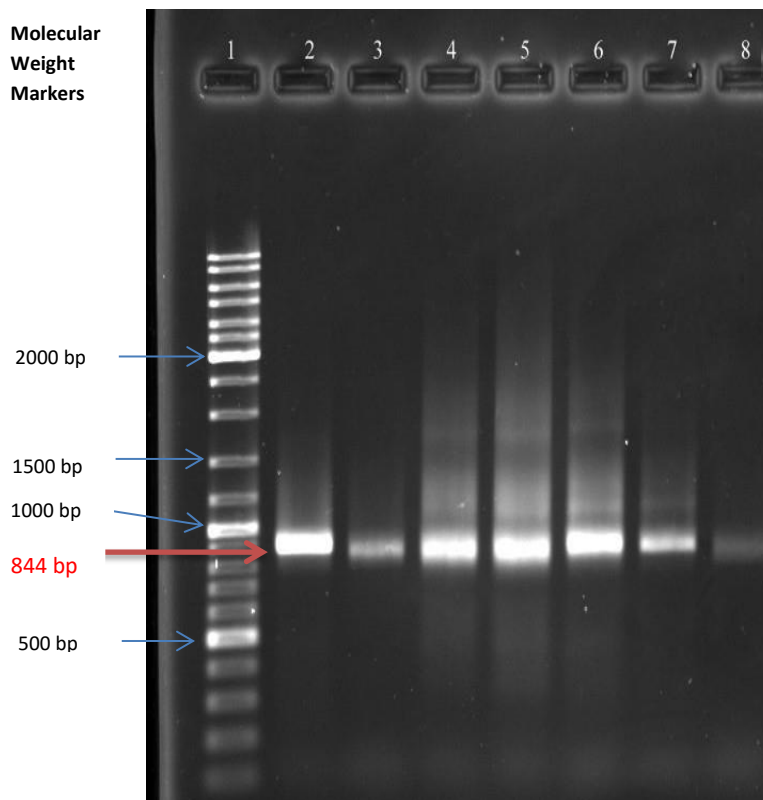


Figure 2.4: PCR amplification of the 16S rDNA of biofilm samples after 16 weeks incubation in loam soil. Lane 1: GeneRuler DNA Ladder Mix (ThermoScientific); 2: positive control (*Bacillus subtilis*); 3: autoclaved control; 4: non-autoclaved control; 5: 5 mM nitrate; 6: 10 mM nitrate; 7: 20 mM nitrate; 8: 40 mM nitrate;

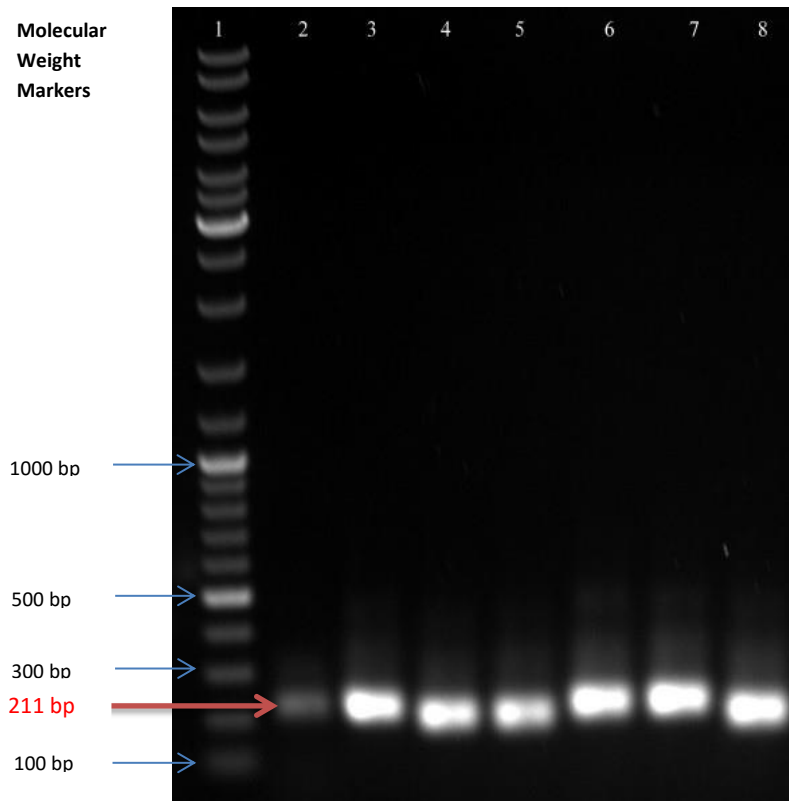


Figure 2.5: PCR amplification with DGGE primers after 16 weeks incubation in loam soil. Lane 1: GeneRuler DNA Ladder Mix (ThermoScientific); 2: positive control (*Bacillus subtilis*); 3: autoclaved control; 4: non-autoclaved control; 5: 5 mM nitrate; 6: 10 mM nitrate; 7: 20 mM nitrate; 8: 40 mM nitrate;

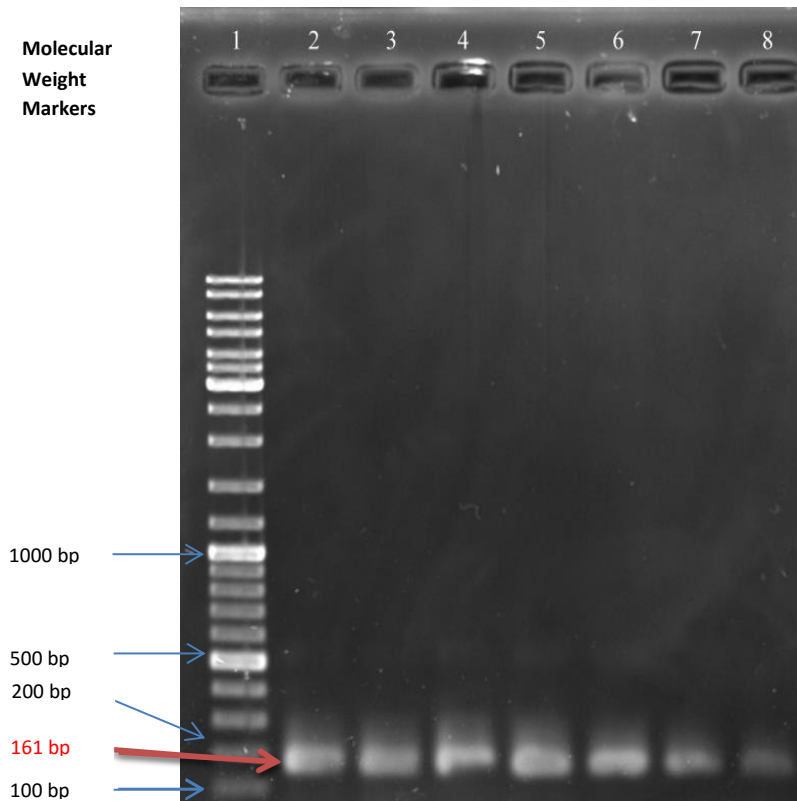


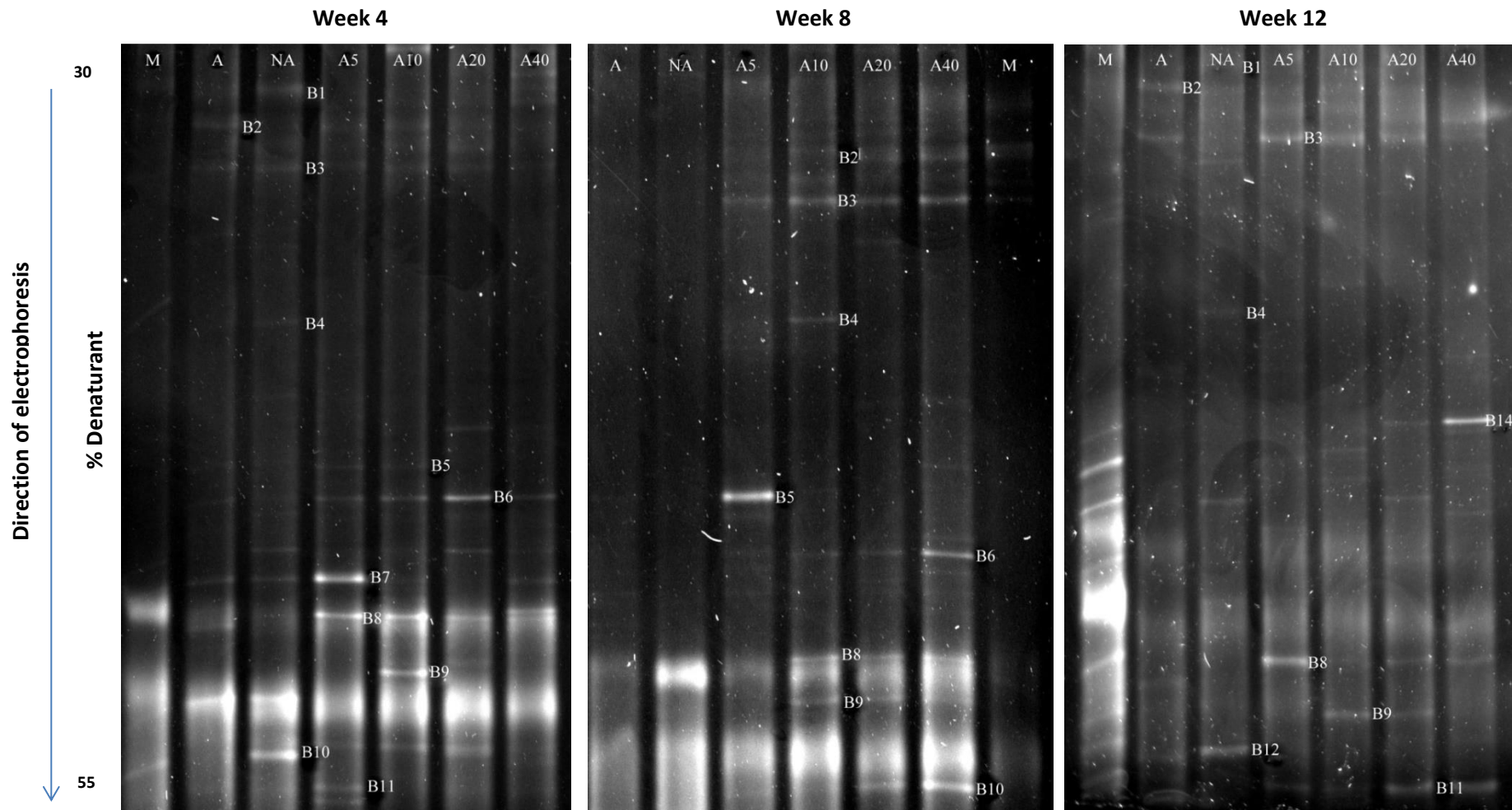
Figure 2.6: PCR amplification of DGGE bands after DGGE analysis at 16 weeks incubation in loam soil. Lane 1: GeneRuler DNA Ladder Mix (ThermoScientific); 2: positive control (*Bacillus subtilis*); 3: autoclaved control; 4: non-autoclaved control; 5: 5 mM nitrate; 6: 10 mM nitrate; 7: 20 mM nitrate; 8: 40 mM nitrate

DGGE amplicons generated multiple bands from the DNA extracts (Figure 2.7) from mild steel coupons over the 24 week sampling period. The number of individual bands is representative of the number of bacterial species present in the sample. Previous studies have suggested that band intensity is indicative of the relative abundancies of certain phylotypes in the sample (Murray *et al.*, 1996). Bands with high intensities were, therefore, taken as the dominant taxa. All bands were excised and sequenced. However, certain bands produced poor quality sequences and were unable to be identified.

Putative identification of the bands excised over the 24 week period are shown in Table 2.5. Sequence data showed that the bacterial diversity revealed phylotypes belonging to 2 major distinct phylogenetic groups, the Firmicutes and α -Proteobacteria. A diverse microbial community was present on the mild steel surface in both controls and nitrate treated systems. The community was found to differ between the non-autoclaved and nitrate treated systems, with a higher bacterial diversity observed in the nitrate treated systems. A total of 21 different bands

were sequenced and identified (Table 2.5). Uncultured *Phenylobacterium* sp. (Band 2) and *Rhizobium* (Band 3) were detected in the coupons in all treatments over the entire 24 week period. *Bacillus* species were found to be dominant in the non-autoclaved control over the early stages of the experiment with *Bacillus subtilis* (Band 10), *Bacillus flexus* (Band 12) and *Bacillus megaterium* (Band 9) detected in the first 16 weeks. Over the latter stages, the banding patterns in the non-autoclaved samples were found to change with uncultured bacterium clone (Band 7), uncultured *Beijerinckiaceae* (Band 18) and *Bradyrhizobium* (Band 19) being the dominant phylotypes.

A more complex bacterial community was detected in the nitrate treated systems, with similar species being detected over the systems treated with different concentrations of nitrate. *Bacillus* species were observed to be the more abundant species, with *Bacillus megaterium* (Bands 8 and 9), *Bacillus subtilis* (Band 10), and *Bacillus flexus* (Bands 11 and 12) detected in the first 16 weeks. A change in the bacterial community is observed over time, however, with *Brevundimonas* (Band 5), uncultured bacterium clone (Band 6) and *Bradyrhizobium* sp. (Band 19) being the dominant phylotypes. By week 20, a clear distinction in banding patterns between the autoclaved, non-autoclaved and nitrate treated systems is observed.



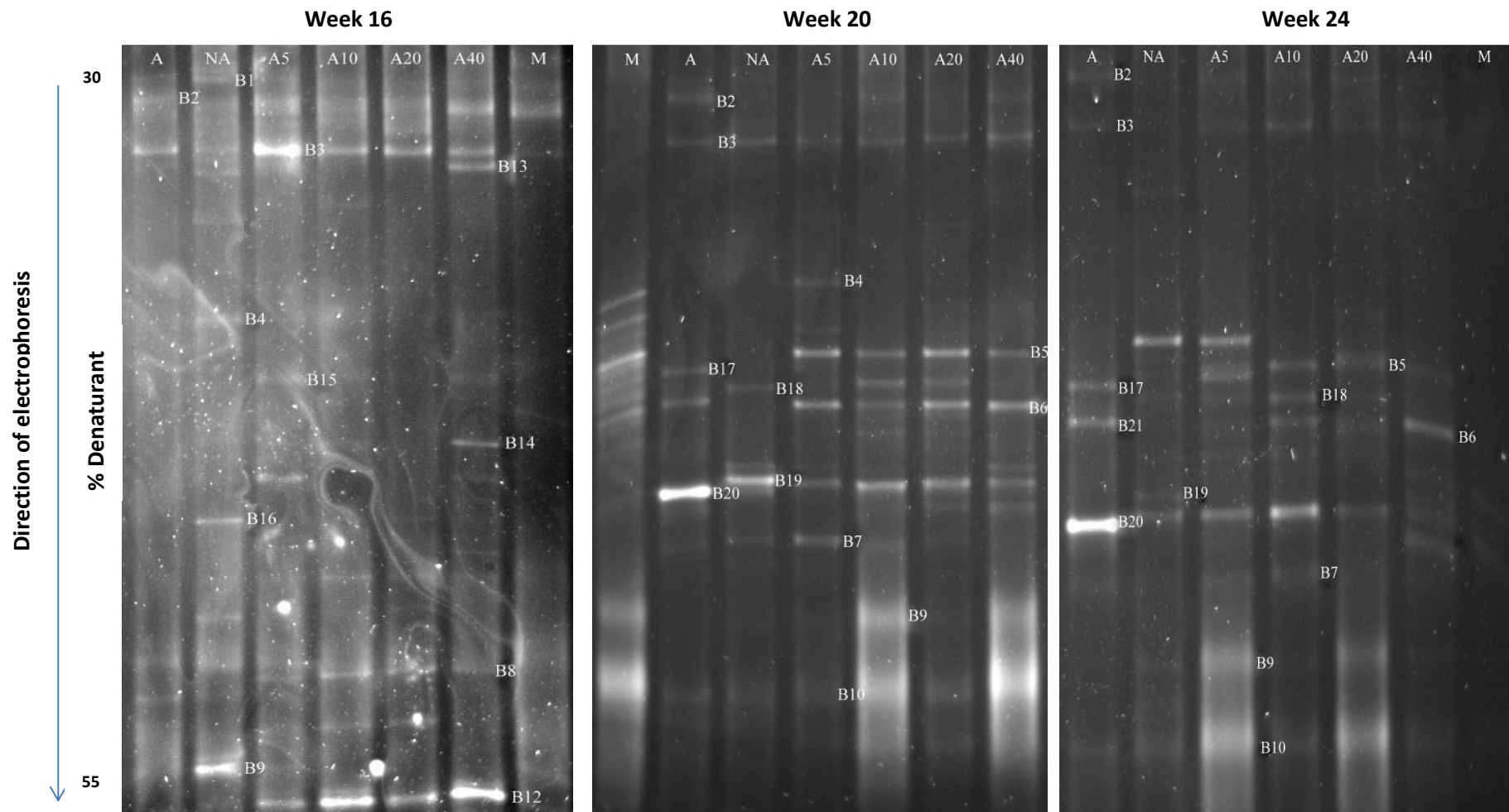


Figure 2.7: DGGE profile of biofilm samples after 4, 8, 12, 16, 20 and 24 weeks incubation in loam soil (Lanes - M: DGGE markers; A: autoclaved control; NA: non-autoclaved control; A5: 5 mM nitrate; A10: 10 mM nitrate; A20: 20 mM nitrate; A40: 40 mM nitrate). The labelled bands indicate gel portions that were sequenced, and identified

Table 2.5: Partial 16S rDNA sequence similarity of the excised bands on DGGE profiles over the 24 week period

Band	THE CLOSEST SEQUENCES (GENBANK NUMBER)	SIMILARITY	PUTATIVE DIVISION	SAMPLE PRESENT
1	<i>Brevundimonas olei</i> strain BGc3 (KF387655)	96%	<i>α-proteobacteria</i>	A
2	Uncultured <i>Phenylobacterium</i> sp. (HE861266)	99%	<i>α-proteobacteria</i>	All Samples
3	<i>Rhizobium</i> sp. SP 2-03 (KM253158)	96%	<i>α-proteobacteria</i>	All Samples
4	Uncultured <i>Xanthomonadaceae</i> bacterium clone GASP-KC3W2 D08 (EU300496)	91%	-	NA, AN
5	<i>Brevundimonas</i> sp. 74 95 4 (KF295785,1)	100%	<i>α-proteobacteria</i>	All Samples
6	Uncultured bacterium clone Pohang WWTP December,2006 3765 (HQ513693,1)	99%	-	A; A5; A10 ;A20; A40
7	Uncultured bacterium clone ncd2550a03c1 (JF224543)	84%	-	A; NA; A5
8	<i>Bacillus megaterium</i> strain CK5.1 (KM434869)	88%	<i>Firmicutes</i>	A5; A10; A20; A40
9	<i>Bacillus megaterium</i> partial (HF584976)	89%	<i>Firmicutes</i>	NA; A10; A20; A40
10	<i>Bacillus subtilis</i> strain NB10 (JX489616,1)	79%	<i>Firmicutes</i>	NA; A5; A10; A20; A40
11	<i>Bacillus flexus</i> strain RC8 (KM505011) band 11	99%	<i>Firmicutes</i>	A5; A10; A20; A40
12	<i>Bacillus flexus</i> strain RC8 (KM505011) band 12	99%	<i>Firmicutes</i>	NA; A5; A10; A20; A40
13	Uncultured <i>Mesorhizobium</i> sp. partial (LM655332,1)	98%	<i>α-proteobacteria</i>	A40
14	<i>Sphingomonas glacialis</i> strain UC7208 (KJ728994,1)	95%	<i>α-proteobacteria</i>	A40
15	<i>Ochrabactrum</i> sp. Yw28 (HQ746581,1)	99%	<i>α-proteobacteria</i>	A5; A10; A20; A40
16	Uncultured <i>Sphingomonas</i> sp. Clone EEMzer0n117 (JX899959,1)	96%	<i>α-proteobacteria</i>	NA; A20; A40
17	<i>Amorphus suaedae</i> strain TC6899 (NR118535,1)	96%	<i>α-proteobacteria</i>	A
18	Uncultured <i>Beijerinckiaceae</i> bacterium partial (LN624894,1)	97%	<i>α-proteobacteria</i>	NA; A5; A10; A20
19	<i>Bradyrhizobium</i> sp. L2D34A partial (LN614689,1)	99%	<i>α-proteobacteria</i>	NA; A5; A10; A20; A40
20	<i>Ochrabactrum</i> sp. Yw28 (DQ468103,1)	100%	<i>α-proteobacteria</i>	A; A10; A20
21	Uncultured <i>Rhizobiales</i> bacterium clone cv-B-04 (KF730289,1)	99%	<i>α-proteobacteria</i>	A; A10

A – Autoclaved, NA- Non-autoclaved, A5 – 5mM nitrate, A10- 10 mM nitrate, A20- 20 mM nitrate, A40- 40 mM nitrate

“-“- Unable to be assigned to a putative division

Figure 2.8 shows the phylogenetic tree of the phylotypes isolated from the non-autoclaved samples. *Brevundimonas* (Band 1) formed a clade with *Phenylobacterium* (Band 2), *Rhizobium* (Band 3), *Ochrobactrum* (Band 20) and *Mesorhizobium* (Band 13). *Bradyrhizobium* (Band 19) formed a clade with *Sphingomonas* (Band 16) and *Bacillus subtilis* (Band 10) formed a clade with *Bacillus flexus* (Band 11), and *Bacillus megaterium* (Band 8).

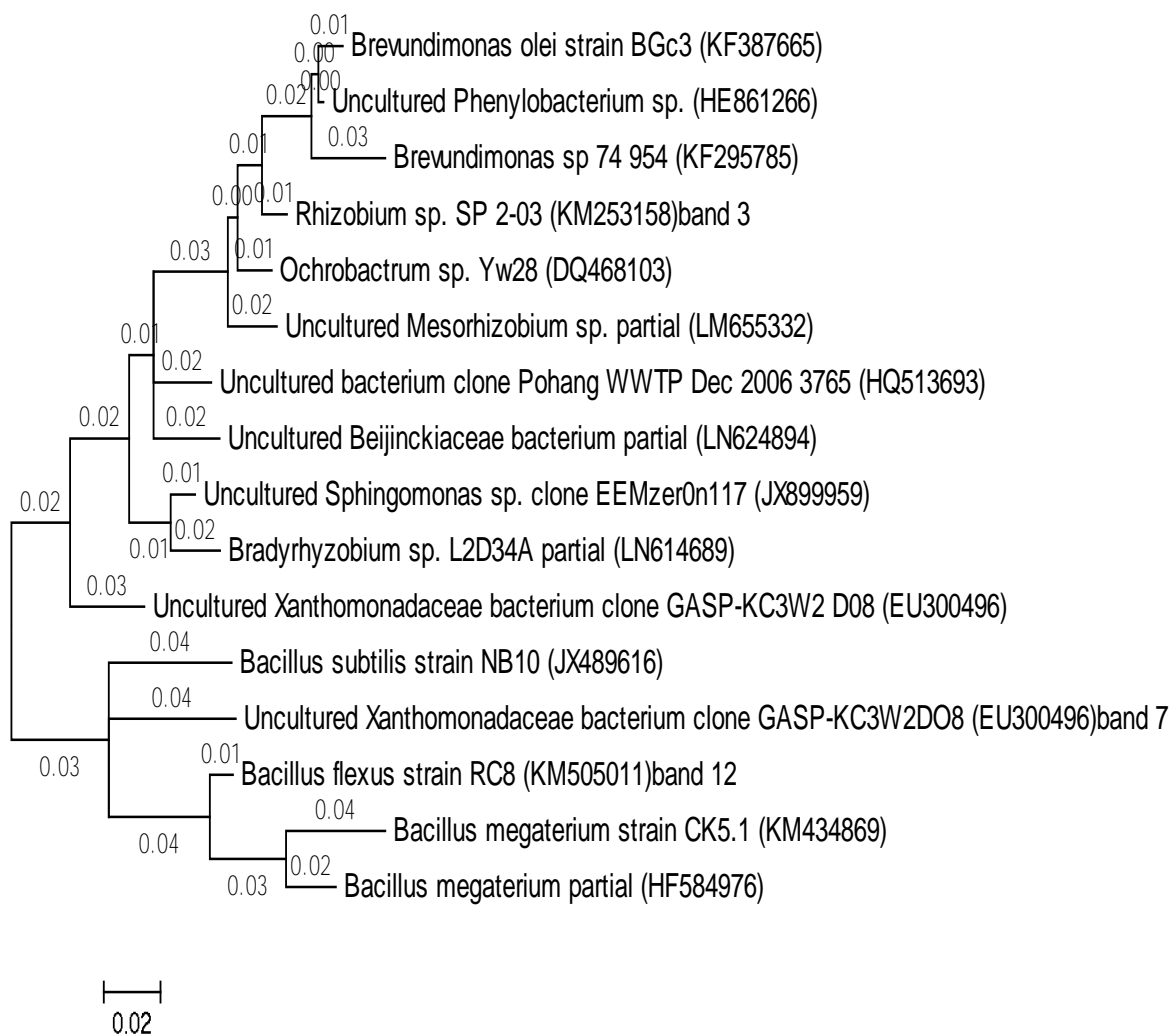


Figure 2.8: The phylogenetic tree generated using the Neighbour-Joining method for the non-autoclaved sample. The bootstrap consensus tree inferred from 500 replicates is taken to represent the evolutionary history of the taxa analysed. The tree is drawn to scale, with branch lengths in the same units as those of the evolutionary distances used to infer the phylogenetic tree. The evolutionary distances were computed using the Maximum Composite Likelihood method and are in the units of the number of base substitutions per site. Codon positions included were 1st+2nd+3rd+Noncoding. Phylogenetic analyses were conducted in MEGA 6

The phylogenetic tree of the phylotypes isolated from the various nitrate treated systems are shown in Figure 2.9. *Brevundimonas* (Band 1) formed a clade with *Phenylobacterium* (Band 2), *Rhizobium* (Band 3) and *Mesorhizobium* (Band 13). *Beijerinckeriaceae* (Band 18) formed a clade with *Sphingomonas glacialis* (Band 14) and *Bradyrhizobium* (Band 19). *Bacillus subtilis* (Band 10) formed a clade with *Bacillus flexus* (Band 11), *Bacillus megaterium* (Band 8) and *Xanthomonadaceae* (Band 4). These microorganisms were also demonstrated to be dominant in the non-autoclaved sample (Figure 2.9).

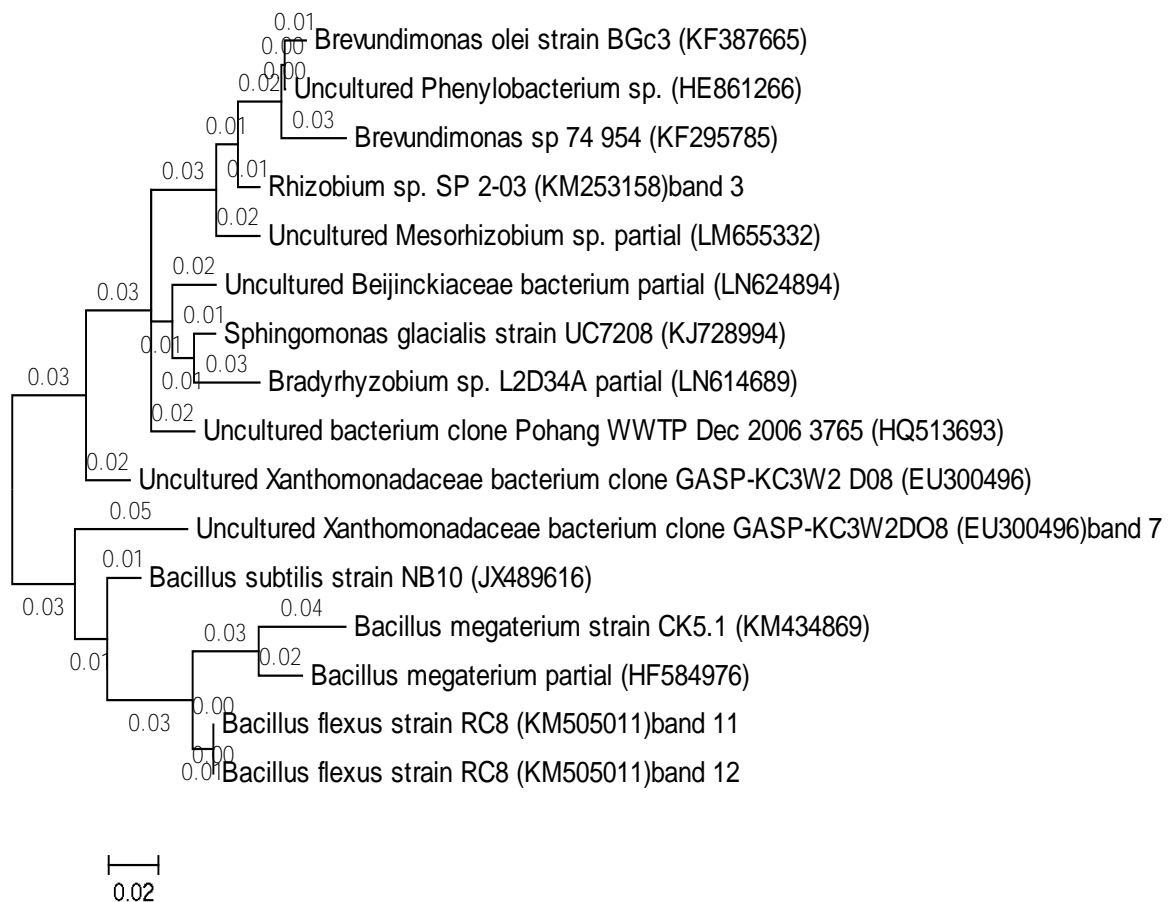


Figure 2.9: The phylogenetic tree generated using the Neighbour-Joining method for the nitrate samples. The bootstrap consensus tree inferred from 500 replicates is taken to represent the evolutionary history of the taxa analysed. The tree is drawn to scale, with branch lengths in the same units as those of the evolutionary distances used to infer the phylogenetic tree. The evolutionary distances were computed using the Maximum Composite Likelihood method and are in the units of the number of base substitutions per site. Codon positions included were 1st+2nd+3rd+Noncoding. Phylogenetic analyses were conducted in MEGA 6

2.4 Discussion

Biofilm formation on the surface of a metal may lead to the alteration of the electrochemical conditions at the metal-solution interface (Videla and Herrera, 2005). This leads to interactions between the metal surface, abiotic corrosion products, as well as the bacterial cells and their metabolites (Beech and Sunner, 2004). Alterations in the types and concentrations of ions, redox potential and pH values occur, leading to either acceleration or inhibition of corrosion. Thus, biofilm formation is key to Microbially Influenced Corrosion (MIC). Biofilm formation may contribute to biocorrosion through the formation of differential aeration/concentration cells, cathodic depolarisation, the degradation of passive films or corrosion inhibitors or the production of corrosive metabolites (Coetser and Cloete, 2005). Microorganisms typically exist as consortia in biofilms, and it has been shown that corrosion rates are much greater in the presence of mixed bacterial cultures than in pure cultures (Beech and Sunner, 2004).

Corrosion product formation involves a number of stages, including rapid pit formation, followed by a number oxygen diffusion rate controlled processes (Pillay and Lin, 2013). As corrosion products build up, oxygen diffusion to the surface slows down. Figure 2.1 shows the weight loss of the mild steel coupons after treatment with different concentrations of nitrate and nitrite. Nitrate treatment led to increased weight loss of the mild steel coupons. Higher concentrations of nitrate led to greater corrosion and weight loss. These observations were confirmed by SEM images which showed extensive corrosion product build up and biofilm formation in the nitrate treated systems. Previous studies have shown an increase in corrosion rate upon nitrate amendment of 5 mM (Pillay and Lin, 2013). The authors postulated that this increase was due to the additional nitrates stimulating the metabolic activities of the corrosive microorganisms. Nitrate reduction typically occurs at the base of the biofilm, where oxygen levels are low (Schwermer *et al.*, 2008). Here the nitrate (NO_3^-) is reduced to nitrite (NO_2^-), and then partly further reduced to nitrogen gas (N_2) and ammonium ion (NH_4^+), possibly as a protective mechanism from the toxic nitrite (Schwermer *et al.*, 2008). Furthermore, at the metal surface, nitrate reducers may use metallic iron and hydrogen gas as alternative sources of electron donors, thus further accelerating corrosion (Schwermer *et al.*, 2008). Schwermer *et al.* (2008) observed that although nitrate amendment resulted in a decrease in SRB activity, corrosion rate did not decrease and may even have increased, although the authors stated this could have been due to the chemical oxidation of metallic iron with nitrate.

Nitrite addition was shown to significantly decrease corrosion rate at concentrations of ≥ 10 , 20 and 40 mM, although corrosion was observed in the system supplemented with 5 mM nitrite. The addition of nitrite has also been shown to inhibit biocorrosion (Rempel *et al.*, 2006). Nitrite may provide a protective effect on the mild steel surface due to the formation of a passive protective layer, when used at concentrations high enough, known as the critical concentration. Below this critical concentration, incomplete passivation may occur, thus accelerating corrosion, as observed upon 5 mM nitrite amendment (Hayyan *et al.*, 2012). The protective layer is composed of an inner conductive Fe_3O_4 film, overlaid by an outer insulating Fe_2O_3 layer (Hayyan *et al.*, 2012). Furthermore, NR-SOB are able to reoxidise sulphide to elemental sulphur or sulphate, using nitrite (Rempel *et al.*, 2006). This results in the net removal of sulphide from the system when there are insufficient organic electron donors available to allow for reduction of all available nitrite. Nitrite also inhibits the enzyme dissimilatory sulphite reductase, which is responsible for the final enzymatic step in the sulphate reduction pathway. However, many SRB have the enzyme nitrite reductase that prevents this inhibition (Hubert *et al.*, 2005). Wen *et al.* (2011) observed that nitrite addition had a greater inhibitory effect on SRB growth and activity than the same concentration of nitrate. A concentration of 20 mM of nitrite was found to completely inhibit any observable corrosion. This corroborates results obtained by Hubert *et al.* (2005) who found that at higher concentrations of 20 mM of nitrite, SRB activity decreased, coupled with a decrease in corrosion rate. At lower concentrations of nitrite, SRB are able to overcome nitrite mediated inhibition.

An increase in protein and carbohydrate content occurred in the coupons treated with nitrate, with higher concentrations seen at week 12, before a decrease in both protein and carbohydrate observed (Tables 2.2 and 2.3). An increase in biofilm formation is observed through SEM, therefore an increase in protein and carbohydrate content is expected. Generally, EPS production is enhanced by the presence of inorganic nutrients such as nitrate (Rajaseker and Ting, 2011). It is still not known which component, be it protein or carbohydrate, plays a larger role in the binding of metal ions, and therefore in the corrosion process. Polysaccharides, a major component of the EPS, can crosslink to metal ions, thus forming a metal concentration cell which can accelerate corrosion (Lewandowski and Beyenal, 2008; Beech, 2004). This could result in the formation of ion concentration cells, thus further accelerating corrosion (Hubert *et al.*, 2005). Interactions occur between the metal ions and the functional groups of proteins and carbohydrates such as carboxyl, phosphate, sulphate, glycerate, pyruvate and succinate groups in the biofilm (Beech and Sunner, 2004). The EPS of a biofilm may also act as a nutrient source when nutrients are limiting

in the system (Pillay and Lin, 2013). This may explain the fluctuation in protein and carbohydrate content seen during the incubation period. No biofilm formation was observed in the nitrite treated coupons, as confirmed by the SEM images, therefore proteins and carbohydrates were undetected. This may explain the lack of corrosion observed in the nitrite treated coupons.

Microbial respiration within biofilms leads to the exclusion of oxygen from the metal surface at the base of the biofilm and the formation of differential aeration cells. This creates local anodic areas at the base of the biofilm, where metal dissolution occurs, and local cathodic areas around the biofilm base, where corrosion products formation occurs (Lee *et al.*, 1995). This leads to a process known as tuberculation. Tubercle formation is observed in the non-autoclaved system, as shown in Figures 2.2NA2 and NA3). A further sign of tuberculation is the formation of deep pits, seen in Figure 2.2AN2.

EDX compositions of the various corrosion products show that the main components of the corrosion products were iron and oxygen. These could indicate the activities of iron oxidising bacteria. Iron oxidisers thrive within the pH range of 6.0-8.0 (Pillay and Lin, 2013), within the pH range of the soil used in this study, although they can survive in more acidic or basic environments. The presence of thick, bulky, reddish brown deposits or rust coloured streaks, may indicate the presence of iron oxidising bacteria (IOB), which can lead to significant localised corrosion (Schiermeyer *et al.*, 2000). IOBs are microaerophilic and are often associated with other types of microorganisms in the aerobic environment (Coetser and Cloete, 2005). They often lead to the formation of differential aeration cells and form iron oxide deposits and tubercles (shown in Figure 2.2NA2 and NA3). The area under the tubercle is excluded from oxygen, and serves as an anode, where metal dissolution occurs, and the areas with access to oxygen serve as the cathode (Lin and Ballim, 2012).

An increase in manganese content was observed in corrosion product 4 (Table 2.4), possibly indicating the presence of manganese utilising bacteria. The oxidation of iron is often closely related to manganese oxidation (Rajaseker *et al.*, 2010), and is a widely distributed ability among the microbial community (Lewandowski and Beyenal, 2008). Metal oxides may also serve as terminal electron acceptors in bacterial respiration (Landoulsi *et al.*, 2008). Sulphur was only detected in corrosion product 2, possibly indicating SRB activity. Oxygen utilisation of oxygen by IOBs reduces the oxygen content at the base of the biofilm, which allow for the growth of

SRB (Emerson *et al.*, 2010). Indeed, IOB and SRB are often found in close association in the natural environment.

DGGE analysis was used to determine diversity of the microbial communities in the biofilm formed on the mild steel coupons and to determine dominant populations. Dominant bands in the gel were excised and sequenced. The microorganisms present were found to belong to 2 major phylogenetic divisions, namely the Firmicutes and the α -Proteobacteria (Table 2.5). A few species (*Bacillus subtilis* (Band 10), *B. flexus* (Band 12) *B. megaterium* (Band 9), *Rhizobium* (Band 3) and *Phenyllobacterium* (Band 2)) were observed growing on the coupons in the earlier periods of the study (Figure 2.10). The dominant species were the *Bacillus* species. This may indicate immature biofilms with limited bacterial diversity. These microorganisms were detected in all treatments, and, as these species are capable of EPS production, may be the primary colonisers in biofilm formation. The most common bacterial species identified were various *Bacillus* species. *Bacillus* species have previously been associated with corroded samples (Rajaseker *et al.*, 2010). These microorganisms are spore formers and show a wide range of physiological diversity, being capable of iron and manganese oxidation, acid production, as well as EPS production (Rajaseker *et al.*, 2010; Oliviera *et al.*, 2011). *Bacillus* species are able to use ions, such as Fe^{2+} , as electron donors (Rajaseker *et al.*, 2010). At low pH, several *Bacillus* species produce metal oxides, accelerating pitting of the metal (Oliviera *et al.*, 2011).

The non-autoclaved sample showed the development of a more diverse bacterial community in the latter stages of the experiment, with the appearance of bands associated with *Beijerinckiceae* and *Bradyrhizobium*. Different banding patterns and greater diversity were observed in the nitrate treated samples when compared to the non-autoclaved samples. Banding patterns amongst the different concentrations of nitrate were similar, suggesting that similar microorganisms, including *Brevundimonas* (Band 5), uncultured bacterium clone (Band 6), *Beijerinckiaceae* (Band 18), uncultured bacterium clone (Band 7), *Bacillus megaterium* (Band 9), and *Bacillus subtilis* (Band 10) were enriched for amongst the different concentrations of nitrate (Figure 2.7). Species such as *Sphingomonas*, *Brevundimonas*, *Bradyrhizobium*, *Rhizobium*, *Rhizobiales* and *Ochrabactrum*, were observed in the latter stages of the experiment in the nitrate treated samples, indicating development of a diverse microbial community in the biofilm sample (Figure 2.11). This could be due to the species needing time to adapt to the different treatments and reach numbers high enough to be detected. *Sphingomonas* has been identified in many different environments including terrestrial, freshwater marine and sediment systems, as well as

polluted environments, and have the ability to degrade pesticides, polyphenols and polycyclic aromatic hydrocarbons (PAHs) (Pillay and Lin, 2013). These microorganisms have been shown to be heavy metal tolerant and have been associated with the corrosion of copper water pipelines (Critchley *et al.*, 2004). *Brevundimonas* sp. are known to produce copious amounts of slime, which could aid in biofilm development and contribute to the corrosion process (Walter *et al.*, 2009). Rhizobia, including *Rhizobium*, *Bradyrhizobium* and *Rhizobiales* were detected in this study. The Rhizobia are a group of Gram-negative bacteria capable of nitrogen fixation and are commonly found in association with plant roots. Rhizobia have been shown to produce siderophores such as ferrichrome, that are able to capture iron ions (Wang *et al.*, 2014). This could affect the corrosion process. *Rhizobium* species, detected in the earlier stages of the study are able to produce copious amounts of EPS that facilitate their attachment to a wide range of biotic and abiotic surfaces. Optimum EPS production in *Rhizobium* was found to occur in the presence of carbohydrates as the carbon source and either ammonium salts such as ammonium nitrate or amino acids as the nitrate source. One can speculate that the presence of nitrate stimulated the production of EPS by the rhizobia, which exacerbated the corrosion process. *Bradyrhizobium*, detected in the latter stages of the study, are much slower growers than *Rhizobium*. *Bradyrhizobium* are able to utilise nitrate in the absence of oxygen, being capable of nitrate reduction to NH_4^+ and N_2 gas (Vairinhos *et al.*, 1989). Respiration by aerobic bacteria would provide a perfect niche for *Bradyrhizobium*, which would utilise the available nitrate in the absence of oxygen. *Ochrabactrum* are another group of bacteria commonly found in association with plant roots. These bacteria are capable of aerobic respiration and anaerobic denitrification as well as nitrate reduction and are able to produce large amounts of exopolysaccharides (Zuo *et al.*, 2008). This species has been shown to have exoelectrogenic activity, by the ability to transfer electrons from an outside source to an external electron acceptor. *Ochrabactrum* have been shown to reduce insoluble metals, such as ferric or manganic ions in the environment (Zuo *et al.*, 2008). It could be that the addition of nitrate stimulated the growth of *Ochrabactrum* species, which, due to their electron transfer abilities, were able to increase the corrosion rate.

SRB were not detected by DGGE analysis. This could be due to the inherent bias in DGGE analysis to detect only dominant microorganisms with a high number of cells. The presence of Bacillales, possible antagonists of SRB (Lopez *et al.*, 2006), may also be a factor. Furthermore, PCR based methods are highly susceptible to inhibition by contaminants purified with metagenomic DNA, such as metal ions, therefore only a part of the community is revealed (Lopez

et al., 2006). Techniques such as fluorescent *in situ* hybridisation, which detect metabolically active cells, may be more successful in detecting SRB.

This study showed that nitrate addition was unable to prevent the biocorrosion of mild steel coupons in loam soil, with higher nitrate concentrations leading to higher corrosion rates. Many studies report varying results with nitrate addition; however, many studies have used lower concentrations of nitrate (Pillay and Lin, 2013). Nitrite addition, however, was shown to prevent corrosion at higher concentrations, with 20 mM nitrite amendment found to be the optimal concentration. The use of nitrate and nitrite addition is still a relatively new, poorly understood technology. Many factors are involved in mild steel corrosion and the interaction between these factors is still not well documented. It is likely that nitrate and nitrite operate differently in various environments and their use in corrosion mitigation requires an individual approach in terms of the evaluation of the environment, the microbial population as well as the metal type.

Chapter 3: The Effect of Nitrite and Nitrate Supplementation on the Corrosion of Mild Steel Coupons in a Loam Soil System: An *in situ* Study

3.1 Introduction

Corrosion is an electrochemical reaction between metals and its environment, consisting of an anodic reaction and a cathodic reaction. The anodic reaction results in the dissolution of the metal, whereas the cathodic reaction results in the reduction of an external electron acceptor. Corrosion occurs immediately after immersion of a pure metal in a soil environment (Al-Judaibi and Al-Moubaraki, 2013). The study of the corrosion of metals is of great economic importance. The direct cost of metals corrosion in the USA alone in 2002 is estimated at 276 billion dollars (Jan-Roblero *et al.*, 2008).

All known materials, such as plastics, metals, minerals and organic materials, can be inhabited by microbes (Al-Judaibi and Al-Moubaraki, 2013). Biocorrosion may occur when microorganisms inhabit the surfaces of metals, forming a biofilm. Biofilms allow microorganisms to alter the electrochemical conditions at the metal surface, thereby contributing to the corrosion process.

Soil represents a very attractive environment for microorganisms, which can grow over a wide range of environmental conditions. Microorganisms have been implicated in the deterioration of many metals, such as iron, copper, aluminium as well as alloys (Oliviera *et al.*, 2011). It is estimated that approximately 50% of underground pipes and structures deteriorate due to the actions of microorganisms (Bano and Qazi, 2011).

Microbially Influenced Corrosion does not involve any new mechanisms of corrosion, rather the presence and activities of microorganisms lead to conditions at the metal surface not normally favoured in similar conditions (Bano and Qazi, 2011). The main microorganism associated with corroding metal structures are the sulphate reducing bacteria, sulphur, iron and manganese oxidisers, extracellular slime producers and acid producers. Studies have derived various individual mechanisms at which these microbes promote the corrosion processes (Videla and Herrera, 2005). Most studies have focussed on the effect of pure cultures on corrosion. Microorganisms in nature, however, occur in complex naturally occurring consortia. It has been shown that greater corrosion rates occur in the presence of microbial consortia in which many physiologically distinct bacteria interact in complex ways when compared to pure cultures (Pope *et al.*, 1984).

In many industries, the use of biocides is commonly used to control growth of SRB and H₂S production (Schwermer *et al.*, 2008). Sulphide produced by SRB is known to react with ferrous

irons, yielding ferrous sulphide, which forms an adhesive film over the metal surface. Ferrous sulphide has been shown to promote further corrosion, and can act as a cathode. However, ferrous sulphide may also have a passivating effect on the metal surface (Valencia-Cantero *et al.*, 2003). The use of biocides to prevent SRB mediated sulphide production is, however, very expensive, and is only effective for a short time, as bacterial biofilms eventually develop resistance to the biocides used (Telang *et al.*, 1997). Biocides are also environmentally toxic (Lin and Ballim, 2012).

Nitrate addition has been proved to be an effective alternative to biocide use (Kumaraswamy *et al.*, 2010). Nitrate addition stimulates the growth of nitrate reducing bacteria (NRB) and inhibits SRB activity. Field trials have reported significant reduction in sulphide levels and corrosion rate upon nitrate addition (Voordouw *et al.*, 2002). MacInerney *et al.* (1993) reported that the addition of ammonium nitrate to an injector led to a 40-60% reduction in sulphide levels, that the authors attributed to the activities of indigenous NRB.

Nitrite addition also constitutes a simple compound that has been used to combat MIC and reduce SRB activity (Sturman and Goeres, 1999). Nitrite is a specific inhibitor of SRB activity, as it prevents the action of the enzyme dissimilatory sulphite reductase, which is responsible for the final enzymatic step in the sulphate reduction pathway (Hubert *et al.*, 2005). Nitrite is also an inhibitor of the anodic reaction by encouraging the formation of a passive layer on the metal surface (Karim *et al.*, 2010).

The previous chapter demonstrated that nitrate addition led to an increase in corrosion rate under laboratory conditions, while 20 mM nitrite supplementation led to a significant decrease in corrosion rate. This study focuses on the effectiveness of nitrite and nitrate supplementation on the corrosion of mild steel coupons in loam soil *in situ*. The microbial population dynamic on the biofilm of mild steel coupons was also investigated.

3.2 Materials and Methods

3.2.1 Soil Sample Collection and Preparation of Mild Steel Coupons

Soil sample collections and preparation of mild steel coupons has been described in Section 2.2, Chapter 2.

3.2.2 *In situ* Experiment: Construction of Loam Soil System Supplemented with Nitrate and Nitrite

Six divisions containing 20 kg of loam soil each were set up and subjected to different nutrient conditions. The experimental setup consisted of a 2m×3m wooden enclosure, divided into 6 1m×1m divisions, each containing the variously treated loam soil. The divisions were underlaid with plastic, so as to prevent seepage of moisture and possible mixing of soils from the different treatments. Autoclaved loam soil was used as the control. The remaining 5 setups consisted of non-autoclaved loam soil, autoclaved and non-autoclaved loam soil supplemented with nitrite and nitrate (200 ml with a final concentration of 20 mM) (determined in Chapter 2 to be the minimal concentration required for complete corrosion inhibition of mild steel). The loam soil was shielded from precipitation but was otherwise subjected to the external environmental conditions. The coupons were buried 5 cm below the surface of the loam soil and incubated for a total of 24 weeks, with sampling occurring every 4 weeks. Corrosion was enhanced by the addition of 200 ml of distilled water at each sampling time (Aung and Tan, 2004).

At each sampling time, coupons were removed in triplicate, treated and weighed as described in Section 2.2.3 in Chapter 2.

3.2.3 Carbohydrate and Protein Analysis from Biofilms of Coupon Surface

The carbohydrate content within the biofilm formed on the mild steel surface was determined using the methodology described in Section 2.2.4 and calculated using standard D-glucose curves.

Protein content on the mild steel surface was determined using the method described in chapter 2.2.4 and calculated using standard bovine serum albumin curves.

3.2.4 Scanning Electron Microscopy (SEM) and Electron Dispersive X-Ray (EDX) Analysis of the Coupon Surface

The mild steel coupons were subjected to chemical fixation and were examined using the FEG SEM equipped with a Bruker EDX detector as described in Section 2.2.5.

3.2.5 Microbial Population Analysis of Biofilm on Corroded Mild Steel Coupons Using Denaturing Gradient Gel Electrophoresis (DGGE)

3.2.5.1 DNA Extraction and Amplification of 16S rDNA

The biofilm sample was scraped off the coupon surface using a sterile surgical blade, and DNA extracted and amplified as described in Section 2.2.6.1.

3.2.5.2 Denaturing Gradient Gel Electrophoresis Analysis

After amplification of the 16S rDNA was confirmed, touchdown PCR was performed with the primers 357F with a 25 bp GC clamp at the 5' end and the universal primer 518R.

The samples were then subjected to DGGE analysis as described in Section 2.2.6.2.

3.2.5.3 DNA Sequencing and Phylogenetic Analysis of DGGE Bands

DNA was extracted from the biofilm on the surface of the mild steel coupons and amplified and separated as described in Sections 2.2.6.1 and 2.2.6.2. Selected DGGE bands were excised using a sterile surgical blade and subjected to PCR amplification according to Ye *et al.* (2009). The excised bands were eluted in 100 µl of millipore water and incubated overnight at 4 °C. Thereafter, the bands were spun down at 10000 rpm for 5 min. The upper layer was extracted and used as the template. The amplified products were sequenced and identified and phylogenetic relationships determined as described in Section 2.2.6.3.

3.2.6 Statistical Analysis

Data were analysed using GraphPad InStat for windows (version 3.10). A one-way ANOVA was used to test mean differences in weight losses of the metal coupons over time. A p-value of <0.05 was considered statistically significant.

3.3 Results

3.3.1 Physical characterisation of loam soil

Table 3.1 shows the physical characteristics of loam soil. The loam soil used in this study was fairly neutral (pH 6.75) and had a moisture content of 8.46%.

Table 3.1: Physical characteristics of soil used in *in situ* study

	Loam soil
pH	6.75
Percentage water content	8.46%
Percentage dry mass	91.54%

3.3.2 Weight loss measurements of mild steel coupons in a loam soil system

Similar to the coupons in Chapter 2, reddish brown as well as black depositions were observed on the surface, attributed to $\text{Fe}(\text{OH})_3$ and Fe_3O_4 , respectively. The weight loss measurements of mild steel coupons immersed in a stimulated loam soil system *in situ* are shown in Figure 3.1. Corrosion rate determined *in situ* was much lower than those observed in the laboratory experiments (Figure 2.1). Weight loss of the mild steel coupons remains relatively constant over the incubation period in both the autoclaved and non-autoclaved systems, with no significant increase over time. Coupons incubated in the autoclaved system did not undergo much weight loss, with maximum weight loss observed to be 3.33 mg/cm^2 . The coupons incubated in the non-autoclaved system demonstrated slightly higher corrosion rates when compared to the autoclaved system, however, this difference was not significant. A maximum corrosion rate of 3.85 mg/cm^2 was observed in the non-autoclaved system.

Supplementation with nitrite led to a slight decrease in corrosion rate compared to the autoclaved and non-autoclaved control, however, this difference was not significant. No significant increase in corrosion was observed over time in the nitrite treated systems. Maximum weight loss in the mild steel coupons in the autoclaved system supplemented with nitrite was observed to be 2.56 mg/cm^2 , a decrease when compared to the autoclaved control of 3.33 mg/cm^2 . No significant difference was observed between the autoclaved and non-autoclaved systems supplemented with nitrite, however, a higher maximum corrosion rate was observed in the non-autoclaved system of 2.82 mg/cm^2 when compared to the autoclaved system of 2.56 mg/cm^2 in the nitrite supplemented systems. Again, a non-significant decrease in the non-autoclaved nitrite supplemented system was observed when compared to the non-autoclaved system.

The autoclaved system supplemented with nitrate showed a significant increase ($p < 0.05$) in weight loss of the mild steel coupons when compared to the autoclaved non-supplemented and nitrite treated systems. An increase in weight loss was observed with time. A maximum corrosion rate of 45.38 mg/cm^2 was demonstrated. The non-autoclaved nitrate supplemented system also demonstrated a significantly greater mild steel weight loss ($p < 0.05$) when compared to the non-

autoclaved non-supplemented and nitrite supplemented systems. Corrosion rate increased with time and a maximum corrosion rate of 44.87 mg/cm^2 was demonstrated. No significant difference was observed between the autoclaved and non-autoclaved nitrate treated systems.

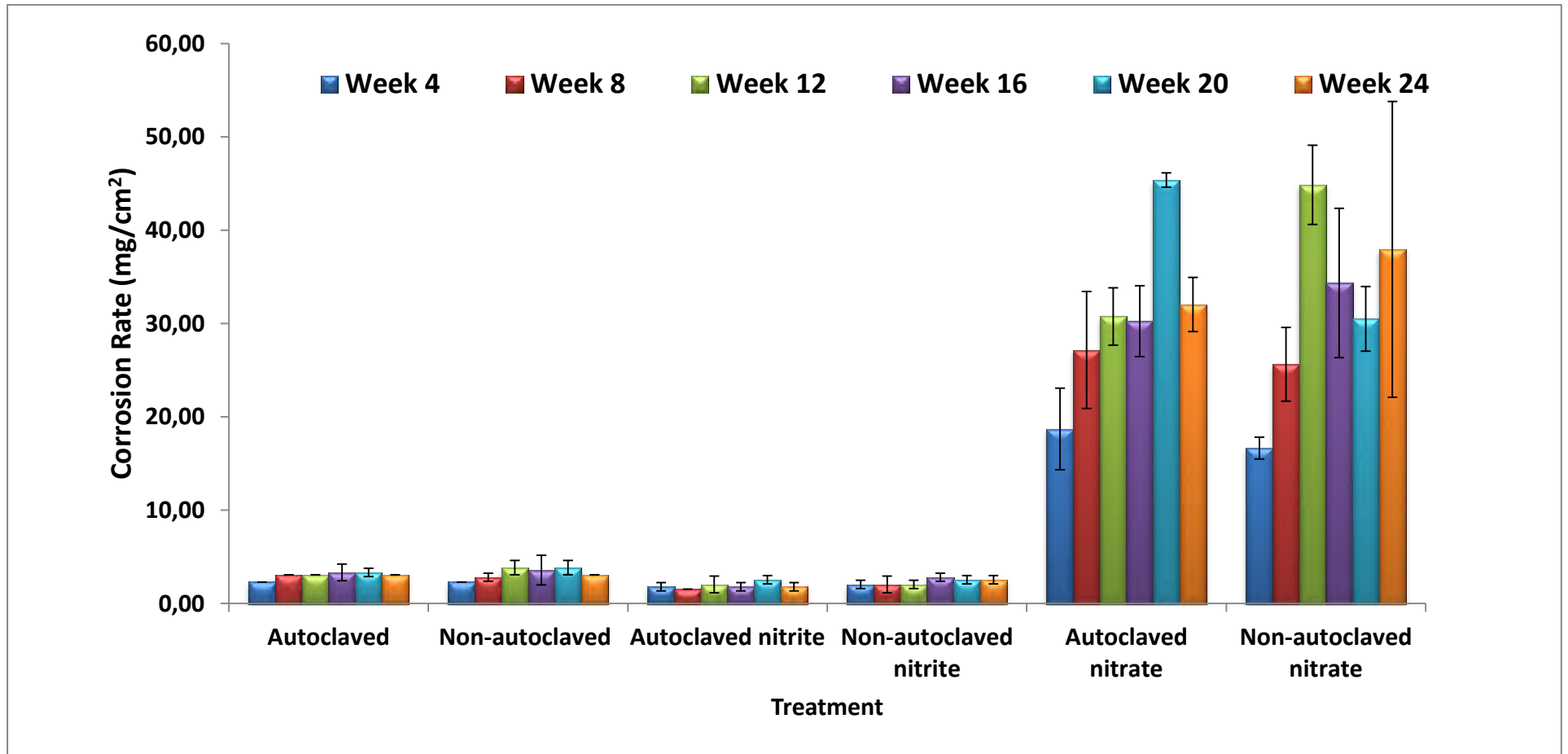


Figure 3.1: Weight loss of mild steel coupons conditions over a period of 24 weeks. Coupons were incubated *in situ* in loam soil containing 20 mM of nitrate and nitrite.

3.3.3: Protein and carbohydrate content of the biofilm on the surface of the mild steel coupon

The protein concentrations of the biofilm formed on the surface of the mild steel coupons are shown in Table 3.2. No detectable protein was observed in the autoclaved and non-autoclaved systems without supplementation over the entire 24 week period, nor in the nitrite treated systems. The autoclaved system treated with nitrate showed an increase in protein from week 4 (2.56 mg/ml) to week 8 (6.53 mg/ml), thereafter a decrease is seen at week 12 (1.28 mg/ml). An increase in protein content was then observed with maximum protein content demonstrated at week 24 (8.76 mg/ml). The non-autoclaved system supplemented with nitrate showed an increase in protein content from week 4 (3.58 mg/ml) to week 8 (4.28 mg/ml). A decrease was then observed at week 12 (2.42 mg/ml). Protein content remained relatively constant between weeks 16 to 24 with highest protein content demonstrated at week 16 (8.79 mg/ml). A medium positive correlation ($r = 0.62$; $p < 0.01$) was observed between corrosion rate and protein concentration in the autoclaved sample, however, no correlation was observed in the non-autoclaved sample.

Table 3.2: Total protein concentration (mg/ml) in biofilm samples extracted from mild steel coupons in loam soil over a period of 24 weeks

	Total protein content (mg/ml) of the biofilm					
	Week 4	Week 8	Week 12	Week 16	Week 20	Week 24
Autoclaved	u.d.	u.d.	u.d.	u.d.	u.d.	u.d.
Non-autoclaved	u.d.	u.d.	u.d.	u.d.	u.d.	u.d.
Autoclaved nitrite	u.d.	u.d.	u.d.	u.d.	u.d.	u.d.
Non-autoclaved nitrite	u.d.	u.d.	u.d.	u.d.	u.d.	u.d.
Autoclaved nitrate	2.56	6.53	1.28	3.89	7.89	8.76
Non-autoclaved nitrate	3.58	4.28	2.42	8.79	7.37	8.38

u.d.: undetectable

The carbohydrate concentrations of the biofilm formed on the surface of the mild steel coupons immersed in the stimulated loam soil system are shown in Table 3.3. No detectable carbohydrate was observed in the non-supplemented autoclaved and non-autoclaved systems, nor in the nitrite

treated systems over the 24 week incubation period. Carbohydrate content in the autoclaved system treated with nitrate was found to increase from week 4 (8.56 mg/ml) to week 12 (9.56 mg/ml). A decrease was seen at week 16 (7.45 mg/ml), thereafter carbohydrate content increased significantly to a maximum observed at week 24 (15.68 mg/ml). A similar trend was demonstrated in the non-autoclaved system treated with nitrate. An increase was observed from week 4 (7.48 mg/ml) to week 12 (10.47 mg/ml). Thereafter, a decrease was observed at week 16 (8.97 mg/ml). An increase was then demonstrated to maximum carbohydrate content at week 24 (20.32 mg/ml). Strong positive correlations between corrosion rate and the carbohydrate content ($r=0.79$; $p<0.01$), and between the protein and hydrocarbon content ($r=0.70$; $p<0.01$) were found in the autoclaved sample. A strong correlation between the protein and hydrocarbon contents ($r=0.70$; $p<0.01$) was observed, but none with the corrosion rates in the non-autoclaved sample.

Table 3.3: Total carbohydrate concentration (mg/ml) in biofilm samples extracted from mild steel coupons in loam soil over a period of 24 weeks

	Total carbohydrate content (mg/ml) of biofilm					
	Week 4	Week 8	Week 12	Week 16	Week 20	Week 24
Autoclaved	u.d.	u.d.	u.d.	u.d.	u.d.	u.d.
Non-autoclaved	u.d.	u.d.	u.d.	u.d.	u.d.	u.d.
Autoclaved nitrite	u.d.	u.d.	u.d.	u.d.	u.d.	u.d.
Non-autoclaved nitrite	u.d.	u.d.	u.d.	u.d.	u.d.	u.d.
Autoclaved nitrate	8.56	8.22	9.56	7.45	12.48	15.68
Non-autoclaved nitrate	7.48	9.58	10.47	8.97	15.16	20.32

u.d.: undetectable

3.3.4 Scanning Electron Microscopy and Electron Dispersive X-ray analysis of Corroded mild steel coupons in an *in situ* loam soil system

3.3.4.1 Scanning Electron Microscopy

Observations of the mild steel coupons immersed in the loam soil system over a 24 week period were conducted using SEM. Figure 3.2 shows the SEM image of mild steel coupons incubated in the autoclaved and non-autoclaved systems after 4, 8 and 20 weeks of incubation. The autoclaved control displayed no microbial growth over the course of the 24 week incubation period, however, corrosion product formation was observed to a small degree. The formation of nodules was observed at week 4, indicated by the arrow (Figure 3.2 A1). At week 8, a heterogeneous layer of corrosion products was observed to cover the surface of the coupon. Towards the end of the incubation period, the formation of deep pits and cracks on the surface is seen to occur, surrounded by corrosion products, as shown in Figure 3.2 A3. Microbial growth was not detected in the non-autoclaved system as well, however, the formation of various tubercles, indicative of microbial activity, was observed over the course of the incubation period (Figure 3.2 NA1, NA2, NA3).

Figure 3.3 shows the surface of the autoclaved and non-autoclaved systems treated with nitrite. Neither microbial activity nor corrosion product formation is observed in the autoclaved and non-autoclaved systems treated with nitrite. Significant corrosion products are not observed in either the autoclaved or non-autoclaved systems throughout the incubation period, in contrast to the non-supplemented systems, however, light corrosion product formation was observed as well as the early phases of pitting corrosion.

Figure 3.4 shows the surface of the coupons incubated in autoclaved and non-autoclaved loam soil supplemented with nitrate. Corrosion was found to be much more severe and occurred at a much higher rate when compared to the non-supplemented and nitrite treated systems, with abundant biofilm growth also observed. At week 4, severe corrosion in the form of deep cracks, as well as sponge-like corrosion product formation, was already seen in the autoclaved system, although microbial growth is not displayed. This corrosion was found to cover the entire surface of the coupon by week 8, in which a thick, heterogeneous layer of corrosion products was observed. Week 20 displayed abundant biofilm growth in the form of cocci shaped bacteria. Corrosion products were found to be interspersed within the biofilm matrix. The non-autoclaved system supplemented with nitrate displayed very similar characteristics when compared to the

autoclaved nitrate treated system. At week 4, spindle-like corrosion product formation as well as deep cracks in the surface are observed although no microbial growth was seen. However, at week 8, abundant non-uniform biofilm formation is demonstrated by the presence of numerous rod shaped bacteria. The bacterial cells were found to be surrounded by corrosion products. As with the autoclaved system, by week 20, severe biofilm and corrosion product formation was found to cover the entire surface of the coupon.

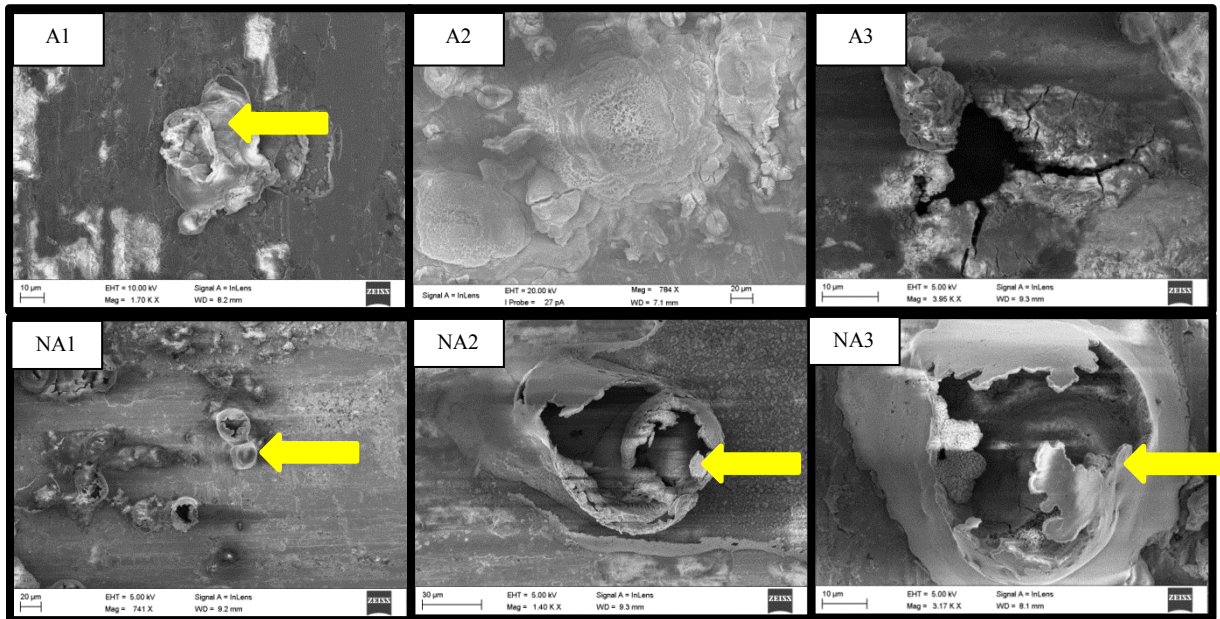


Figure 3.2: Some typical examples of SEM images of the surface of mild steel coupons in a stimulated loam soil system after various weeks of incubation. (A1, A2, A3) – Autoclaved system after 4, 8 and 20 weeks, respectively; (NA1, NA2, NA3) – Non-autoclaved system after 4, 8 and 20 weeks, respectively.

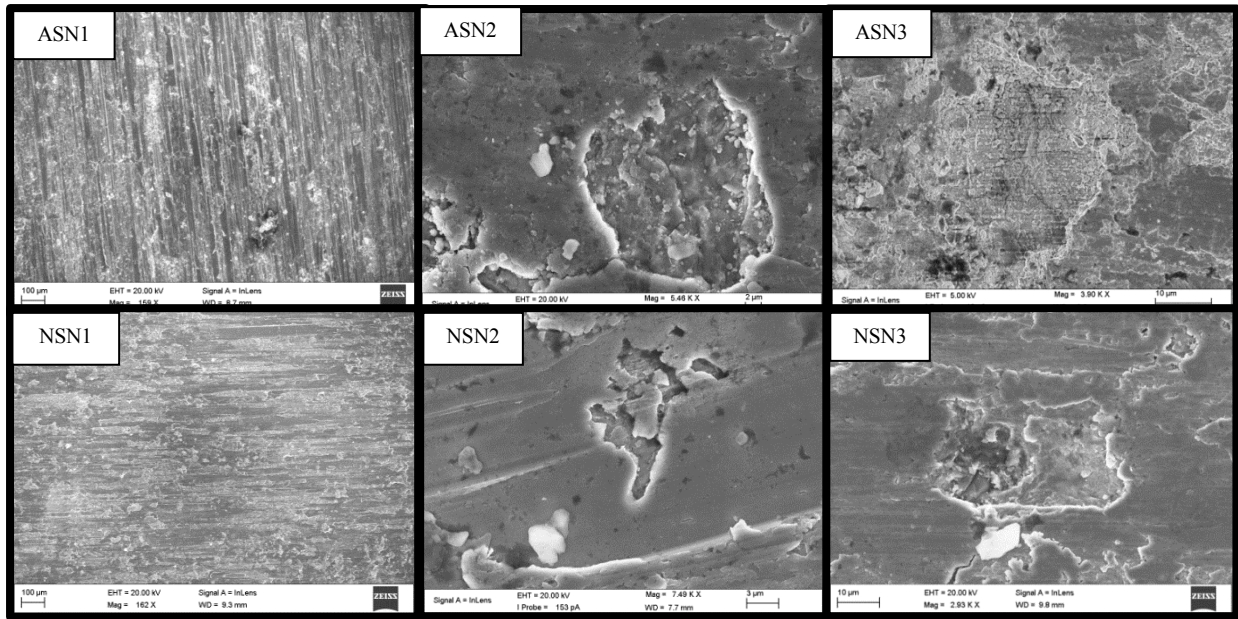


Figure 3.3: Some typical examples of SEM images of the surface of mild steel coupons in a stimulated loam soil system after various weeks of incubation. (ASN1, ASN2, ASN3) – Autoclaved system supplemented with 20 mM nitrite after 4, 8 and 20 weeks, respectively; (NSN1, NSN2, NSN3) – Non-autoclaved system supplemented with 20 mM nitrite after 4, 8 and 20 weeks, respectively

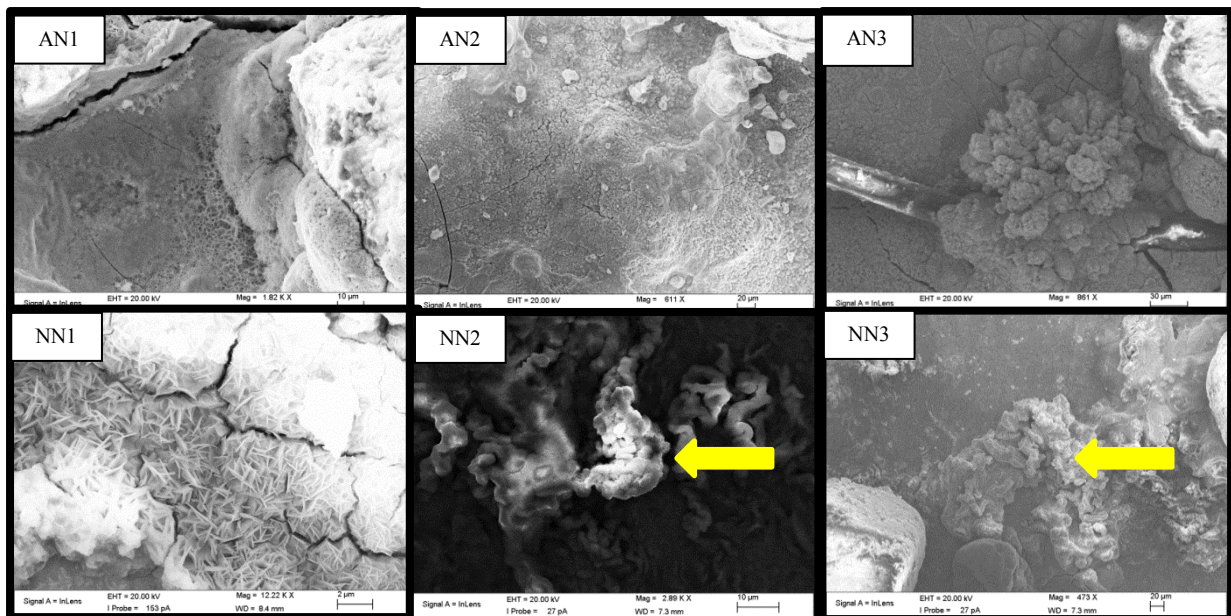


Figure 3.4: Some typical examples of SEM images of the surface of mild steel coupons in a stimulated loam soil system after various weeks of incubation. (AN1, AN2, AN3) – Autoclaved system supplemented with 20 mM nitrate after 4, 8 and 20 weeks, respectively; (NN1, NN2, NN3) – Non-autoclaved system supplemented with 20 mM nitrate after 4, 8 and 20 weeks, respectively

3.3.4.2 Energy Dispersive X-ray analysis of mild steel coupons

The different corrosion products formed on the surface of both the untreated and treated mild steel coupons were examined using EDX analysis for their elemental composition as described in Section 2.3. The various different types of corrosion products analysed amongst all systems are shown in Figure 3.5, and the elemental composition of these corrosion products is shown in Table 3.3.

The untreated mild steel coupon was mainly composed of iron (88.22 %), carbon (4.87 %), and oxygen (3.53 %), with trace amounts of manganese, fluorine, aluminium, and silicon (0.2%, 1.78%, 0.4% and 1.01% respectively) also present. All corrosion products were composed of varying percentages of iron and oxygen, indicating the occurrence of iron oxidation, as well as carbon, with varying degrees of trace minerals also present.

Corrosion product 1 (IC1) was a biofilm detected in the autoclaved nitrate treated system, with corrosion products interspersed within the biofilm. IC1 mainly consisted of 61.84 % iron and 30.84% oxygen, with increased amounts of carbon (5.22%) compared to the untreated coupon. Trace amounts of Mn, K, Ca, Ti, Cr, Co, Cu and Ta were also detected but were absent on the untreated coupon surface.

Corrosion product 2 (IC2) was a thin, tightly adhered corrosion product detected in the non-autoclaved control. IC2 was observed to be composed of 61.53 % iron and 32.43 % oxygen, similarly to IC1, however, lower amounts of carbon were present (3.27 %) when compared to IC1 and the untreated coupon surface. Mn was not detected in IC2, however, trace amounts of Si, Ca, Co, Ni, Br and Tb were detected.

Corrosion product 3 (IC3) was a sponge-like, porous, thick, voluminous corrosion product detected on the surface of the non-autoclaved mild steel coupon surface. It was found to contain a similar elemental composition to IC2, with iron (59.49%), oxygen (35.56%), carbon (3.66%) and Si (0.63%) detected in similar amounts. IC3, however, contained Mn (0.07%), as well as higher amounts of Co and Ni and trace amounts of Ca.

Corrosion product 4 (IC4) was detected in the coupons incubated in the autoclaved loam soil. It consisted of spindle shaped corrosion products arranged in a manner resembling a cotton-ball

structure. IC4 contained the highest oxygen content (41.13%) and lowest iron content (50.56%) when compared to the other corrosion products examined. However, the carbon content (4.69%) was similar to the untreated mild steel surface. An increase in manganese content (2.9%) was observed in IC4, possibly indicating the activities of metal reducing bacteria. Phosphorous was detected in trace amounts (0.09%), which could indicate the presence of microbial cells. Trace amounts of Ca and Si were also observed in IC4.

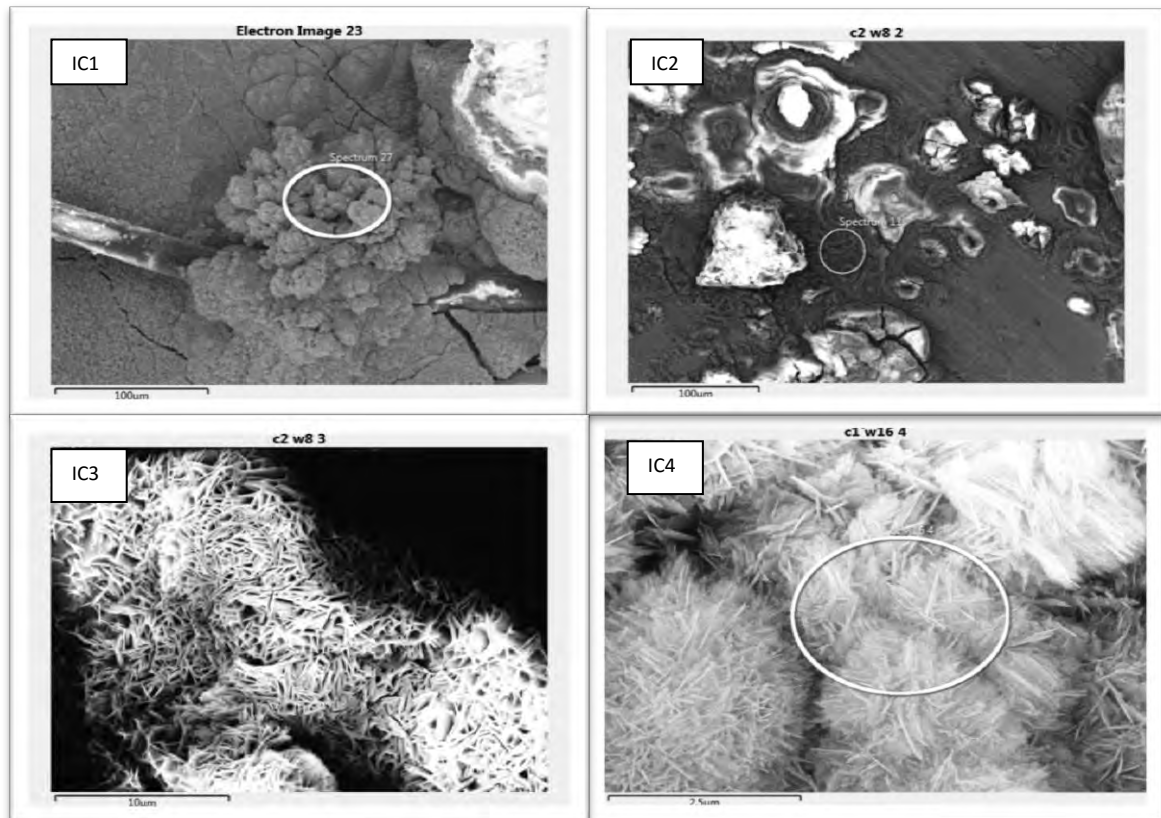


Figure 3.5: Corrosion products investigated using EDX analysis. IC1- Corrosion product 1 (Autoclaved 20 mM nitrate supplemented system- week 12), IC2- corrosion product 2 (Non-autoclaved system- week 8), IC3- corrosion product 3 (Non-autoclaved system- week 8), IC4- corrosion product 4 (Autoclaved-system- week 16).

Table 3.4: Elemental composition of different corrosion products formed on the surface of the treated and untreated mild steel coupons analysed by EDX analysis

	Sample				
	Untreated Coupon	Corrosion product 1	Corrosion product 2	Corrosion product 3	Corrosion product 4
Element	Wt%				
Fe	88.22	61.84	61.53	59.49	50.56
O	3.53	30.84	32.43	35.56	41.13
C	4.87	5.22	3.27	3.66	4.69
Mn	0.2	0.15	-	0.07	2.9
F	1.78	-	-	-	-
Al	0.4	0.06	-	-	-
Si	1.01	0.17	0.63	0.63	0.22
K	-	0.13	-	-	-
Ca	-	0.13	0.49	0.2	0.41
Ti	-	0.07	-	-	-
Cr	-	0.16	-	-	-
Co	-	0.16	0.18	0.32	-
Cu	-	0.16	-	-	-
Ni	-	-	0.06	0.08	-
Ta	-	0.7	-	-	-
Br	-	-	0.31	-	-
Tb	-	-	0.1	-	-
P	-	-	-	-	0.09

Samples: Corrosion product 1 (Autoclaved 20 mM nitrate supplemented system- week 12), Corrosion product 2 (Non-autoclaved system- week 8), Corrosion product 3 (Non-autoclaved system- week 8), Corrosion product 4 (Autoclaved-system- week 16)

3.3.5 DGGE analysis of biofilm communities on corroded mild steel coupons and phylogenetic affiliation of dominant bacteria

Total DNA was extracted from the biofilm formed on the surface of the mild steel coupons in the various treated and non-treated systems, amplified and separated using DGGE as described in Section 2.5. No discernible biofilm was detected on the surface of the nitrite treated systems throughout the study period; therefore the nitrite treated coupons were excluded from the rest of the study. DGGE amplicons generated multiple bands from the DNA extracts from the mild steel coupons over the 24 week sampling period. The number of individual bands is representative of the number of bacterial species present in the sample. Limited bacterial diversity was present on the mild steel surface in both control, nitrite and nitrate treated systems. However, community complexity increased with time. Many bands were shared amongst the different samples.

Similarities and putative identification of the bands excised over the 24 week period are shown in Table 3.4. A total of 14 sequenced bands showed high sequence homology with known database sequences. However, 5 of these sequences showed high sequence similarity to uncultured bacteria. Taxonomic classification of the sequence data (Table 3.4) showed that the bacterial diversity exhibited phylotypes belonging to 3 major distinct phylogenetic groups, the Firmicutes, α -Proteobacteria, and γ -Proteobacteria, with the remaining classified as uncultured bacteria. Dominant species were found to differ between the nitrate-treated systems and the autoclaved and non-autoclaved systems.

Figure 3.6 displays the banding patterns of the biofilm formed on the surface of the mild steel coupons in the autoclaved, non-autoclaved and nitrate treated systems over the first 12 weeks of the study. The dominant taxa in the non-supplemented systems were found to vary at each sampling time, however, the dominant taxon in the nitrate treated systems was found to be *Bacillus subtilis* (Band 25). The autoclaved system displayed no bands over the first 12 weeks, whereas the autoclaved nitrate treated system displayed no bacterial diversity at weeks 4 and 8, with only one band, Band 7 being detected at week 12, corresponding to an uncultured bacterium. The non-autoclaved systems displayed greater bacterial diversity when compared to the autoclaved systems. Many bands were shared amongst the non-autoclaved non-supplemented and non-autoclaved nitrate treated system. Bands corresponding to uncultured bacteria (Band 7 and Band 27), *Ochrabactrum* (Band 20), uncultured *Shigella* (Band 23) *Solibacillus silvestris* (Band 24) and *Bacillus subtilis* (Band 25) were detected in the non-autoclaved system in the first 12 weeks of the study, with the dominant bands varying between uncultured bacteria at weeks 4 and 8 (Band 20 and Band 27, respectively) to *Bacillus subtilis* at week 12. The non-autoclaved

nitrate treated system also displayed bands showing similarity to *Ochrabactrum*, *Solibacillus silvestris* (Band 24), *Bacillus subtilis* (Band 25), however, *Bacillus aryabhatai* (B and 22) was detected at week 4, as well as an uncultured bacterium (Band 26) at week 8. *Bacillus subtilis* remained the dominant phylotype within the first 12 weeks of the study.

Increased bacterial diversity was observed over the latter 12 weeks of the study amongst all systems when compared to the earlier 12 weeks, as shown in Figure 3.7, which displays the banding patterns of the biofilm formed on the mild steel coupons over weeks 16, 20 and 24. Many phlotypes were found amongst all systems, particularly, *Bacillus subtilis* (Band 25), *Bacillus megaterium* (Band 28), uncultured *Porphyrobacter* (Band 30), uncultured *Xanthomonadaceae* (Band 31) and an uncultured bacterium (Band 32). The autoclaved system also displayed bands corresponding to 2 uncultured bacteria (Band 7 and Band 23). Similar bands were detected in the autoclaved nitrate treated system when compared to the autoclaved system, however, *Bacillus aryabhatai* (Band 22) was also detected. *Bacillus subtilis* was determined to be the dominant taxon in the autoclaved nitrate treated system. The non-autoclaved system displayed greater bacterial diversity when compared to the remaining systems. Bands corresponding to *Bacillus aryabhatai* (Band 22), *Solibacillus silvestris* (Band 24), *Rhizobium* (Band 29) and uncultured bacteria (Band 26 and Band 27) were detected, however, the dominant taxa varied per sampling time, with *Bacillus aryabhatai* and *Bacillus megaterium* dominant at weeks 16 and 20, respectively, and *Solibacillus silvestris*, *Rhizobium* and uncultured *Porphyrobacter* dominant at week 24. The non-autoclaved nitrate treated system displayed lower bacterial diversity when compared to the non-autoclaved non-supplemented system. *Rhizobium* (Band 29) and uncultured bacterium (Band 7) were detected, however, the dominant taxon was found to be *Bacillus subtilis* (B25).

Table 3.5: Partial 16S rDNA sequence similarity of the excised bands on DGGE profiles over the 24 week period

Band	THE CLOSEST SEQUENCES (GENBANK NUMBER)	SIMILARITY	PUTATIVE DIVISION	SAMPLE PRESENT
7	Uncultured bacterium clone ncd2550a03c1 (JF224543)	84%	-	A; NA; AN;
20	<i>Ochrobactrum</i> sp. Yw28 (DQ468103,1)	100%	<i>α-proteobacteria</i>	NA; NN
22	<i>Bacillus aryabhatai</i> partial (LN650466,1)	98%	Firmicutes	NA; AN; NN;
23	Uncultured <i>Shigella</i> sp. clone C307 (JF833742)		<i>γ-proteobacteria</i>	A; NA;
24	<i>Solibacillus silvestris</i> strain CM3HG10 (KM277365,1)	93%	Firmicutes	NA; NN;
25	<i>Bacillus subtilis</i> strain NB10 (JX489616,1)	79%	Firmicutes	A; NA; AN, NN
26	Uncultured bacterium clone ncd94b04c1 (HM256679,1) band 26	79%	-	NA; NN;
27	Uncultured bacterium clone ncd94b04c1 (HM256679,1) band 27	79%	-	NA;
28	<i>Bacillus megaterium</i> strain CK5.1 (KM434869) band 28	88%	Firmicutes	A; NA; AN, NN
29	<i>Rhizobium</i> sp. SP 2-03 (KM253158)	96%	<i>α-proteobacteria</i>	NA; AN;
30	Uncultured <i>Porphyrobacter</i> sp. clone UVmas2 38 (JQ701377,1)	95%	<i>α-proteobacteria</i>	A; NA; AN, NN
31	Uncultured <i>Xanthomonadaceae</i> bacterium clone GASP-KC3W2 D08 (EU300496)	91%	-	A; NA; AN, NN
32	Uncultured bacterium clone ncd2550a03c1 (JF224543)	84%	-	A; NA; AN, NN

A- Autoclaved, NA- Non-autoclaved; AN- autoclaved supplemented with nitrate, NN- Non-autoclaved supplemented with nitrate

“-“ – Unable to be assigned to a putative division

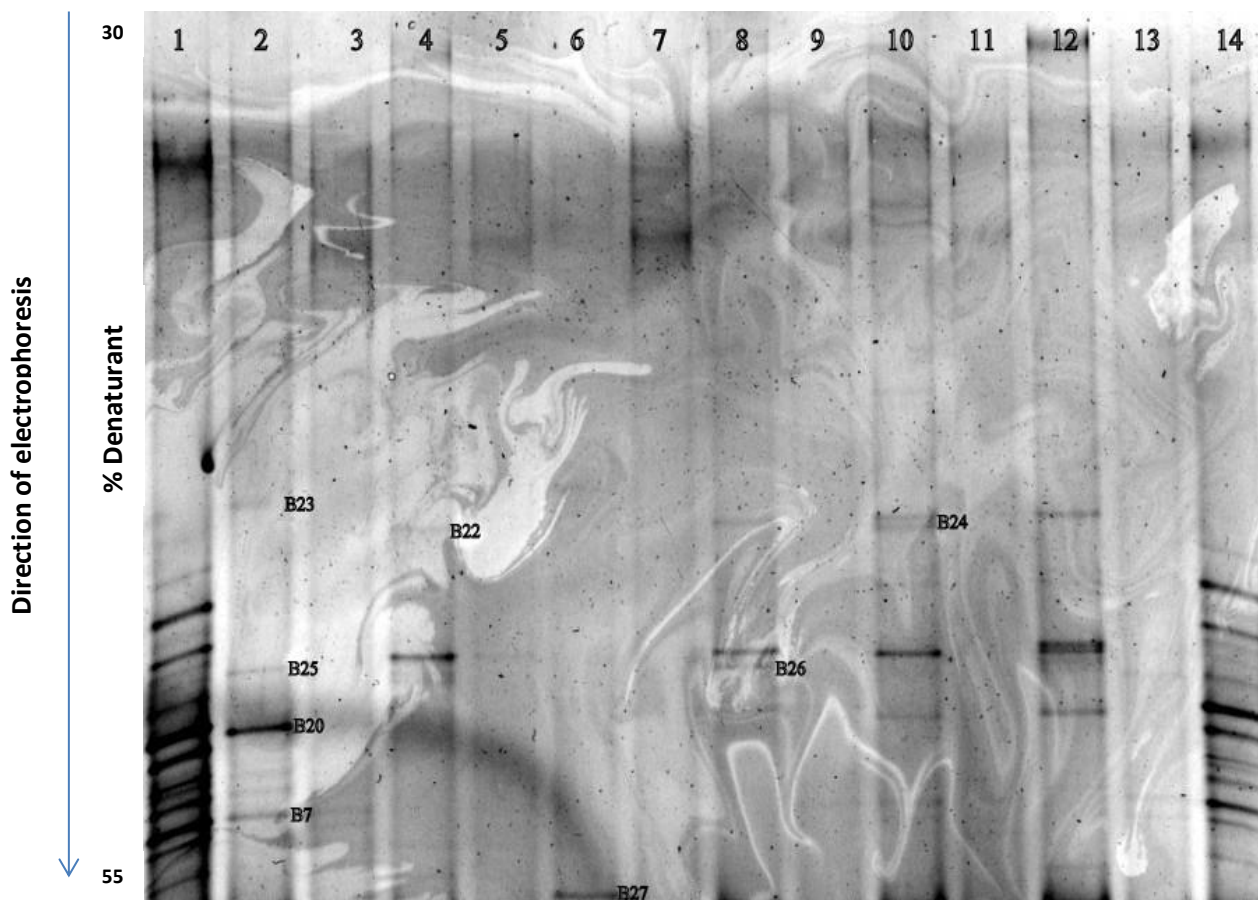


Figure 3.6: DGGE profile of biofilm samples after 4, 8 and 12 weeks incubation in loam soil (Lanes 1, 14: DGGE markers; 2: non-autoclaved (week 4); 3: autoclaved control (week 4); 4: non-autoclaved supplemented with nitrate (week 4); 5: autoclaved supplemented with nitrate (week 4); 6: non-autoclaved (week 8); 7: autoclaved control (week 8); 8: non-autoclaved supplemented with nitrate (week 8); 9: autoclaved supplemented with nitrate (week 8); 10: non-autoclaved (week 12); 11: autoclaved control (week 12); 12: non-autoclaved supplemented with nitrate (week 12); 13: autoclaved supplemented with nitrate (week 12); The numbers indicate gel portions that were sequenced and identified

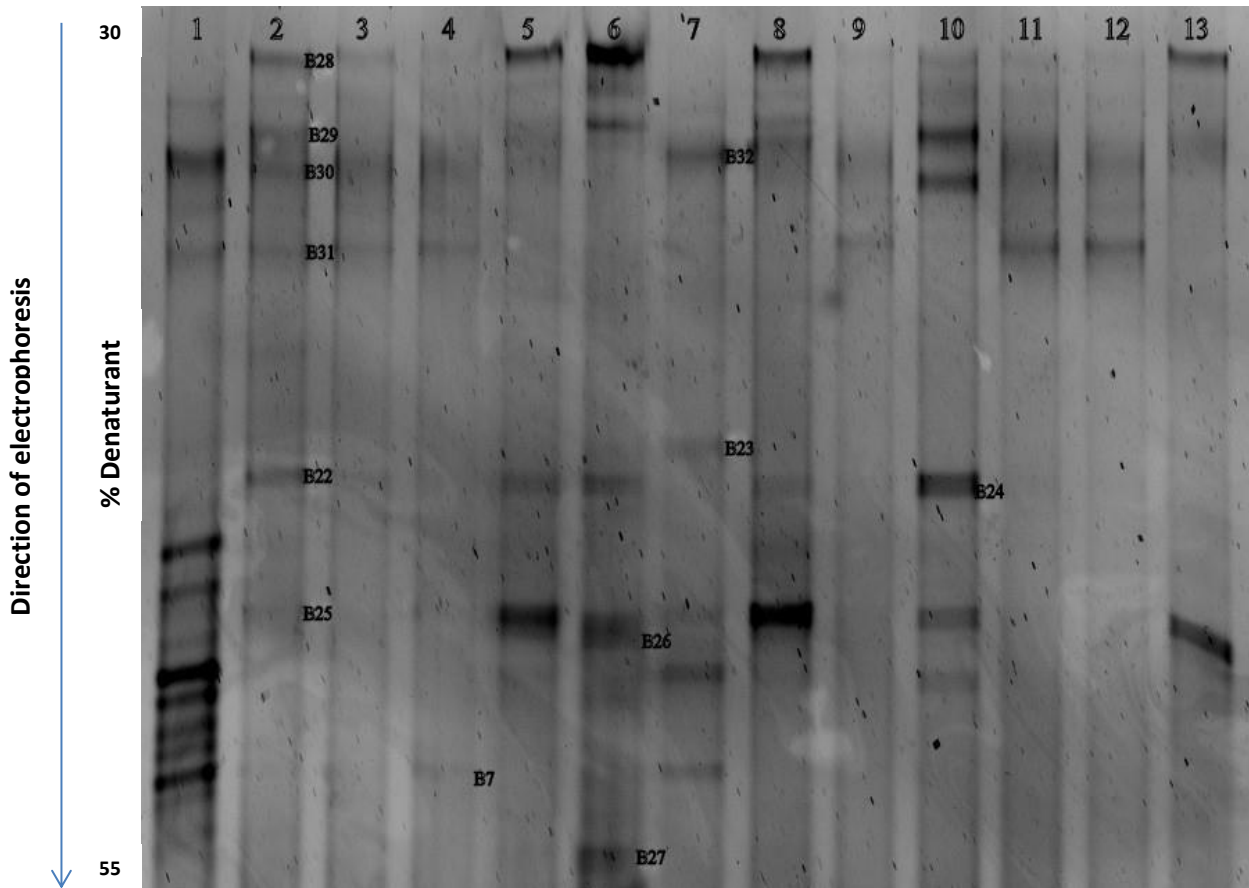


Figure 3.7: DGGE profile of biofilm samples after 16, 20 and 24 weeks incubation in loam soil (Lanes 1: DGGE markers; 2: non-autoclaved (week 16); 3: autoclaved control (week 16); 4: non-autoclaved supplemented with nitrate (week 16); 5: autoclaved supplemented with nitrate (week 16); 6: non-autoclaved (week 20); 7: autoclaved control (week 20); 8: non-autoclaved supplemented with nitrate (week 20); 9: autoclaved supplemented with nitrate (week 20); 10: non-autoclaved (week 24); 11: autoclaved control (week 24); 12: non-autoclaved supplemented with nitrate (week 24); 13: autoclaved supplemented with nitrate (week 24); The numbers indicate gel portions that were sequenced and identified

Figure 3.8 shows the phylogenetic tree of the phylotypes isolated from the autoclaved samples. Uncultured *Xanthomonadaceae* (Band 31) formed a clade with *Bacillus megaterium* (Band 28) and *Bacillus subtilis* (Band 25) and uncultured *Shigella* (Band 23) formed a clade with uncultured *Porphyrobacter* (Band 30) and Uncultured *Xanthomonadaceae* (Band 31).

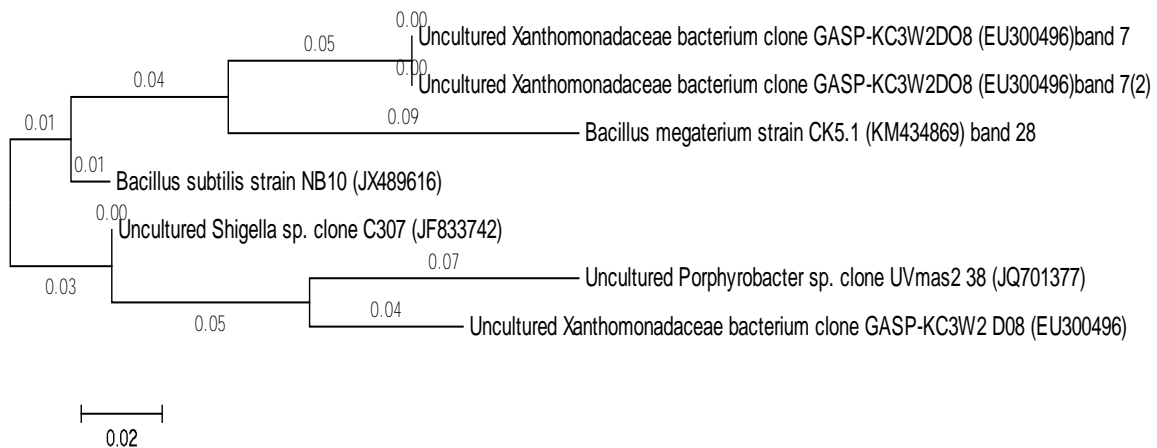


Figure 3.8: The phylogenetic tree generated using the Neighbour-Joining method for the autoclaved samples. The bootstrap consensus tree inferred from 500 replicates is taken to represent the evolutionary history of the taxa analysed. The tree is drawn to scale, with branch lengths in the same units as those of the evolutionary distances used to infer the phylogenetic tree. The evolutionary distances were computed using the Maximum Composite Likelihood method, and are in the units of the number of base substitutions per site. Codon positions included were 1st+2nd+3rd+Noncoding. Phylogenetic analyses were conducted in MEGA6

Figure 3.9 shows the phylogenetic tree of the phylotypes isolated from the non-autoclaved samples. *Bacillus aryabhatai* (Band 22) formed a clade with *Bacillus megaterium*, *Solibacillus silvestris* (Band 24), uncultured *Xanthomonaceae* (Band 31) and uncultured bacterium clone (Band 26). *Rhizobium* (Band 29) species formed a clade with *Ochrabactrum* (Band 20), uncultured *Porphyrobacter* (Band 30) and uncultured *Xanthomonadaceae* (Band 31), the latter 2 both present in the autoclaved sample as well.

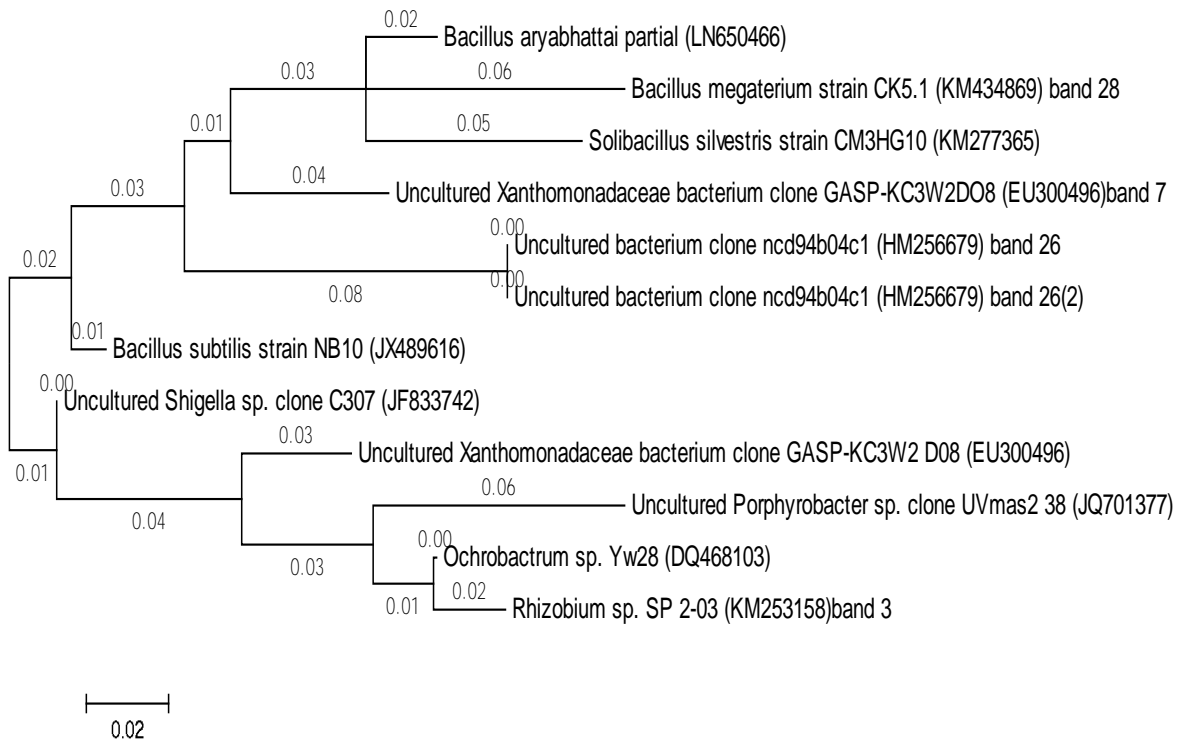


Figure 3.9: The phylogenetic tree generated using the Neighbour-Joining method for the non-autoclaved samples. The bootstrap consensus tree inferred from 500 replicates is taken to represent the evolutionary history of the taxa analysed. The tree is drawn to scale, with branch lengths in the same units as those of the evolutionary distances used to infer the phylogenetic tree. The evolutionary distances were computed using the Maximum Composite Likelihood method, and are in the units of the number of base substitutions per site. Codon positions included were 1st+2nd+3rd+Noncoding. Phylogenetic analyses was conducted in MEGA6

Figure 3.10 shows the phylogenetic tree of the phylotypes isolated from the nitrate-treated autoclaved samples. Uncultured *Xanthomonadaceae* formed a clade with *Bacillus subtilis*, present in the non-autoclaved non-supplemented samples, and *Bacillus aryabhatai* (Band 22) formed a clade with *Bacillus megaterium* (Band 28) and an uncultured bacterium clone (Band 26).

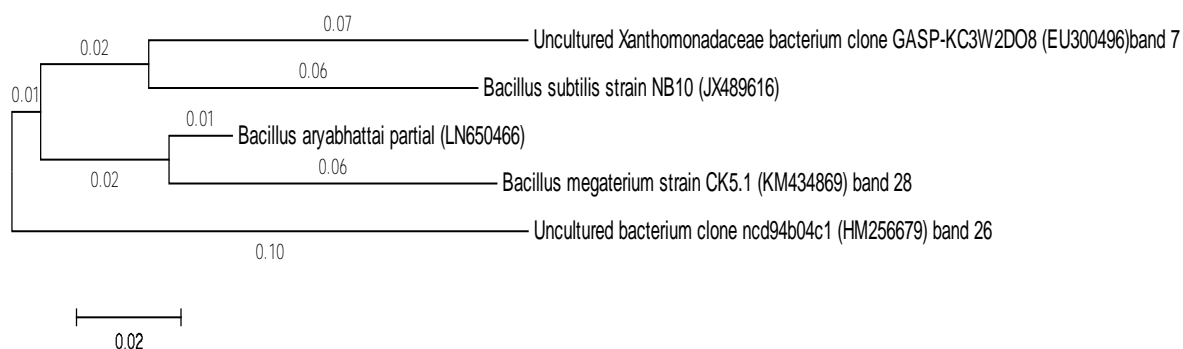


Figure 3.10: The phylogenetic tree generated using the Neighbour-Joining method for the autoclaved sample supplemented with nitrate. The bootstrap consensus tree inferred from 500 replicates is taken to represent the evolutionary history of the taxa analysed. The tree is drawn to scale, with branch lengths in the same units as those of the evolutionary distances used to infer the phylogenetic tree. The evolutionary distances were computed using the Maximum Composite Likelihood method, and are in the units of the number of base substitutions per site. Codon positions included were 1st+2nd+3rd+Noncoding. Phylogenetic analyses was conducted in MEGA6

Figure 3.11 shows the phylogenetic tree of the phylotypes isolated from the nitrate-treated non-autoclaved samples. *Solibacillus silvestris* (Band 24) formed a clade with *Bacillus megaterium* (Band 28) and *Bacillus aryabhatai* (Band 22) and uncultured *Xanthomonadaceae* (Band 31), present in the non-autoclaved non-supplemented sample as well. Uncultured bacterium clone (Band 26) formed a clade with *Bacillus subtilis* (Band 25). Uncultured *Xanthomonadaceae* (Band 31) formed a clade with uncultured *Porphyrobacter* (Band 30), *Ochrabactrum* (Band 20) and *Rhizobium* (Band 29), as observed in the non-autoclaved, non-supplemented samples.

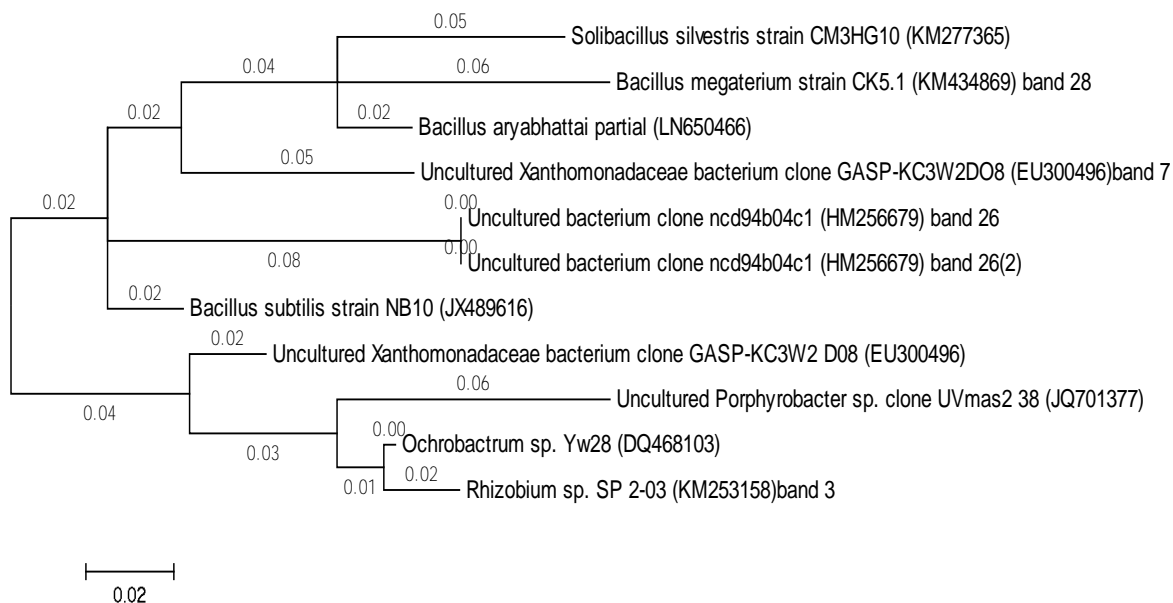


Figure 3.11: The phylogenetic tree generated using the Neighbour-Joining method for the non-autoclaved sample supplemented with nitrate. The bootstrap consensus tree inferred from 500 replicates is taken to represent the evolutionary history of the taxa analysed. The tree is drawn to scale, with branch lengths in the same units as those of the evolutionary distances used to infer the phylogenetic tree. The evolutionary distances were computed using the Maximum Composite Likelihood method, and are in the units of the number of base substitutions per site. Codon positions included were 1st+2nd+3rd+Noncoding. Phylogenetic analyses was conducted in MEGA6

3.4 Discussion

When pure metals or their alloys are exposed to a soil environment, they begin to corrode immediately (Al-Judaibi and Al-Moubaraki, 2013). Corrosion in soils are much more difficult to predict when compared to other environments due to its complexity. Soil corrosion occurs due to the interaction of a variety of factors, including metal type, pH, moisture, redox potential, microbial activity and the type of soil (Singh *et al.*, 2008; Ekine and Emujakporue, 2012). These factors interact in a variety of complex ways that could influence the corrosivity of the soil. For this reason corrosivity tests on a particular location are only applicable to that location.

Moisture content in the soil was determined to be 8.46%, a decrease when compared to the 15.38% moisture content observed in the soil used in chapter 2. The pH was found to be 6.75. Soils at this pH are generally not very corrosive (Ismail and El-Shamy, 2009), however, this is within the pH range (4.5-9) required for microbial activity to occur (Pillay and Lin, 2013).

Corrosion rates determined *in situ* were much lower than those observed in the laboratory experiments. This could have been due to the lower moisture content of the soil when compared to that used in Chapter 2. Furthermore, the jars used in Chapter 2, due to them being closed, would prevent evaporation of moisture. However, the open nature of the *in situ* setup, as well as the prevention of precipitation, would likely lead to even lower moisture within the soil. The presence of water is a prerequisite for the formation of corrosion cells and represents a critical electrolyte for electrochemical reactions to occur (Ismail and El-Shamy, 2009). Evaporation in soils influences the concentration of ions such as sulphate and chloride. Moisture content, along with oxygen are major corrosion rate determining factors. Weight loss of the mild steel coupons remained relatively constant over the incubation period in both the autoclaved and non-autoclaved systems, with no significant increase over time. This may also be explained by the low moisture content of the soil. Dry soils are generally not very corrosive (Ismail and El-Shamy, 2009).

The coupons incubated in the non-autoclaved system demonstrated slightly higher but non-significant corrosion rates when compared to the autoclaved system. This could be explained by the autoclaved system needing much more time to develop a microbial community, which could affect corrosion to a significant degree when compared to the non-autoclaved control. The addition of nitrate to the loam soil had a similar effect as observed in Chapter 2, however, corrosion rates were much lower than corrosion rates obtained in the laboratory experiments. A significant increase in corrosion rate was observed in both the autoclaved and non-autoclaved nitrate amended systems. There have been studies in which nitrate failed to control sulphide production and corrosion (Kumaraswamy *et al.*, 2011). Rempel *et al.* (2006) observed that amendments of nitrate lead to an increase in corrosion rate, as well as pitting. Ammonium nitrate has also been shown to increase the stress corrosion cracking of mild steel at higher concentrations. This is due to the high cathodic depolarisation power of nitrate, as well as the complexing action of ammonium ions which facilitates the anodic reaction (Mohammed *et al.*, 2009). Nitrite addition did decrease corrosion rate when compared to the autoclaved and non-autoclaved systems, however, this difference was not significant. Low amounts of corrosion was observed over the 24 week period, compared to no observable corrosion in the laboratory studies. A possible explanation could be due to the lower moisture content in the soil. Wen *et al.* (2011) noted that the lower the moisture content of the soil, the more heterogeneous the soil was. The more heterogeneous and complex the soil is, the more complex the corrosion process. Minimal difference was observed between the autoclaved and non-autoclaved nitrate, nitrite and non-

supplemented systems. Microbial introduction into the autoclaved systems would allow for the development of a microbial community upon the metal coupons, thus accounting for little difference noted between the autoclaved and non-autoclaved systems.

A lack of corrosion product and biofilm formation was observed in the autoclaved, non-autoclaved and nitrite treated systems. This led to no observable carbohydrate and protein content on the mild steel coupons in these treated systems. This is in contrast to results in Chapter 2 in which the autoclaved and non-autoclaved samples displayed the presence of carbohydrates and proteins. The lack of biofilm formation could explain the lower corrosion rates obtained in the *in situ* study. Proteins and carbohydrates were observed on the nitrate treated coupons, albeit at lower concentrations than in the laboratory experiments, possibly explaining the lower corrosion rates. An increase in carbohydrate and protein was observed over the 24 week incubation period. This could be linked to biofilm formation. Furthermore, a strong positive correlation was determined between the corrosion rate and carbohydrate concentration ($r = 0.79$; $p < 0.01$) in the nitrate supplemented autoclaved sample, as well as strong correlations between protein and hydrocarbon content ($r = 0.70$; $p < 0.010$), possibly indicating participation of biofilm protein and carbohydrate components in the corrosion process. Biofilms of various microorganisms containing EPS could create local concentration cells and also provide the water necessary for electrolyte formation (Stadler *et al.*, 2008). The presence of a biofilm may increase corrosion if the concentration of harmful anions such as chloride is increased below the biofilm.

SEM observations of the autoclaved system show the gradual build-up of a heterogeneous layer of corrosion products, to the formation of deep pits (Figure 3.2 A1, A2, A3), which are characteristic of local corrosion. The non-autoclaved system shows the formation of nodules which subsequently increase in size with longer incubation times (Figure 3.2 NA1, NA2, NA3). Microbial activity was not detected on the nitrite treated coupons, however, light general corrosion was observed as shown in Figure 3.3 ASN1, ASN2, ASN3 and Figure 3.4 NSN1, NSN2, NSN3. SEM images show extensive corrosive product formation and microbial growth in the latter stages of the experiment. A porous corrosion product layer was seen at week 4 in the autoclaved system treated with nitrate (Figure 3.4 AN1). Needle-like corrosion products are observed in the non-autoclaved system, as well as the formation of deep cracks (Figure 3.4 AN2, AN3, NN1). By week 24, biofilm formation is seen on the nitrate treated coupons, shown by the arrows in Figure 3.4 NN2 and NN3. However, the presence of bacterial growth does not always determine the occurrence of MIC. Pillay and Lin (2013) state that there is no relationship

between the presence or amount of planktonic or sessile bacteria and pitting corrosion. Therefore, bacterial presence does not necessarily indicate biocorrosion.

EDX analysis correlates with that of the laboratory study in which the corrosion products are composed mostly of iron and oxygen. This may indicate the activities of IOB, which are often found in consortia with SRB. The interaction between SRB and IOB accelerates metals corrosion (Xu *et al.*, 2007). Bacteria capable of iron oxidation are often capable of manganese oxidation, as these processes are often closely related (Rajaseker *et al.*, 2007b). An increase in manganese content is observed in corrosion product 4, and was also detected in corrosion products 1 and 3. Manganese oxidising bacteria are aerobes which form manganese oxides.

Mn^{2+} is oxidised to manganese oxyhydroxide ($MnOOH$), which is thereafter deposited onto the metal surface. $MnOOH$ is then oxidised to manganese dioxide (MnO_2), which is also deposited onto the metal surface. These oxides on the metal surface are then reduced back to Mn^{2+} using electrons released at anodic sites. Soluble Mn^{2+} is then reoxidised to by the MOB in a continuous cycle, producing renewable reactants such as $MnOOH$ and MnO_2 that act as cathodic reactants (Lewandowski and Beyenal, 2008). Manganese dioxides are some of the most powerful oxidising agents. Trace amounts of silicon, calcium, cobalt and other minerals were detected in various amounts in the corrosion products as shown in Table 3.3. Some metal oxidising bacteria can selectively remove certain elements within the alloy, such as silicon from the metal matrix, and deposit organic and inorganic materials on the metal surface, increasing its susceptibility to corrosion (Pillay and Lin, 2013).

The microbial diversity observed for all samples was low, when compared to microbial diversity in Chapter 2. A possible explanation could be due to the open nature of the *in situ* system when compared to the laboratory studies. Temperature fluctuations may have led to a less favourable growth environment when compared to the stable temperatures present in the laboratory. However, various studies that show that bacterial diversity involved in the corrosion of metals is usually low (Oliviera *et al.*, 2011). Relatively low bacterial diversity has been observed in samples obtained from biofilms in gas pipelines and seawater pipelines (Jan-Roblero *et al.* 2004; Zhu *et al.* 2003; Zhang and Fang, 2001). A total of 13 clones were obtained from the surface of the mild steel coupons over all treatments, belonging to three major phylogenetic groups, the Firmicutes, α -Proteobacteria and γ -Proteobacteria. Many bands were shared over the different treatments, and were also detected in Chapter 2. However, certain unique microorganisms were

detected that were not present in Chapter 2, including *Bacillus aryabhatai*, *Shigella* and *Porphyrobacter*. Banding patterns in the autoclaved and non-autoclaved systems were different to those of the nitrate treatments systems, indicating a change in bacterial diversity due to nitrate addition. Bacterial diversity was found to increase with time. Limited bands were observed during the first 3 weeks of the study. Microorganisms and their metabolic products, such as organic and inorganic acids can affect the anodic and cathodic processes in the metal surface. However the extent of corrosion is not necessarily linked to number of cells present, rather the metabolic status of the cells is believed to be the more pertinent parameter (Beech *et al.* 1994).

Bacillus species was found to be the most common species present on the corroded metal coupons, which correlates with results observed in Chapter 2. *Ochrabactrum* and *Bacillus* species were found to be the dominant species in the non-autoclaved system over the first 12 weeks of the experiment. *Bacillus subtilis* species remained the dominant species in the non-autoclaved treated system amended with nitrate. No bands were detected in the autoclaved systems in the first 12 weeks. This could be due to the microorganisms requiring time to adapt and reach numbers high enough to be detected using DGGE.

DGGE patterns in weeks 16, 20, and 24 show increased bacterial diversity. *Bacillus* sp., *Rhizobium*, and uncultured *Porphyrobacter* were the dominant bands in the non-autoclaved system with *Solibacillus* becoming the dominant microorganism by week 24. *Bacillus* species were found to dominate the nitrate amended systems at weeks 16 and 20. *Shigella* species was detected in the autoclaved system at week 20. *Shigella* are a group of Gram-negative, facultative anaerobic, non-spore forming, rod shaped bacteria.

As in Chapter 2, SRB were not detected in the corrosive biofilm formations. However, this could be due to the difficulties in detecting bacterial species present in low numbers by DGGE analysis, which shows a bias towards dominant species. There have been studies that have failed to detect SRB using PCR based methods such as DGGE, but detected SRB in the same sample using methods detecting metabolically active cells, such as fluorescent *in situ* hybridisation (FISH) (Pillay and Lin, 2013; Kumaraswamy *et al.*, 2011).

Bacillus species were the most frequently detected bacterial species. There are many reports on the protective effect of *Bacillus* species on metal surfaces (Jayaraman *et al.*, 1997; Volkland *et*

al., 2000). In this study, *Bacillus aryabhatai*, *Bacillus subtilis* and *Bacillus megaterium* were detected, however, a protective effect was not observed, as pitting corrosion was quite severe in the nitrate treated coupons. *Bacillus* species have also been detected in many corrosive bacterial biofilms (Lopez *et al.* 2006; Rajaseker *et al.* 2007b, 2010). At low pH, these bacteria produce metal oxides which may increase metal corrosion.

Results obtained in this *in situ* study correlate with those in the laboratory experiment, in which nitrate led to an increase in weight loss in the mild steel coupons. This means that nitrate stimulated the corrosion of mild steel in loam soil. However, nitrite addition was found to decrease the weight loss of the coupons, although this was not significant when compared to the control. It is known that results obtained in laboratory studies do not always translate into results in the field. Corrosion is a dynamic process subject to fluctuations in many different factors, and is sensitive to changes in the local environment, especially in moisture content. Changes in bacterial species composition present within biofilms may produce different corrosion results, even in seemingly identical systems. Therefore, more research needs to focus on the interaction of the different factors involved in the corrosion of metals.

Chapter 4: Biocorrosion by bacterial species isolated from corroded mild steel coupons: The effect of nitrite supplementation

4.1 Introduction

Corrosion is the disintegration of any substance due to a chemical reaction with its environment (Herbert *et al.*, 2002). Due to their opportunistic behaviour, microorganisms are known to influence the energy yielding corrosion reaction, often enhancing corrosion in order to harvest the energy released. This phenomenon is known as microbiologically influenced corrosion, or MIC (Herbert *et al.*, 2002). By definition, MIC is the initiation, facilitation or exacerbation of the corrosion process due to the activities of microorganisms. It has been postulated that microorganisms can accelerate the corrosion process by as much as 1000-10000 times (Herbert *et al.*, 2002). MIC is, in fact, a widely occurring phenomenon and occurs in probably all industries, including the sugar, dentistry, paper and pulp, shipping, petroleum and gas industries (Rajaseker *et al.*, 2010). The annual costs with regards to corrosion related problems worldwide are estimated to cost as much as \$3 trillion dollars, with MIC estimated to contribute to approximately 50% of this total (Herbert *et al.*, 2002).

Microbiologically influenced corrosion acceleration (MIC) in nature is not caused by one type of microorganism, nor is it limited to one mechanism. The most well studied bacteria with regards to MIC are the anaerobes, including the sulphate reducing bacteria and the acid producing bacteria, and the aerobic bacteria, including manganese and iron oxidisers and the extracellular slime producers (Maluckov, 2012). MIC occurs due to the synergistic action of a number of different bacterial groups that share a common environment.

The first step in the biocorrosion process is the formation of a biofilm. A biofilm is composed of microbial cells held together by a thick slime known as the extracellular polymeric substance (Lin and Ballim, 2012). The biofilm can influence MIC in the following ways: i) the creation of oxygen heterogeneities and therefore differential aeration cells ii) increasing mass transport resistance at the interface of the biofilm and metal surface iii) production of corrosive substances such as acids iv) removal or disruption of passive protective layers and v) changing redox conditions at the interface of the metal and bulk solution (Lewandowski and Beyenal, 2008).

Most studies have focussed on the corrosion acceleration abilities of biofilms, although some studies have shown biofilms to have a protective effect on metal surfaces. Microorganisms have been known to contribute to corrosion inhibition, and they do this by various mechanisms, such as the neutralisation or breakdown of corrosive substances present in the environment, the formation of protective films or stabilisation of already present protective films, or the induction of a decrease in the corrosiveness of the medium (Akpabio *et al.*, 2011).

The formation of biofilms on the surfaces of metals has been shown to decrease the rate of corrosion due to the consumption of the cathodic reactant, oxygen, therefore rendering it unavailable for the corrosion reaction (Lewandowski and Beyenal, 2008). The rate of mild steel corrosion was shown to be markedly decreased due to the formation of a uniform biofilm layer (Lewandowski and Beyenal, 2008). The decrease was attributed to the microbial respiration occurring within the biofilm, which resulted in a decrease in the availability of oxygen at the surface of the metal and thus a decrease in the cathodic reaction.

Studies into the identities and role of certain microbial species in the biocorrosion process may be exploited to induce microbial inhibition of corrosion as a method to prevent the occurrence of MIC encountered in the various fields (Videla and Herrera, 2005). The previous chapter showed that nitrate addition led to an increase in corrosion rate of mild steel, while nitrite addition induced a decrease in a loam soil environment. In this chapter, microbial species were isolated from corroded mild steel coupons in the above mentioned system. DNA sequence analysis was used to identify these isolates and phylogenetic analysis to determine similarity. The effect of nitrite supplementation on the corrosion of mild steel by these isolates was investigated.

4.2 Materials and Methods

4.2.1 Experimental Set-Up

The loam soil system was setup according to Orfei *et al.* (2006) as described in Chapter 2. The mild steel coupons were treated and pre-weighed prior to immersion and incubation into the systems described in chapter 2. Every 4 weeks, up to a maximum of 24 weeks, mild steel coupons were removed from their respective experimental setup in triplicate and used to isolate bacteria.

4.2.2 The isolation of the cultivatable fraction of bacterial isolates within the biofilm formed on the surface of the mild steel coupons

The coupons were extracted from the nitrite experimental set up and swabbed (25 mm Gamma sterilized cotton swabs) onto nutrient agar plates. The plates were then incubated at 30°C overnight or until bacterial growth was observed. Isolates were then purified using the four way streak technique onto nutrient agar plates. Once individual isolates were obtained, they were subjected to Gram staining and spore staining according to the standard methods (Dhanasekaran *et al.*, 2009; Correia *et al.*, 2010) and 16S rDNA identification (Marchesi *et al.*, 1998).

4.2.3 Preparation of the inoculum and mild steel coupons

The mild steel coupons were pre-treated as described in Chapter 2. The inoculum was prepared by growing the cultures in 30 ml of nutrient broth at 30°C overnight at 150 rpm. The cultures were centrifuged at 10000 rpm for 5 min, and washed 3 times using a 0.85% (w/v) saline solution, and thereafter suspended in a smaller volume of 0.85% (w/v) saline solution. The inoculum was then standardised to an absorbance of 1 at 600nm.

4.2.4 Determination of the corrosion activities of the bacterial isolates isolated form bacterial biofilms formed of corroding mild steel surfaces

Four sets of experiments were prepared. The mild steel coupons were suspended in a vertical position in a 250 ml Erlenmeyer flask containing 100 ml sterilised deionised water, 1 ml of standardised inoculum and varying concentrations (5, 10 and 20 mM) of sodium nitrite. To create a corrosive environment, 3.5% (w/v) NaCl was added to the flasks. Five, 10, and 20 mM of sodium nitrite were used. Flasks were incubated at 30°C at 100 rpm to obtain a homogenous medium. The pH of the bulk medium was measured every 2 days. After a period of 7 days, the mild steel coupons were removed and weighed according to the method described in Chapters 2 and 3 previously.

4.2.5 DNA Extraction

DNA was extracted from the bacterial isolates using the boiling-centrifugation method (Freschi *et al.*, 2005). A loopful of culture from the pure isolates was placed in an Eppendorf tube containing 400 µl of sterile distilled water. The mixture was boiled at 100°C for 10 min, then

centrifuged at 10000 rpm for 5 min. The supernatant was used as the template for PCR amplification.

4.2.6 Amplification of 16S rDNA and Sequencing

The conserved region of 16S rDNA was amplified using the forward primer 63F and reverse primer 907R. The reaction mixture contained 1 µl each of forward and reverse primers (10 µM), 25 µl ReadyMix Taq PCR Reaction Mix with MgCl₂ (2×) (Fermentas Life Sciences) and 1 µl of template DNA from each isolate was used. PCR amplification conditions were achieved using Sambrook *et al.* (1989), using the ThermoHybrid PCR Express Thermal Cycler (Ashford, Middlesex) under the following cycling parameters: 30 cycles of initial denaturation at 95°C for 1 min, 55°C for 1 min and 72°C for 1.5 min, followed by the final elongation step at 72°C for 5 min (1 cycle). PCR products were confirmed using electrophoresis on a 1% agarose gel at 100V for 30 min in 1× Tris-Acetate – EDTA running buffer. Product size was determined using the GeneRuler DNA ladder mix (ThermoScientific). The gel was then stained using ethidium bromide and visualised using the Chemi Genius2 BIO Imaging System and Gene Snap software (Syngene, UK).

4.2.7 Database Searches and Phylogenetic Analysis

The amplified 16S rDNA PCR products were sequenced by Inqaba Biotech (South Africa). An NCBI BLAST search (<http://www.ncbi.nlm.nih.gov/BLAST>) was performed and aligned with the closest matching 16S rDNA sequences (Altschul *et al.*, 1990; Altschul *et al.*, 1997).

4.2.8 Statistical Analysis

One way ANOVA was used to examine the statistical significance between the different treatments with the isolates on the rate of corrosion on mild steel coupons. Probability was set at < 0.05.

4.3 Results

4.3.1 Identification of bacterial isolates

A total of 11 isolates were obtained from the surface of the nitrite treated mild steel coupons. DNA was extracted from the isolated species, and 16S rDNA amplified as described in section 4.2.6. A 1% agarose gel was used to evaluate the amplified PCR products and is shown in the Appendix (III). The resulting PCR products were sequenced and a BLAST search was performed to determine their putative identities. The putative identities of the bacteria present on the surface of the nitrite treated coupons are shown in Table 4.1. The isolates were found to belong to 2 main divisions, namely the Actinobacteria and Firmicutes. Of the 11 isolated species, 8 isolates were found to belong to *Bacillus*, whereas 2 were *Rhodococcus* species and one *Arthrobacter* species was observed.

Table 4.1: Putative identities of bacteria isolated from the surface of nitrite treated mild steel coupons

No	THE CLOSEST SEQUENCES (GENBANK NUMBER)	SIMILARITY	PUTATIVE DIVISION
2	<i>Arthrobacter nicotianae</i> strain VITNJ6 (KM047491)	99%	Actinobacteria
4	<i>Bacillus sp.</i> hb68 (KF863863)	98%	Firmicutes
5	<i>Bacillus cereus</i> strain P83 (KC876035)	99%	Firmicutes
6	<i>Rhodococcus qinqshenqii</i> strain B2 (KJ028076)	99%	Actinobacteria
8	<i>Bacillus pumilus</i> strain KD3 (EU500930)	99%	Firmicutes
9	<i>Bacillus cereus</i> strain 03BB87 (CP009941)	99%	Firmicutes
10	<i>Bacillus sp.</i> hb68 (KF863863)	98%	Firmicutes
11	<i>Bacillus cereus</i> strain RV.B2.90 (HQ197382)	99%	Firmicutes
13	<i>Rhodococcus equi</i> strain ATCC33372 (DQ150572)	99%	Actinobacteria
14	<i>Bacillus sp.</i> GZB (HQ603746)	99%	Firmicutes
16	<i>Bacillus simplex</i> strain IHB B 15619 (KM817245)	99%	Firmicutes

4.3.2 Weight loss measurements of mild steel coupons in the presence of bacterial isolates supplemented with nitrite

Upon removal of the metal coupons, reddish brown as well as black depositions were observed on the surface. The reddish brown colour can be attributed to the many phases of iron oxides and hydroxides that correspond to the formula, FeOOH, whereas the black colour formed may be attributed to the formation of magnetite (Fe₂O₃) (De Melo *et al.*, 2011).

Figure 4.1 shows the weight loss of the coupons in the presence of different isolates supplemented with various concentrations of nitrite. Generally, a decrease in corrosion was seen with higher concentrations of nitrite. The control showed a decrease in weight loss upon 5 mM nitrite amendment (13.85 mg/cm^2) when compared to no nitrite (16.41 mg/cm^2), however, upon 10 mM treatment weight loss increased to (17.02 mg/cm^2). The lowest corrosion rate is seen at 20 mM nitrite amendment (8.73 mg/cm^2).

A similar trend was seen for isolate 2, 6, 10, 11, and 16 when compared to the control with the highest corrosion rate seen upon 10 mM nitrite amendment. Isolates 4, 13 and 14 showed decreasing corrosion rates upon increasing nitrite concentration. In isolate 4, the addition of 20 mM nitrite led to a significant decrease in corrosion rate when compared to no nutrient addition, from 20.77 mg/cm^2 to 8.62 mg/cm^2 . Isolate 2 showed significant decrease in corrosion rate upon 5 mM nitrite addition (13.08 mg/cm^2) when compared to no nutrient (27.44 mg/cm^2), with corrosion further decreasing till 20 mM nitrite addition (7.16 mg/cm^2). Isolate 8 showed significant decrease in corrosion rate upon 20 mM supplementation from 18.21 mg/cm^2 to 9.35 mg/cm^2 when compared to no nutrient addition. The addition of 5 mM (13.59 mg/cm^2) and 20 mM (12.95 mg/cm^2) nitrite to isolate 11 led to significant decrease in corrosion rate when compared to no nutrient (26.15 mg/cm^2). For isolate 13, 10 mM (9.63 mg/cm^2) and 20 mM (9.28 mg/cm^2) addition significantly decreased the corrosion rate when compared to no nitrite addition (18.72 mg/cm^2). Significant differences were seen upon 20 mM nitrite addition to isolates 14 and 16 (10.63 mg/cm^2 and 5.77 mg/cm^2 respectively) when compared to no nitrite addition (20.00 mg/cm^2 and 17.69 mg/cm^2 , respectively).

Lowest corrosion rates were seen for isolate 5 at 20 mM nitrite (7.16 mg/cm^2), and for isolate 16 at 20 mM (5.77 mg/cm^2). The highest corrosion rates were seen for isolates 5 and 11 without nutrient addition (27.55 mg/cm^2 and 26.15 mg/cm^2 , respectively), in which significantly greater corrosion rates were observed compared to the control.

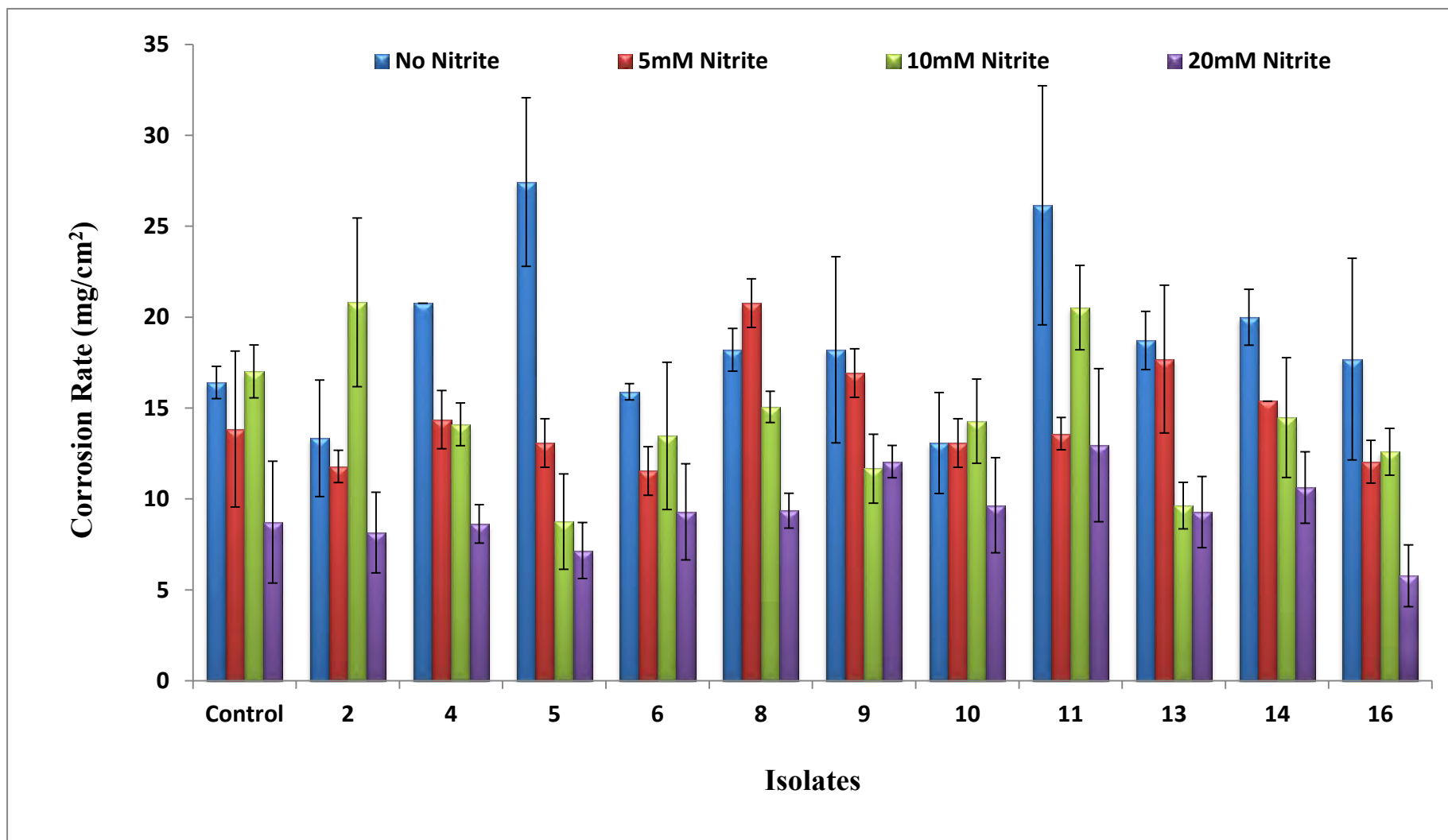


Figure 4.1: Weight loss of mild steel coupons following exposure to various isolates under different concentrations of nitrite

4.3.3 pH changes over the incubation period

Figure 4.2 shows the pH changes in the corrosive medium of *Arthrobacter nicotianae* (Isolate 2) that occurred over the incubation period. The pH was measured every 2 d. With no addition of nitrite, the pH was found to gradually increase from 6.3 at the beginning of the incubation period to 8.33 at day 6. The addition of 5 and 10 mM nitrite led to a drastic increase in pH from the start of experiment (6.23 and 6.21 respectively) to Day 2 (11.00 and 10.65, respectively). The pH remains relatively constant over the rest of the incubation period. With the addition of 20 mM nitrate, pH increased gradually from Day 0 (7.05) to 10.78 at day 4, remaining relatively constant over the rest of the experiment. A similar trend was observed over the remaining isolates and is shown in Appendix IV.

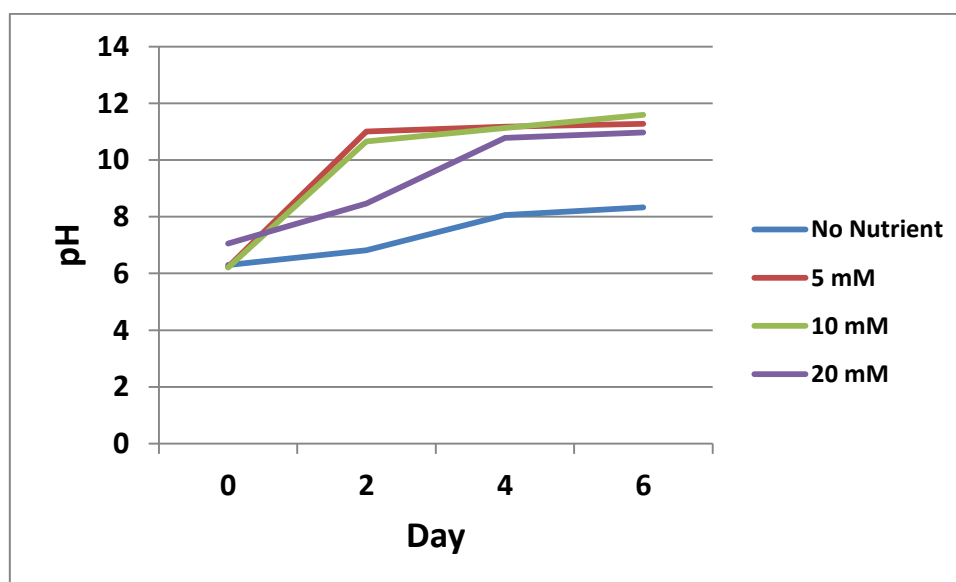


Figure 4.2: pH changes of *Arthrobacter nicotianae* under various nitrite concentrations

4.4 Discussion

Results in Chapter 2 showed that higher concentrations of nitrite led to inhibition of mild steel corrosion in a laboratory environment. However, *in situ* experiments in Chapter 3 were less successful, with nitrite addition having no significant effect on corrosion rate. It is clear from this study that the bacterial isolates with or without nitrite addition affected the corrosion rate of mild steel. The addition of nitrite led to a decrease in corrosion rate, with higher concentrations of nitrite leading to lower corrosion rates in general (Figure 4.1). In some cases the addition of 10 mM nitrite to isolates 2, 6, 10, and 11 increased corrosion rate when compared to the other concentrations of nitrite. Lowest corrosion rates were seen upon addition of 20 mM nitrite.

Higher corrosion rates without nutrient addition were seen for isolates 4, 5 and 11. Bacteria may increase corrosion by the creation of oxygen concentration cells, the production of corrosive metabolic products or the degradation of passive protective layers (Coetser and Cloete, 2005). Bano and Qazi (2011) describe a possible explanation for biocorrosion. They state that a thick biofilm forms on the surface of a susceptible metal. The microorganisms multiply and form nodules, which are colonies of cells containing metabolic by-products and corrosion products. These formations trap ions and prevent the surface below them from oxygen access. This leads to the formation of an oxygen concentration cell and increases corrosion. It could be possible that the lack of nutrients in the system lead to a non-uniform biofilm layer on the mild steel surface, which occludes oxygen from the metal surface, creating local anodic and cathodic areas, thus increasing corrosion.

Higher concentrations of nitrite led to lower corrosion rates in the presence of the various bacterial isolates. Microorganisms can contribute to corrosion inhibition in various ways (Videla and Herrera, 2005), such as neutralisation of corrosive substances, formation or stabilisation of protective films, and decreasing medium corrosiveness. The use of biofilms has been demonstrated to induce the protection of metals from corrosion (Jayaraman *et al.*, 1997). Zuo *et al.* (2005) demonstrated that live biofilms protected aluminium from a corrosive medium. The beneficial effect of the biofilms was lost after the bacteria were killed. The formation of biofilms on the surfaces of metals has been shown to decrease the rate of corrosion, due to the consumption of the cathodic reactant, oxygen, therefore rendering it unavailable for the corrosion reaction (Lewandowski and Beyenal, 2008). The rate of mild steel corrosion was shown to be markedly decreased due to the formation of a uniform biofilm layer (Lewandowski and Beyenal, 2008). The decrease was attributed to the microbial respiration occurring within the biofilm, which resulted in a decrease in the availability of oxygen at the surface of the metal and thus a decrease in the cathodic reaction. However, the inhibition of corrosion by this mechanism requires the biofilm to uniformly cover the entire surface of the metal and have a uniform microbial activity (Lewandowski and Beyenal, 2008). Due to the fact that biofilms in nature are not uniformly distributed and do not have uniform microbial activity, Lewandowski and Beyenal (2008) proposed that the inhibitory effect of microbial biofilms is not likely to occur in nature. It is also possible that the EPS component of the biofilm may be responsible for the protective effects. The EPS of most bacterial species is negatively charged, and could repel chloride ions from the metal surface (Zuo *et al.*, 2005). Rajaseker and Ting (2011) reported that EPS production by *Bacillus megaterium* and *Pseudomonas* sp. increased in the presence of inorganic

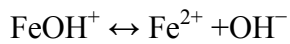
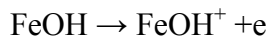
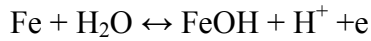
nutrients when compared to organic nutrients. It is possible that the presence of inorganic nitrite encouraged the formation of EPS by the bacterial species which had a protective effect on the metal surface.

Sequence analysis of the amplified DNA sequences revealed that the majority of the microbial isolates were of *Bacillus* sp., which is affiliated to the Firmicutes phylum. The influence of *Bacillus* sp. in biocorrosion has been documented (Pillay and Lin, 2013). The remaining three isolates were found to be *Rhodococcus* and *Arthrobacter* affiliated with the Actinobacteria phylum.

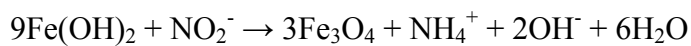
Bacillus species have been found to be capable of iron oxidation and reduction, and manganese oxidation (Kan *et al.*, 2011). They are suggested to be the primary colonisers in biofilm formation and are known to produce EPS, as well as acids, that can accelerate the corrosion of steels (Pillay and Lin, 2013). Isolates 4, 5 and 11, all accelerated corrosion of mild steel without nutrient addition, and all belonged to *Bacillus* species. Iron and manganese oxidisers are capable of oxidising ferrous (Fe^{2+}) and manganous (Mn^{2+}) into ferric (Fe^{3+}) and manganic (Mn^{4+}) ions, which would then be deposited as MnO_2 and Fe_2O_3 on the surface of the metal, leading to corrosion (Rajaseker *et al.*, 2011). These corrosion products are unlikely to precipitate completely on a non-passivated metal, such as mild steel. As a result, ferric ions and manganic ions in solution then serve as highly reactive species which accelerate corrosion. As saltwater contains chloride ions, the iron oxidising bacteria may be directly linked to the production of ferric chloride. FeCl_3 is a highly corrosive substance which acts like dilute HCl and can concentrate under nodules (Rajaseker *et al.*, 2007b). Chloride ions can migrate into crevices by neutralizing the increased charge via anodic dissolution, and are then able to combine with the oxidation of ferrous and manganous ions to ferric and manganic ions (Rajaseker *et al.*, 2011). The effect of Actinobacteria on biocorrosion has not been well documented.

One cannot ignore the passivating effect of nitrite itself on the mild steel surface in addition to its effect on microbial activity. Nitrite can act as a passivating inhibitor of corrosion that leads to a protective oxide film on the metal surface (Hayyan *et al.*, 2012). The protective oxide formed on the treated metal surface with nitrites consists mainly of Fe_2O_3 and Fe_3O_4 (Hayyan *et al.*, 2012). However, at low concentrations, nitrite may cause imperfect passivity and in effect accelerate corrosion.

The increase in pH of the corrosion medium can be attributed to the following reactions which show the dissolution of iron at the surface of the coupon, and results in the release of hydroxide ions into the medium (Chongdar *et al.*, 2005):



Higher pH values were observed in the flasks supplemented with nitrite. Nitrite reacts with iron hydroxides according to the following reactions, resulting in the release of OH⁻ ions into solution (Hayyan *et al.*, 2012):



This study showed that isolated aerobic microbial organisms do affect the corrosion process of mild steel, and can have an accelerating or a protective effect. However, the corrosive process is complex and the factors that govern whether the effect is positive or negative are still not well understood and require further study.

Chapter 5: Concluding Remarks

It is estimated that at least 40% of all internal pipeline corrosion in the gas and oil industry and approximately 50% of underground pipes deteriorate due to the actions of microorganisms (Bano and Qazi, 2011). Biocorrosion is, therefore of great economic importance, with the cost of repair and replacement of piping material reaching considerable proportions. Microorganisms have been implicated in the corrosion of various types of metals, including iron, copper, and aluminium as well as their alloys (Oliviera *et al.*, 2011). Various mechanisms of biocorrosion have been discovered and studied, as well as the various physiologically distinct microorganisms that have been shown to have the potential to participate in the corrosion reaction. Microbial activity on metal surfaces can result in severe localised corrosion and rapid metal loss, due to changes in the surface microchemistry initiated by microbial metabolism (Rajaseker and Ting, 2011). Aerobic bacteria generally have a much greater growth rate and metabolism when compared to anaerobic bacteria (Pillay and Lin, 2012). These bacteria, therefore, have a higher potential to influence the corrosion reaction (Santana *et al.*, 2012). The isolation and identification of microorganisms involved in biocorrosion is essential if one is to research methods to prevent and control this phenomenon (Correia *et al.*, 2010).

The addition of nitrate to control microbial corrosion damage has the potential to be a more effective, cheaper and less toxic method when compared to biocide use (Kumaraswamy *et al.*, 2011). In this study, however, nitrate addition was found to stimulate the weight loss of mild steel in loam soil over a 24 week period. SEM images showed an increase in corrosion product and biofilm formation upon the addition of nitrate. The increase in weight loss could be due to the nitrate stimulating the growth and activities of the microorganisms present in the biofilm formed on the metal surface. Upon removal of the mild steel coupons, reddish brown and black deposits were observed to have developed on the coupon surface. Upon further analysis using EDX, the main components of the corrosion products were determined to be iron and oxygen, possibly indicating the presence and activities of iron oxidising bacteria. The presence of tubercle formation, a possible indicator of iron oxidiser activity, detected by SEM, further corroborates the possible presence of iron oxidisers.

Nitrite addition was observed to induce a decrease in corrosion rate, especially at higher concentrations. The laboratory experiments showed that at 20 mM nitrite, neither visible corrosion nor biofilm formation was observed, as determined through SEM analysis. Nitrite is

one of the most commonly used anodic inhibitors of corrosion (Hayyan *et al.*, 2012). The *in situ* experiments showed a decrease in weight loss when compared to the controls and nitrate addition. However, in contrast to the laboratory experiments, weight loss was observed to occur.

Isolation and identification of bacterial species growing on the nitrite treated coupons revealed eleven isolates. Of these two *Rhodococcus* species and one *Arthrobacter* species were present, with the remaining eight species belonging to the *Bacillus* genus. It was observed that nitrite addition, in conjunction with the bacteria isolated in this study, induced a decrease in corrosion rate in general. The most common bacteria discovered belonged to the genus *Bacillus*. This is the predominant species involved in the corrosion process and its activities are enhanced in the presence of oxygen (Pillay and Lin, 2012). Several studies have shown the potential of *Bacillus* species to mitigate corrosion (Jayaraman *et al.*, 1997). These results show that individual isolates can affect the corrosion process of mild steel, and may also be used in an attempt to mitigate metal loss.

DGGE analysis was used to study the population dynamics within the biofilms formed on the corroding mild steel coupons. The microorganisms detected across the laboratory and *in situ* experiments belonged to three different phylogenetic groups, the alpha-, and gamma-Proteobacteria and the Firmicutes. Certain species were common amongst all treatments, namely *Phenylobacterium* and *Rhizobium*. However, nitrate treatment was found to induce a shift in bacterial populations to NRB. In general, though, the microbial diversity within the corroded metal coupon was low, corroborating previous studies showing microbial diversity involved in corroding metals are usually low (Oliviera *et al.*, 2011). By far, the most abundant and dominant microorganisms were the *Bacillus* species. *Bacillus* are capable of iron and manganese oxidation, as well as acid production (Pillay and Lin, 2012), and have previously been isolated from corroded metal samples (Oliviera *et al.*, 2011; Valencia-Cantero *et al.*, 2003). Furthermore, these microbes, through respiration and therefore oxygen depletion, may allow for the growth of anaerobic bacteria such as SRB.

The present study showed that nitrate was unable to prevent the corrosion of mild steel coupons, but actually accelerated it, possibly due to the stimulation of the growth of indigenous microbial populations on the metal surface. The addition of nitrite however, was shown to induce a reduction in weight loss of the mild steel coupons, possibly due to the formation of a passive

protective film and preventing the growth a microbial population on the metal surface. Although no corrosion was observed in the laboratory studies upon 20 mM nitrite addition, some corrosion was observed to occur in the *in situ* experiments. Therefore, further studies need to be conducted with regards to the effect of environment type as well as microbial population on corrosion. The presence of humidity, warm temperature, and organic matter can influence the activities of the microorganisms present, influencing their corrosive potential. Furthermore, even slight changes in microbial populations may result in drastically different metabolic capabilities, which may explain why, in two environments under the exact same treatments and environmental conditions, corrosion results may differ.

Many different mechanisms have been proposed as pertinent to biocorrosion. This reflects the range of physiological capabilities of microorganisms found within biofilms (Pillay and Lin, 2012). This study observed that individual aerobic isolates were able to affect the corrosion dynamics of mild steel. A better understanding of the roles of different microorganisms within the microbial communities with the potential to affect the corrosion reaction could be used to develop a deeper insight into biocorrosion and new methods for its mitigation and control (Beech and Sunner, 2004; Beech *et al.*, 2005).

References

- Adeosun, S.O., and O.S. Sanni.** 2013. Degradation propensity of welded mild steel in coastal soil of university of Lagos. *International Journal of Chemical, Nuclear, Materials and Metallurgical Engineering.* **7(1):**84-88
- Akpabio, E.J., E.J. Akott and M.E. Akpan.** 2011. Inhibition and control of Microbiologically Influenced Corrosion in oilfield materials. *Environmental Research Journals.* **5 (2):** 59 - 65
- Al-Judaibi, A., and A. Al-Moubaraki.** 2013. Microbial analysis and surface characterization of SABIC carbon steel corrosion in soils of different moisture levels. *Advances in Biological Chemistry.* **3:**264-273
- Altschul, S.F., W. Gish, W. Miller, E.W. Myers, and D.J. Lipman.** 1990. Basic local alignment search tool. *Molecular Biology.* **215:**403-410
- Altschul, S.F., T.L. Madden, A.A. Schaffer, J. Zhang, Z. Zhang, W. Miller, and D.J. Lipman.** 1997. Gapped BLAST and PSI-BLAST: a new approach of protein database search programs. *Nucleic Acids Research.* **25:**3389-3402
- Amann, R.I., J. Stromley, R. Devereux, R. Key, and D.A. Stahl.** 1992. Molecular and microscopic identification of sulfate-reducing bacteria in multispecies biofilms. *Applied and Environmental Microbiology.* **58(2):**614-623
- Aung, N.N., and Y.-J. Tan.** 2004. A new method of studying buried steel corrosion and its inhibition using the wire beam electrode. *Corrosion Science.* **46:**3057–3067
- Avci, G.G., and D. Abanoz.** 2004. Corrosion protection of steel by hybrid sol-gel coating. *Key Engineering Materials.* **264-268:**387-390
- Bachmann, R.T., and R.G.J. Edyvean.** 2006. AFM study of the colonisation of stainless steel by *Aquabacterium commune*. *International Biodeterioration and Biodegradation.* **58(3-4):**112–118
- Bano, S.A., and J.I. Qazi.** 2011. Soil buried mild steel corrosion by *Bacillus cereus*-SNB4 and its inhibition by *Bacillus thuringiensis*-SN8. *Pakistan Journal of Zoology.* **43(3):**555-562
- Barett, E.L., and M.A. Clark.** 1987. Tetrathionate reduction and production of hydrogen sulfide from thiosulfate. *Microbiology Reviews.* **51:**192–205
- Barton, L.L.** 1997. Sulphate-reducing Bacteria. International workshop on Industrial Biofouling and Biocorrosion. Mulheim, Germany

- Beech, I.B.** 1996. The potential use of atomic force microscopy for studying corrosion of metals in the presence of bacterial biofilms – an overview. *International Biodeterioration and Biodegradation*. 141 – 149
- Beech, I.B.** 2004. Corrosion of technical materials in the presence of biofilms-current understanding and state-of-the art methods of study. *International Biodeterioration & Biodegradation*. **53**:177–183
- Beech, I.B., J.A. Sunner and K. Hiraoka.** 2005. Microbe-surface interactions in biofouling and biocorrosion processes. *International Microbiology*. **8**: 157 – 168
- Beech, I.B., and C.W.S. Cheung.** 1995. Interactions of exopolymers produced by sulphate-reducing bacteria with metal ions. *International Biodeterioration and Biodegradation*. **35**:59–72
- Beech, I.B., and C.C. Gaylarde.** 1999. Recent advances in the study of biocorrosion—an overview. *Revista de Microbiologia*. **30**:177-190
- Beech, I., A. Bergel, A. Mollica, Hans-Curt Flemming, V. Scotto, and W. Sand.** 2000. Simple methods for the investigation of the role of biofilms in corrosion. *Brite Euram Thematic network on MIC of industrial materials*. 1-27
- Beech, I.B., and J. Sunner.** 2004. Biocorrosion: towards understanding interactions between biofilms and metals. *Current Opinion in Biotechnology*. **15**:181–186
- Beech, I.B., J.A. Sunner, and K. Hiraoka.** 2005. Microbe-surface interactions in biofouling and biocorrosion processes. *International Microbiology*. **8**:157 – 168
- Bodtker, G., T. Thorstenson, B.–L.P. Lillebo, B.E. Thobjornsen, R.H. Ulvoen, E. Sunde and T. Torsvik.** 2008. The effect of long-term nitrate treatment on SRB activity, corrosion rate and bacterial community composition in offshore H₂O injection systems. *Journal of Industrial Microbiology and Biotechnology*. **35 (12)**:1625–1636
- Borenstein, S.W.** 1994. *Microbiologically Influenced Corrosion Handbook*, Industrial Press Inc., New York
- Bradford, M.** 1976. A rapid and sensitive method for the quantitation of microgram quantities of protein utilizing the principle of protein-dye binding. *Analytical Biochemistry*. **72**:248–254
- Brenda, J.L., and J.S. Lee.** 2009. Factors contributing to corrosion of steel pilings in Duluth Superior harbor. *Corrosion*. **65(11)**:707-716
- Bryant, R.D., and E.J Laishley.** 1989. The role of hydrogenase in anaerobic biocorrosion. *Canadian Journal of Microbiology*. **36**:259-264

- Chongdar, S., G. Gunasekaran, and P. Kumar.** 2005. Corrosion inhibition of mild steel by aerobic biofilm. *Electrochimica Acta*. **50**:4655-4665
- Chou, T.P., C. Chandrasekaran, S. Limmer, C. Nguyen, and G.Z. Cao.** 2002. Organic-inorganic sol-gel coating for corrosion protection of stainless steel. *Journal of Material Science Letters*. **21**:251-255
- O'Halloran, R.J., M.M. Critchley, and R. Pasetto.** 2004. Microbiological influences in 'blue water' copper corrosion. *Journal of Applied Microbiology*. **97(3)**:590-597
- Coetser, S.E., and T.E. Cloete.** 2005. Biofouling and biocorrosion in industrial water systems. *Critical reviews in Microbiology*. **31(4)**:213-232
- Compere, C., and N. Le Bozec.** 1997. Influence of stainless steel surface treatment on the oxygen reduction reaction in seawater. *Corrosion Science*. **43(4)**:765-786
- Córdoba, V.C., M.A. Mejía, F. Echeverría, M. Morales, and J.A. Calderón.** 2011. Corrosion mitigation of buried structures by soils modification. *Ingeniare Revista Chilena de Ingeniería*. **19(3)**:486-497
- Correia, A.F., J.F.O. Segovia, R.M. Bezerra, M.C.A. Goncalves, S.S. Ornelas, D. Silveira, J.C.T. Carvalho, S.P.S.S. Diniz, and L.I.B. Kanzaki.** 2010. Aerobic and facultative microorganisms isolated from corroded metallic structures in a hydroelectric power unit in the Amazon Region of Brazil. *Air, Soil and Water Research*. **3**:113-121
- De Bruyn, E.** 1992. Microbial ecology of sulphide-producing bacteria in water cooling systems. PhD Thesis. University of Pretoria. South Africa
- De Freitas, V., C. Lins, M.L.M. Ferreira, and P.A. Saliba.** 2012. Corrosion Resistance of API X52 Carbon Steel in Soil Environment. *Journal of Materials Research and Technology*. **1(3)**:161-166
- de Melo, I.R., S.L.U. Filho, F.J.S. Oliveira, and F.P. de França.** 2011. Formation of biofilms and biocorrosion on AISI-1020 carbon steel exposed to aqueous systems containing different concentrations of a diesel/biodiesel mixture. *International Journal of Corrosion*. **6(2)**:197-202
- Dhanasekaran, D., N. Thajuddin, M. Rashmi, T.L. Deepika, and M. Gunasekaran.** 2009. Screening of biofouling activity in marine bacterial isolate from ship hull. *International Journal of Environmental Science and Technology*. **6(2)**:197-202
- Dunbar, J., S. Takala, Barns S.M., Davis J.A., Kuske C.R.** 1999. Levels of bacterial community diversity in four arid soils compared by cultivation and 16S rRNA gene cloning. *Applied and Environmental Microbiology*. **65**:1662-1669

- Dzieriewicz, Z., B. Cwalina, E. Chodurek, and T. Wilczok.** 1997. The relationship between microbial metabolic activity and biocorrosion of carbon steel. *Research in Microbiology*. **148**:785-793
- Eckford, R.E., and P.M. Fedorak.** 2002. Planktonic nitrate-reducing bacteria and sulfate-reducing bacteria in some Western Canadian oil field waters. *Journal of Industrial Microbiology and Biotechnology*. **29(2)**:83–92
- Eduardo, V.-C., J.J. Peña-Cabriales, and E. Martínez-Romero.** 2003. The Corrosion effects of Sulfate- and Ferric-Reducing Bacterial Consortia on Steel. *Geomicrobiology Journal*. **20(2)**:157-169
- Ekine, A.S., and G.O. Emujakporue.** 2012. Investigation of corrosion of buried oil pipeline by the electrical geophysical methods. *Environmental Research Journal*. **6(1)**:19–21
- Elboujdaini, M.** 2011. Hydrogen-induced cracking and sulfide stress cracking. Uhlig's corrosion handbook. Wiley, New Jersey
- Emerson, D., E.J. Fleming, and J.M. McBeth.** 2010. Iron-Oxidizing Bacteria: An Environmental and Genomic Perspective. *Annual Reviews in Microbiology*. **64**:561–83
- Enning, D., H. Venzlaff, J. Garrelfs, H.T. Dinh, V. Meyer, K. Mayrhofer, A.W. Enning, D., and J. Garrelfs.** 2014. Corrosion of Iron by Sulfate-Reducing Bacteria: New Views of an Old Problem. *Applied and Environmental Microbiology*. **80(4)**:1226-1236
- Hassel, M. Stratmann, and F. Widdel.** 2012. Marine sulfate-reducing bacteria cause serious corrosion of iron under electroconductive biogenic mineral crust. *Environmental Microbiology*. **14(7)**:1772–1787
- Freschi, C.R., L.F. de Oliveira e Silva Carvalho, and C.J.B. de Oliveira.** 2005. Comparison of DNA-extraction methods and selective enrichment broths on the detection of *Salmonella typhimurium* in swine feces by Polymerase Chain Reaction (PCR). *Brazilian Journal of Microbiology*. **36**:363-367
- Gadd, G.M.** 2010. Metals, minerals and microbes: geomicrobiology and bioremediation. *Microbiology*. **156**:609-643
- Garcia, F., A.L.R. Lopez, J.C. Guille, L.H. Sandoval, C.R. Gonzalez, V. Castano.** 2012. Corrosion inhibition in copper by isolated bacteria. *Anticorrosion Methods and Materials*. **59**:10-17
- Gevertz, D., A.J. Telang, G. Voordouw, and G.E. Jenneman.** 2000. Isolation and characterization of strains CVO and FWKO B, two novel nitrate-reducing, sulfide-oxidizing

bacteria isolated from oil field brine. *Applied and Environmental Microbiology*. **66(6)**:2491–2501

Gu, T. 2012. New understandings of biocorrosion mechanisms and their classifications. *Journal of Microbial and Biochemical Technology*. **4(4)**:3-6

Hamilton, W.A. 1985. Sulphate reducing bacteria and anaerobic corrosion. *Annual Review of Microbiology*. **39**:195–217

Hamilton, W.A. 2003. Microbially influenced corrosion as a model system for the study of metal microbe interactions: A unifying electron transfer hypothesis. *Biofouling*. **19(1)**:65-76

Hayyan, M., S.A. Sameh, A. Hayyan, and I.M. Al-Nashef. 2012. Utilizing of Sodium Nitrite as Inhibitor for Protection of Carbon Steel in Salt Solution. *International Journal of Electrochemical Science*. **7**:6941–6950

Herbert, H.P.F., Li.-C. Xua, and K.-Y. Chan. 2002. Effects of toxic metals and chemicals on biofilm and biocorrosion. *Water Research*. **36**:4709–4716

Hubert, C., M. Nemati, G. Jenneman, and G. Voordouw. 2005. Corrosion risk associated with microbial souring control using nitrate or nitrite. *Applied Microbiology and Biotechnology*. **68**:272–282

Ismail, A.I.M., and A.M. El-Shamy. 2009. Engineering behaviour of soil materials on the corrosion of mild steel. *Applied Clay Science*. **42**:356–362

Jan-Roblero, J., J.M. Romero, M. Amaya, and S. Le Borgne. 2004. Phylogenetic characterization of a corrosive consortium isolated from a sour gas pipeline. *Applied Microbiology and Biotechnology*. **64**:862-867

Javaherdashti, R. 2009. A Brief Review of General Patterns of MIC of Carbon Steel and Biodegradation of Concrete. *IUFS Journal of Biology*. **68(2)**:65-73

Jayaraman, A., J.C. Earthman, and Y.K. Wood. 1997. Corrosion inhibition by aerobic biofilms on SAE 1018 steel. *Applied Microbiology and Biotechnology*. **47**:62-68

Juzeliunas, E., R. Ramanauskas, A. Lugauskas, K. Leinartas, M. Samulevicien, and A. Sudavicius. 2006. Influence of wild strain *Bacillus mycooides* on metals: From corrosion acceleration to environmentally friendly protection. *Electrochimica Acta*. **51**:6085-6090

Kan, J., P. Chellamuthu, A. Obratzsova, J.E Moore, and K.H. Nealson. 2011. Diverse bacterial groups are associated with corrosive lesions at a Granite Mountain Record Vault (GMRV). *Journal of Applied Microbiology*. **111(2)**:329-337

- Karim, S., C.M. Mustafa, Md. Assaduzzaman, and M. Islam.** 2010. Effect of nitrite ion on corrosion inhibition of mild steel in simulated cooling water. *Chemical engineering research bulletin.* 14:87-91
- Kelly, R.G., J. R. Scully, D. W. Shoesmith and R. G. Buchheit.** 2007. Electrochemical Techniques in Corrosion Science and Engineering
- Kjeldsen, K.U., B.V. Kjellerup, K. Egli, B. Frolund, P.H. Nielsen, and K. Ingvorsen.** 2007. Phylogenetic and functional diversity of bacteria in biofilms from metal surfaces of an alkaline district heating system. *FEMS Microbiology Ecology.* 61:384-397
- Korenblum, E., E. Valoni, M. Penna, and L. Seldin.** 2010. Bacterial diversity in water injection systems of Brazilian offshore oil platforms. *Applied Microbiology and Biotechnology.* 3:791-800
- Kumaraswamy, R., S. Ebert, M.R. Gray, P.M. Fedorak, and J.M. Foght.** 2010. Molecular- and cultivation-based analyses of microbial communities in oil field water and in microcosms amended with nitrate to control H₂S production. *Applied Microbiology and Biotechnology.* 89(6):2027-2242
- Landoulsi J., K. Elkirat, T., C. Richard, D. Feron, and S. Pulvin.** 2008. Enzymatic Approach in Microbial-Influenced Corrosion: A Review Based on Stainless Steels in Natural Waters. *Environmental Science and Technology.* 42:2233–2242
- Lee, W., Z. Lewandowski, P.H. Nielsen, and W.A. Hamilton.** 1995. Role of sulphate-reducing bacteria in corrosion of mild steel: a review. *Biofouling.* 8:165-194
- Lewandowski, Z., and H. Beyenal.** 2008. Mechanisms of Microbially Influenced Corrosion. *Springer Series on Biofilms.* 4:35-64
- Lin, J., and Ballim, R.** 2012. Biocorrosion control: Current strategies and promising alternatives. *African Journal of Biotechnology.* 11(91):15736-15747
- Little, B.J., and J.S. Lee.** 2007. Microbiologically Influenced Corrosion. Wiley, USA
- Lopez, M.A., F.J.Z.D. de la Serna, J. Jan-Roblero, J.M. Romero, and C. Hernandez-Rodriguez.** 2006. Phylogenetic analysis of a biofilm bacterial population in a water pipeline in the Gulf of Mexico. *FEMS.* 58:145-154
- Magot, M., G. Ravot, X. Campaignolle, B. Ollivier, B.K.C Patel, M.L Fardeau, P. Thomas, J.L Crolet, and J.L Garcia.** 1997. *Dethiosulfobivrio peptidovorans* gen. nov., sp. nov., a new anaerobic slightly halophilic, thiosulfatereducing bacterium from corroding offshore oil wells. *International Journal of Systematic Bacteriology.* 47:818–824

- Malucknov, B.S.** 2012. Corrosion of steels induced by microorganisms. *Metallurgical Material Engineers*. **18(3)**:223–231
- Mansouri, H., S.A. Alavi, and M. Yari.** 2012. A Study of *Pseudomonas Aeruginosa* Bacteria in Microbial Corrosion. *ICCEES*. 42-47
- Marchesi, J., R.T. Sato, A.J. Martin, S.J. Hiam, and W. Wade.** 1998. Design and evaluation of bacterium-specific PCR primers that amplify genes coding for bacterial 16S rRNA. *Applied and Environmental Microbiology*. **64**:795- 799
- Marquis, F.D.S.** 1989. Strategy of macro and microanalysis in microbial corrosion. *Applied Science*. 125–151
- Marshall, K.C., and B.L. Blainey.** 1991. Role of bacterial adhesion in biofilm formation and biocorrosion. *Biofouling and Biocorrosion in Industrial Water Systems*. 24-46
- McCauley, A., C. Jones, and J. Jacobsen.** 2003. Soil pH and organic matter. *Nutrient Management-a self study course from the MSU extension service continuing education series*. **8**:1–12
- McInerney, M.J., K.L. Sublette, V.K. Bhupathiraju, J.D. Coates, R.M. Knapp, and T.P.A.A. Eugene.** 1993. Causes and Control of Microbially Induced Souring. *Developments in Petroleum Science*. **39**:363-371
- Mohammed, T., N. Otsuki, M. Hisada, and T. Shibata.** 2001. Effect of crack width and bar type on corrosion of steel in concrete. *Journal of Materials in Civil Engineering*. **13(3)**:194-201
- Moradi, M., J. Duan, H. Ashassi-Sorkhabi, and X. Luan.** 2011. De-alloying of 316 stainless steel in the presence of a mixture of metal oxidizing bacteria. *Corrosion Science*. **53(12)**:4282-4290
- Morcillo, M., D. de la Fuente, I. Díaz, and H. Cano.** 2011. Atmospheric corrosion of mild steel. *Revista de Metalurgia*. **47(5)**:426-444
- Muddlman, D.C., A. Gusev, A. Proctor, and D.M. Hercules.** 1994. Quantitative measurement of cyclosporin A in blood by Time-of-flight Mass Spectrometry. *Analytical Chemistry*. **66**:2623
- Murray, A.E., J.T. Hollibough, and C. Orrego.** 1996. Phylogenetic compositions of bacterioplankton from two California Estuaries compared by Denaturing Gradient Gel Electrophoresis of 16S rDNA fragments. *Applied and Environmental Microbiology*. **62(7)**:2676-2680

- Newman, R.C., K. Rumash, and B.J. Webster.** 1992. The effect of pre-corrosion on the corrosion rate of steel in neutral solutions containing sulfide: relevance to microbially influenced corrosion. *Corrosion Science*. **33**:1877–1884
- Nik, W.B.W., F. Zulkifli, M.M. Rahman, and R. Rosliza.** 2011. Corrosion Behavior of Mild Steel in Seawater from Two Different Sites of Kuala Terengganu Coastal Area. *International Journal of Basic & Applied Sciences*. **11(6)**:75-80
- Olesen, B.H., R. Avci, and Z. Lewandowski.** 2000. Manganese dioxide as a potential cathodic reactant in corrosion of stainless steels . *Corrosion Science*. **42**:211-227
- Oliveira, V.M., P.F. Lopes-Oliveira, M.R.Z. Passarini, C.B.A. Menezes, W.R.C. Oliveira, A.J. Rocha, and L.D. Sette.** 2011. Molecular analysis of microbial diversity in corrosion samples from energy transmission towers. *Biofouling: The Journal of Bioadhesion and Biofilm Research*. **27(4)**:435-447
- Orfei, L., S. Simison, and J.P. Busalmen.** 2006. Stainless steels can be cathodically protected using energy stored at the marine sediment/seawater interface. *Environmental Science and Technology*. **40**:6473-6478
- Paradies, H.H., W.R. Fisher, I. Haenssel, and D. Wagner.** 1992. Characterisation of metal biofilm interactions by extended absorption fine structure spectroscopy. *Microbial Corrosion Publication, European Federation of Corrosion Publication*. 168–189
- Pfennig, N.** 1984. Microbial behaviour in natural environments. The Microbe: Part II. Procarvates and Eukaryotes. Oxford University Press, Oxford
- Pillay, C., and J. Lin.** 2013. Metal corrosion by aerobic bacteria isolated from stimulated corrosion systems: Effects of additional nitrate sources. *International Biodeterioration & Biodegradation*. **83**:158-165
- Pope, D. H., D. J. Duquette, A. H. Johannes, and P. C. Wayner.** 1984. Microbially influenced corrosion of industrial alloys. *Materials Performance*. **23**:14-18
- Rajasekar, A., S. Maruthamuthu, N. Palaniswamy and A. Rajendran.** 2007a. Biodegradation of corrosion inhibitors and their influence on petroleum product pipeline. *Microbiological Research*. **162**:355-368
- Rajasekar, A., T.G. Babu, S.K. Pandian, S. Maruthamuthu, N. Palaniswamy, and A. Rajendran.** 2007b. Biodegradation and corrosion behaviour of manganese oxidizer *Bacillus cereus* ACE4 in diesel transporting pipeline. *Corrosion Science*. **49**:2694–2710

- Rajasekar, A., B. Anandkumar, S. Maruthamuthu, Y.P. Ting, and P.K.S.M. Rahman.** 2010. Characterization of corrosive bacterial consortia isolated from petroleum-product-transporting pipelines. *Applied Microbiology and Biotechnology*. **85**:1175-1188
- Rajasekar, A., and Y.-P., Ting.** 2011. Role of Inorganic and Organic Medium in the Corrosion Behavior of *Bacillus megaterium* and *Pseudomonas* sp. in Stainless Steel SS 304. *Industrial and Engineering Chemistry Research*. **50**:12534-12541
- Rempel, C.L., E.R.W. Evitts, and E.M. Nemati.** 2006. Dynamics of corrosion rates associated with nitrite or nitrate mediated control of souring under biological conditions simulating an oil reservoir. *Journal of Industrial Microbiology and Biotechnology*. **33**:878–886
- Ryhl-Svendsen, M.** 2008. Corrosivity measurements of indoor museum environments using lead coupons as dosimeters. *Journal of Cultural Heritage*. **9**:285-293
- Russell, A.D.** 2003. Similarities and differences in the responses of microorganisms to biocides. *Journal of Antimicrobial Chemotherapy*. **52**:750-763
- Sambrook, J., E.F. Fritsch, and T. Maniatis.** 1989. Molecular cloning: a laboratory manual. Cold Spring Harbor Laboratory, Cold Spring Harbor, New York
- Santana, J.J., B.M. Fernández-Pérez, J. Morales, H.C. Vasconcelos, R.M. Souto, and S. González.** 2012. Characterization of the Corrosion Products Formed on Zinc in Archipelagic Subtropical Environments. *International Journal of Electrochemical Science*. **7**:12730-12741
- Saravia, S.G., R.S., Guiamet, and H.A., Videla.** 2003. Prevention and protection of the effects of biocorrosion and biofouling, minimizing the environmental impact. *Revista de Metalurgia*. 49-54
- Schiermeyer, E.M., P.P. Provencio, and D.E. Northup.** 2000. Microbially induced iron oxidation: What, where, how. (<http://www.osti.gov/>)
- Schwermer, C.U., G. Lavik, R.M.M. Abed, B. Dunsmore, T.G. Ferdelman, P. Stoodley, A. Gieseke, and D. de Beer.** 2008. Impact of nitrate on the structure and function of bacterial biofilm communities in pipelines used for injection of seawater into oil fields. *Applied and Environmental Microbiology*. 2841–2851
- Setareh, M., and R. Javaherdashti.** 2003. Assessment and control of MIC in a sugar cane factory. *Metals and Corrosion*. **54(4)**:259-263
- Shi, X., N. Xie, and J. Gong.** 2011. Recent progress in the research on microbially influenced corrosion: A bird's eye view through the engineering lens. *Recent Patents on Corrosion Science*. **1**:118-131

- Shimura, T., and K. Aramaki.** 2008. Improvement of the film thickness by modification of the hydroxymethylbenzene SAM with tetraethoxysilane and octanediol for protection of iron from corrosion in 0.5M NaCl. *Corrosion Science*. **50**:1397-1405
- Singh, D.D.N., S. Yadav, and J.K. Saha.** 2008. Role of climatic conditions on corrosion characteristics of structural steels. *Corrosion Science*. **50**:93–110
- Soracco, R.J., D.H. Pope, J.M. Eggers, and T.N. Effinger.** 1988. Microbiologically influenced corrosion investigations in electric power generating stations. *Proc. NACE Corrosion*. 88
- Sreekumari, K.R., K. Nandakumar, and Y. Kikuchi.** 2001. Bacterial adhesion to weld metals: significance of substratum microstructure. *Biofouling*. **17**:303-316
- Stadler, R., W. Fuerbeth, K. Harneit, M. Grooters, M. Woellbrink, and W. Sand.** 2008. First evaluation of the applicability of microbial extracellular polymeric substances for corrosion protection of metal substrates. *Electrochimica Acta*. **54**:91–99
- Sturman, P.J. and D.M. Goeres.** 1999. Control of hydrogen sulfide in oil and gas wells with nitrite injection. SPE paper 56772, SPE Annual Conference, Houston, TX
- Sutherland, I.W.** 1985. Biosynthesis and composition of Gram negative bacterial extracellular and cell wall polysaccharides. *Annual Review of Microbiology*. **39**:243–262.
- Tabari, K., M. Tabari, and O. Tabari.** 2011. Application of biocompetitive exclusion in prevention and controlling biogenetic H₂S of petroleum reservoirs. *Australian Journal of Basic Applied Science*. **5(12)**:715-718.
- Tamura, K, J. Dudley, M. Nei, and S. Kumar.** 2007. MEGA4: Molecular Evolutionary Genetics Analysis (MEGA) software version 4.0. *Molecular Biology and Evolution*. **24**:1596-1599
- Telang, A. J., S. Ebert, J.M. Foght, D.W.S. Westlake, G.E. Jenneman, D. Gevertz, and G. Voordouw.** 1997. Effect of nitrate injection on the microbial community in an oil field as monitored by reverse sample genome probing. *Applied and Environmental Microbiology*. **63**:1785-1793
- Thomas R. J.** 2002. Biological Corrosion Failures. ASM Handbook. ASM International
- Uhlig, H.H.** 2000. Uhlig's Corrosion Handbook. Wiley, London
- Vairinhos, F., W. Wallace, and D.J.D. Nicholas.** 1989. Simultaneous Assimilation and Denitrification of Nitrate by *Bradyrhizobium japonicum*. *Journal of General Microbiology*. **135**:189-193

- Valencia-Cantero E., J.J. Peña-Cabriales, and E. Martínez-Romero.** 2003. The Corrosion Effects of Sulfate- and Ferric-Reducing Bacterial *Consortia on Steel*. *Geomicrobiology Journal*. **20(2):**157-169
- Videla, H.A., and L.K. Herrera.** 2005. Microbiologically influenced corrosion: looking to the future. *International Microbiology*. **8:**169-180
- Volkland, H.-P., H. Harms, K.K. Oskar.** 2000. Corrosion inhibition of mild steel by bacteria. Biofouling: *The Journal of Bioadhesion and Biofilm Research*. **15(4):**287-297
- Voordouw, G., M. Nemati, and G.E. Jenneman.** 2002. Use of nitrate-reducing, sulfide oxidizing bacteria to reduce souring in oil fields: interactions with SRB and effects on corrosion. Paper No. 02034. Proceedings of NACE Corrosion 2002, Denver, CO
- Walsh, D.,E. Willis, and T. Van Diepen.** 1994. The effect of microstructure on microbial interaction with metals accent welding. *Corrosion*. 612-622
- Walter, M.C., T. Rattei, R. Arnold, U. Guldener, M. Munsterkotter, K. Nenova, G. Kastenmuller, P. Tischler, A. Wolling, A. Volz, N. Pongratz, R. Jost, H.W. Mewes, and D. Frishman.** 2009. PEDANT covers all complete RefSeq genomes. *Nucleic Acids Resources*. **37:**408–411
- Wan, Y., L. Ding, X. Wang, Y. Li, H. Sun, and Q. Wang.** 2013. Corrosion Behaviors of Q235 Steel in Indoor Soil. *International Journal of Electrochemical Science*. **8:**12531–12542
- Wang, W., Z. Qiu, H. Tan, and L. Cao.** 2014. Siderophore production by actinobacteria. *An International Journal on the Role of Metal Ions in Biology, Biochemistry and Medicine*. **27:**9739
- Wen, W., D. Jizhou, C. Liye, and S. Hongbo.** 2011. Isolation of a nitrate-reducing bacteria strain from oil field brine and the inhibition of sulfate-reducing bacteria. *African Journal of Biotechnology*. **10(49):**10019-10029
- Widdel, F.** 1988. Microbiology and ecology of sulfate-and sulfur-reducing bacteria. *In Biology of Anaerobic Micro-organisms*. 469–585
- Wilkie, A.C.** 2005. Anaerobic digestion: biology and benefits. *Natural Resource Agriculture and Engineering Service*. **176:**63-72
- Xu, C., Y. Zhang, G. Cheng, and W. Zhu.** 2007. Localized corrosion behaviour of 316L stainless steel in the presence of sulfate-reducing and iron-oxidizing bacteria. *Materials Science and Engineering*. **443:**235-241

- Ye, W., X. Liu, S. Lin, J. Tan, J. Pan, D. Li, and H. Yang.** 2009. The vertical distribution of bacterial and archaeal communities in the water and sediment of Lake Taihu. *FEMS Microbiology and Ecology*. **70(2):**263-276
- Zhang, T., and H.H.P. Fang.** 2001. Phylogenetic diversity of a SRB-rich marine biofilm. *Applied Microbiology and Biotechnology*. **57:**437-440
- Zhu, X.Y., J. Lubeck, and J.J. Kilbane.** 2003. Characterization of microbial communities in gas industry pipelines. *Applied and Environmental Microbiology*. **69:**5354-5363
- Zhu, Q., H.T. Zhu, A.K. Tieu, and C. Kong.** 2011. Three dimensional microstructure study of oxide scale formed on a high-speed steel by means of SEM, FIB and TEM. *Corrosion Science*, doi: 10.1016/j.corsci.2011.07.004
- Zinkevich, V., I. Bogdarina, H. Kang, M.A.W. Hill, R. Tapper, and I.B. Beech.** 1996. Characterisation of exopolymers produced by different isolates of marine sulphate-reducing bacteria. *International Biodeterioration and Biodegradation*. **37(3-4):**163–172
- Zuo, R.** 2007. Biofilms: strategies for metal corrosion inhibition employing microorganisms. *Applied Microbiology and Biotechnology*. **76:**1245–1253
- Zuo, R., D. Ornek, B.C. Syrett, R.M. Green, C.-H. Hsu, F.B. Mansfeld, and T.K. Wood.** 2004. Inhibiting mild steel corrosion from sulfate-reducing bacteria using antimicrobial-producing biofilms in Three-Mile-Island process water. *Applied Microbiology and Biotechnology*. **64:**275–283
- Zuo, R., E. Kus, F. Mansfeld, and T.K. Wood.** 2005. The importance of live biofilms in corrosion protection. *Corrosion Science*. **47:**279–287

Appendix I: Raw weight loss data and corrosion rate calculations

Table A1: Raw corrosion rate data from laboratory study

Autoclaved Control						Non-autoclaved					
	Initial Weight	Final Weight	% Weight loss	Mean	STD DEV		Initial Weight	Final Weight	% Weight loss	Mean	STD DEV
A1	5,15	5,11	0,78			A1	5,27	5,21	1,14		
A2	5,27	5,23	0,76	0,77	0,01	A2	5,2	5,15	0,96	1,15	0,19
A3	5,26	5,22	0,76			A3	5,23	5,16	1,34		
B1	5,19	5,11	1,54			B1	5,19	5,12	1,35		
B2	5,19	5,15	0,77	1,09	0,40	B2	5,23	5,15	1,53	1,41	0,11
B3	5,19	5,14	0,96			B3	5,2	5,13	1,35		
C1	5,18	5,12	1,16			C1	5,21	4,93	5,37		
C2	5,28	5,16	2,27	1,82	0,69	C2	5,25	5,05	3,81	4,20	1,03
C3	5,43	5,32	2,03			C3	5,25	5,07	3,43		
D1	5,21	5,13	1,54			D1	5,11	4,85	5,09		
D2	5,3	5,06	4,53	2,53	1,80	D2	5,25	5,06	3,62	4,99	1,32
D3	5,27	5,19	1,52			D3	5,28	4,95	6,25		
E1	5,22	5,03	3,64			E1	5,31	4,96	6,59		
E2	5,16	5,06	1,94	3,24	1,18	E2	5,22	4,9	6,13	6,16	0,42
E3	5,3	5,08	4,15			E3	5,22	4,92	5,75		
F1	5,21	5,11	1,92			F1	5,24	4,84	7,63		
F2	5,15	5,01	2,72	2,37	0,47	F2	5,25	5,03	4,19	4,89	2,47
F3	5,24	5,11	2,48			F3	5,27	5,12	2,85		

A: Week 4; B: Week 8; C: Week 12; D: Week 16; E: Week 20; F: Week 24

Table A1: Raw corrosion rate data from laboratory study (Cont.)

Ammonium Nitrate (5uM)						Ammonium Nitrate (10uM)					
	Initial Weight	Final Weight	% Weight loss	Mean	STD DEV		Initial Weight	Final Weight	% Weight loss	Mean	STD DEV
A1	5,19	5,17	0,39			A1	5,22	5,07	2,87		
A2	5,28	5,23	0,95	0,89	0,48	A2	5,26	5,1	3,04	3,07	0,21
A3	5,2	5,13	1,35			A3	5,17	5	3,29		
B1	5,25	5,07	3,43			B1	5,23	4,9	6,31		
B2	5,21	5,05	3,07	3,12	0,29	B2	5,29	5,01	5,29	6,37	1,10
B3	5,25	5,1	2,86			B3	5,2	4,81	7,50		
C1	5,23	5,06	3,25			C1	5,2	4,69	9,81		
C2	5,24	4,89	6,68	4,39	1,99	C2	5,24	4,75	9,35	8,84	1,31
C3	5,27	5,1	3,23			C3	5,17	4,79	7,35		
D1	5,25	4,95	5,71			D1	5,27	4,44	15,75		
D2	5,18	4,96	4,25	6,67	3,01	D2	5,25	4,55	13,33	14,68	1,23
D3	5,28	4,75	10,04			D3	5,21	4,43	14,97		
E1	5,36	4,73	11,75			E1	5,25	4,26	18,86		
E2	5,25	4,57	12,95	11,68	1,31	E2	5,25	4	23,81	20,80	2,64
E3	5,22	4,68	10,34			E3	5,22	4,19	19,73		
F1	5,26	4,68	11,03			F1	5,23	4,05	22,56		
F2	5,24	4,53	13,55	11,78	1,53	F2	5,27	4,06	22,96	22,67	0,25
F3	5,29	4,72	10,78			F3	5,2	4,03	22,50		

A: Week 4; B: Week 8; C: Week 12; D: Week 16; E: Week 20; F: Week 24

Table A1: Raw corrosion rate data from laboratory study (Cont.)

Ammonium Nitrate (20uM)						Ammonium Nitrate (40uM)					
	Initial Weight	Final Weight	% Weight loss	Mean	STD DEV		Initial Weight	Final Weight	% Weight loss	Mean	STD DEV
A1	5,25	5,08	3,24			A1	5,25	5,1	2,86		
A2	5,24	5,18	1,15	2,48	1,16	A2	5,24	5,13	2,10	2,10	0,76
A3	5,23	5,07	3,06			A3	5,24	5,17	1,34		
B1	5,28	4,94	6,44			B1	5,2	4,61	11,35		
B2	5,27	4,97	5,69	5,75	0,66	B2	5,22	4,45	14,75	12,15	2,31
B3	5,28	5,01	5,11			B3	5,22	4,68	10,34		
C1	5,23	4,65	11,09			C1	5,29	4,37	17,39		
C2	5,19	4,56	12,14	11,28	0,78	C2	5,25	4,2	20,00	19,72	2,20
C3	5,28	4,72	10,61			C3	5,24	4,1	21,76		
D1	5,29	4,34	17,96			D1	5,17	4,01	22,44		
D2	5,18	4,49	13,32	13,87	3,84	D2	5,25	3,81	27,43	26,63	3,85
D3	5,22	4,68	10,34			D3	5,23	3,66	30,02		
E1	5,2	4,15	20,19			E1	5,22	3,62	30,65		
E2	5,27	4,04	23,34	21,47	1,66	E2	5,32	3,67	31,02	30,57	0,49
E3	5,27	4,17	20,87			E3	5,26	3,68	30,04		
F1	5,33	4,11	22,89			F1	5,24	3,72	29,01		
F2	5,27	4,22	19,92	21,45	1,48	F2	5,27	3,69	29,98	30,04	1,06
F3	5,29	4,15	21,55			F3	5,14	3,54	31,13		

A: Week 4; B: Week 8; C: Week 12; D: Week 16; E: Week 20; F: Week 24

Table A1: Raw corrosion rate data from laboratory study (Cont.)

Sodium Nitrite (5uM)						Sodium Nitrite (10uM)					
	Initial Weight	Final Weight	% Weight loss	Mean	STD DEV		Initial Weight	Final Weight	% Weight loss	Mean	STD DEV
A1	5,24	5,24	0			A1	5,29	5,29	0,00		
A2	5,25	5,24	0,19	0,06	0,11	A2	5,24	5,24	0,00	0,00	0
A3	5,26	5,26	0,00			A3	5,24	5,24	0,00		
B1	5,27	5,19	1,52			B1	5,2	5,2	0,00		
B2	5,22	5,12	1,92	1,59	0,30	B2	5,23	5,23	0,00	0,00	0
B3	5,25	5,18	1,33			B3	5,26	5,26	0,00		
C1	5,24	5,1	2,67			C1	5,23	5,23	0,00		
C2	5,28	5,1	3,41	2,73	0,66	C2	5,32	5,32	0,00	0,00	0
C3	5,25	5,14	2,10			C3	5,2	5,2	0,00		
D1	5,25	5,01	4,57			D1	5,33	5,32	0,19		
D2	5,22	5,05	3,26	4,01	0,68	D2	5,17	5,17	0,00	0,06	0
D3	5,22	5	4,21			D3	5,27	5,27	0,00		
E1	5,22	4,94	5,36			E1	5,19	5,19	0,00		
E2	5,3	5,03	5,09	5,55	0,56	E2	5,19	5,17	0,39	0,25	0
E3	5,18	4,86	6,18			E3	5,39	5,37	0,37		
F1	5,19	4,63	10,79			F1	5,27	5,25	0,38		
F2	5,26	4,77	9,32	9,44	1,30	F2	5,16	5,14	0,39	0,38	0
F3	5,24	4,81	8,21			F3	5,31	5,29	0,38		

A: Week 4; B: Week 8; C: Week 12; D: Week 16; E: Week 20; F: Week 24

Table A1: Raw corrosion rate data from laboratory study (Cont.)

Sodium Nitrite (20uM)						Sodium Nitrite (40uM)					
	Initial Weight	Final Weight	% Weight loss	Mean	STD DEV		Initial Weight	Final Weight	% Weight loss	Mean	STD DEV
A1	5,19	5,19	0,00			A1	5,26	5,26	0,00		
A2	5,21	5,21	0,00	0,00	0	A2	5,23	5,23	0,00	0,00	0
A3	5,28	5,28	0,00			A3	5,32	5,32	0,00		
B1	5,29	5,29	0,00			B1	5,18	5,18	0,00		
B2	5,22	5,22	0,00	0,00	0	B2	5,3	5,3	0,00	0,00	0
B3	5,32	5,32	0,00			B3	5,2	5,2	0,00		
C1	5,24	5,24	0,00			C1	5,19	5,19	0,00		
C2	5,27	5,27	0,00	0,00	0	C2	5,21	5,21	0,00	0,00	0
C3	5,25	5,25	0,00			C3	5,28	5,28	0,00		
D1	5,17	5,17	0,00			D1	5,22	5,22	0,00		
D2	5,25	5,25	0,00	0,00	0	D2	5,22	5,22	0,00	0,00	0
D3	5,2	5,2	0,00			D3	5,2	5,2	0,00		
E1	5,16	5,16	0,00			E1	5,2	5,2	0,00		
E2	5,24	5,24	0,00	0,00	0	E2	5,19	5,19	0,00	0,00	0
E3	5,24	5,24	0,00			E3	5,18	5,18	0,00		
F1	5,24	5,24	0,00			F1	5,19	5,19	0,00		
F2	5,21	5,21	0,00	0,00	0	F2	5,23	5,23	0,00	0,00	0
F3	5,25	5,25	0			F3	5,24	5,24	0,00		

A: Week 4; B: Week 8; C: Week 12; D: Week 16; E: Week 20; F: Week 24

Table A2: Raw corrosion rate data from *in situ* study

Autoclaved						Non Autoclaved					
	Before	After	Weight Loss (mg/cm ²)	Mean	STD DEV		Before	After	Weight Loss (mg/cm ²)	Mean	STD DEV
A1	3,69	3,66	2,31			A1	3,82	3,79	2,31		
A2	3,62	3,59	2,31	2,31	0,00	A2	3,68	3,65	2,31	2,31	0,00
A3	3,68	3,65	2,31			A3	3,74	3,71	2,31		
			0,00								
B1	3,49	3,45	3,08			B1	3,70	3,67	2,31		
B2	3,43	3,39	3,08	3,08	0,00	B2	3,70	3,66	3,08	2,82	0,44
B3	3,54	3,50	3,08			B3	3,51	3,47	3,08		
C1	3,63	3,59	3,08			C1	3,58	3,53	3,85		
C2	3,82	3,78	3,08	3,08	0,00	C2	3,74	3,68	4,62	3,85	0,77
C3	3,91	3,87	3,08			C3	3,80	3,76	3,08		
D1	3,63	3,58	3,85			D1	3,58	3,54	3,08		
D2	3,63	3,60	2,31	3,33	0,89	D2	3,63	3,56	5,38	3,59	1,60
D3	3,87	3,82	3,85			D3	3,49	3,46	2,31		
E1	3,72	3,67	3,85			E1	3,63	3,57	4,62		
E2	3,79	3,75	3,08	3,33	0,44	E2	3,47	3,43	3,08	3,85	0,77
E3	3,77	3,73	3,08			E3	3,74	3,69	3,85		
F1	3,59	3,55	3,08			F1	3,84	3,80	3,08		
F2	3,93	3,89	3,08	3,08	0,00	F2	3,62	3,58	3,08	3,08	0,00
F3	3,63	3,59	3,08			F3	3,69	3,65	3,08		

A: Week 4; B: Week 8; C: Week 12; D: Week 16; E: Week 20; F: Week 24

Table A2: Raw corrosion rate data from *in situ* study (Cont.)

	Autoclaved + Nitrite						Non autoclaved + Nitrite				
	Before	After	Weight Loss (mg/cm ²)	Mean	STD DEV		Before	After	Weight Loss (mg/cm ²)	Mean	STD DEV
A1	3,80	3,78	1,54			A1	3,74	3,71	2,31		
A2	3,68	3,66	1,54	1,79	0,44	A2	3,64	3,62	1,54	2,05	0,44
A3	3,36	3,33	2,31			A3	3,65	3,62	2,31		
B1	3,66	3,64	1,54			B1	3,67	3,65	1,54		
B2	3,78	3,76	1,54	1,54	0,00	B2	3,61	3,59	1,54	2,05	0,89
B3	3,80	3,78	1,54			B3	3,63	3,59	3,08		
C1	3,66	3,64	1,54			C1	3,73	3,70	2,31		
C2	3,86	3,84	1,54	2,05	0,89	C2	3,63	3,60	2,31	2,05	0,44
C3	3,63	3,59	3,08			C3	3,72	3,70	1,54		
D1	3,55	3,52	2,31			D1	3,77	3,73	3,08		
D2	3,61	3,59	1,54	1,79	0,44	D2	3,65	3,61	3,08	2,82	0,44
D3	3,65	3,63	1,54			D3	3,71	3,68	2,31		
E1	3,50	3,47	2,31			E1	3,66	3,63	2,31		
E2	3,68	3,65	2,31	2,56	0,44	E2	3,76	3,72	3,08	2,56	0,44
E3	3,86	3,82	3,08			E3	3,66	3,63	2,31		
F1	3,84	3,82	1,54			F1	3,62	3,59	2,31		
F2	3,65	3,63	1,54	1,79	0,44	F2	3,33	3,29	3,08	2,56	0,44
F3	3,78	3,75	2,31			F3	3,76	3,73	2,31		

A: Week 4; B: Week 8; C: Week 12; D: Week 16; E: Week 20; F: Week 24

Table A2: Raw corrosion rate data from *in situ* study (Cont.)

	Autoclaved + Nitrate						Non-Autoclaved + Nitrate				
	Before	After	Weight Loss (mg/cm ²)	Mean	STD DEV		Before	After	Weight Loss (mg/cm ²)	Mean	STD DEV
A1	3,65	3,39	20,00			A1	3,68	3,48	15,38		
A2	3,78	3,49	22,31	18,72	4,37	A2	3,92	3,70	16,92	16,67	1,18
A3	3,73	3,55	13,85			A3	3,61	3,38	17,69		
B1	3,67	3,41	20,00			B1	3,68	3,29	30,00		
B2	3,32	2,93	30,00	27,18	6,27	B2	3,99	3,67	24,62	25,64	3,95
B3	3,60	3,19	31,54			B3	3,62	3,33	22,31		
C1	3,68	3,28	30,77			C1	3,90	3,26	49,23		
C2	3,55	3,19	27,69	30,77	3,08	C2	3,72	3,19	40,77	44,87	4,24
C3	3,64	3,20	33,85			C3	3,78	3,20	44,62		
D1	3,85	3,49	27,69			D1	3,86	3,33	40,77		
D2	3,70	3,25	34,62	30,26	3,79	D2	3,82	3,49	25,38	34,36	8,01
D3	3,71	3,34	28,46			D3	3,96	3,48	36,92		
E1	3,59	3,01	44,62			E1	3,80	3,36	33,85		
E2	3,97	3,38	45,38	45,38	0,77	E2	3,49	3,14	26,92	30,51	3,47
E3	3,74	3,14	46,15			E3	3,78	3,38	30,77		
F1	3,86	3,40	35,38			F1	3,55	2,90	50,00		
F2	3,92	3,52	30,77	32,05	2,91	F2	3,83	3,26	43,85	37,95	15,85
F3	3,94	3,55	30,00			F3	3,64	3,38	20,00		

A: Week 4; B: Week 8; C: Week 12; D: Week 16; E: Week 20; F: Week 24

Table A3: Weight loss data by individual isolates at various nitrite concentrations

	control			mean	std dev	5mM Nitrite			mean	std dev
	initial	final	% loss			initial	final	% loss		
	3,51	3,29	16,92			3,43	3,31	9,23		
0	3,66	3,44	16,92	16,41	0,89	3,72	3,53	14,62	13,85	4,28
	3,76	3,56	15,38			3,48	3,25	17,69		
	3,66	3,50	12,31			3,75	3,61	10,77		
2	3,71	3,49	16,92	13,33	3,20	3,68	3,52	12,31	11,79	0,89
	3,71	3,57	10,77			3,64	3,48	12,31		
	3,87	3,60	20,77			3,61	3,43	13,85		
4	3,42	3,15	20,77	20,77	0,00	3,72	3,51	16,15	14,36	1,60
	3,63	3,36	20,77			3,85	3,68	13,08		
	3,69	3,27	32,31			3,62	3,47	11,54		
5	3,56	3,26	23,08	27,44	4,64	3,93	3,75	13,85	13,08	1,33
	3,68	3,33	26,92			3,66	3,48	13,85		
	3,81	3,60	16,15			3,61	3,44	13,08		
6	3,54	3,33	16,15	15,90	0,44	3,56	3,42	10,77	11,54	1,33
	3,69	3,49	15,38		1,60	3,64	3,50	10,77		
	3,64	3,40	18,46		1,54	3,94	3,68	20,00		
8	4,01	3,79	16,92	18,21	1,18	3,87	3,58	22,31	20,77	1,33
	3,69	3,44	19,23			3,59	3,33	20,00		
	3,81	3,59	16,92			3,67	3,46	16,15		
9	3,75	3,57	13,85	18,21	5,12	3,66	3,42	18,46	16,92	1,33
	3,89	3,58	23,85			3,83	3,62	16,15		
	3,86	3,66	15,38			3,77	3,61	12,31		
10	3,70	3,52	13,85	13,08	2,77	3,77	3,58	14,62	13,08	1,33
	3,76	3,63	10,00			3,67	3,51	12,31		
	3,88	3,45	33,08			3,67	3,50	13,08		
11	3,94	3,61	25,38	26,15	6,57	3,56	3,37	14,62	13,59	0,89
	3,58	3,32	20,00			3,74	3,57	13,08		
	3,70	3,48	16,92			3,64	3,45	14,62		
13	3,94	3,68	20,00	18,72	1,60	3,66	3,37	22,31	17,69	4,07
	3,63	3,38	19,23			3,61	3,40	16,15		
	3,51	3,27	18,46			3,68	3,48	15,38		
14	3,90	3,62	21,54	20,00	1,54	3,86	3,66	15,38	15,38	0,00
	3,81	3,55	20,00			3,82	3,62	15,38		
	3,64	3,33	23,85			3,53	3,39	10,77		
16	3,55	3,38	13,08	17,69	5,55	3,71	3,55	12,31	12,05	1,18
	3,64	3,43	16,15			3,71	3,54	13,08		

Table A3: Weight loss data by individual isolates at various nitrite concentrations (cont.)

	10mM Nitrite			mean	std dev	20mM Nitrite			mean	std dev
	initial	final	% loss			initial	final	% loss		
	5,23	5,02	15,56			4,97	4,88	6,67		
0	3,67	3,43	18,46	17,02	1,45	3,65	3,56	6,92	8,73	3,35
	5,22	4,99	17,04			5,26	5,09	12,59		
	3,81	3,47	26,15			5,17	5,03	10,37		
2	5,01	4,76	18,52	20,82	4,64	5,37	5,29	5,93	8,15	2,22
	5,12	4,88	17,78			5,12	5,01	8,15		
	3,82	3,65	13,08			5,09	4,99	7,41		
4	3,58	3,38	15,38	14,10	1,18	3,59	3,47	9,23	8,62	1,05
	3,76	3,58	13,85			3,46	3,34	9,23		
	3,68	3,56	9,23			5,08	5,00	5,93		
5	5,16	5,01	11,11	8,76	2,63	4,98	4,89	6,67	7,16	1,54
	5,06	4,98	5,93			5,11	4,99	8,89		
	3,78	3,61	13,08			3,67	3,51	12,31		
6	5,09	4,96	9,63	13,47	4,05	5,34	5,24	7,41	9,29	2,64
	3,67	3,44	17,69			5,06	4,95	8,15		
	5,09	4,88	15,56			3,84	3,73	8,46		
8	5,09	4,88	15,56	15,06	0,86	3,69	3,57	9,23	9,35	0,96
	5,37	5,18	14,07			5,14	5,00	10,37		
	5,37	5,23	10,37			3,87	3,70	13,08		
9	3,56	3,42	10,77	11,66	1,90	3,89	3,74	11,54	12,05	0,89
	3,61	3,43	13,85			3,58	3,43	11,54		
	5,34	5,16	13,33			5,00	4,91	6,67		
10	5,02	4,85	12,59	14,28	2,32	3,63	3,48	11,54	9,66	2,62
	3,60	3,38	16,92			3,79	3,65	10,77		
	3,71	3,45	20,00			5,37	5,24	9,63		
11	3,57	3,27	23,08	20,53	2,33	3,85	3,70	11,54	12,95	4,21
	5,22	4,97	18,52			3,65	3,42	17,69		
	5,08	4,96	8,89			5,18	5,07	8,15		
13	5,34	5,22	8,89	9,63	1,28	3,70	3,55	11,54	9,28	1,96
	5,32	5,17	11,11			5,18	5,07	8,15		
	5,37	5,22	11,11			3,86	3,75	8,46		
14	3,77	3,58	14,62	14,47	3,29	3,67	3,51	12,31	10,63	1,97
	3,81	3,58	17,69			5,02	4,87	11,11		
	5,14	4,98	11,85			5,14	5,07	5,19		
16	5,36	5,20	11,85	12,59	1,28	5,37	5,31	4,44	5,77	1,70
	5,16	4,97	14,07			3,89	3,79	7,69		

Appendix II: EDX Spectra

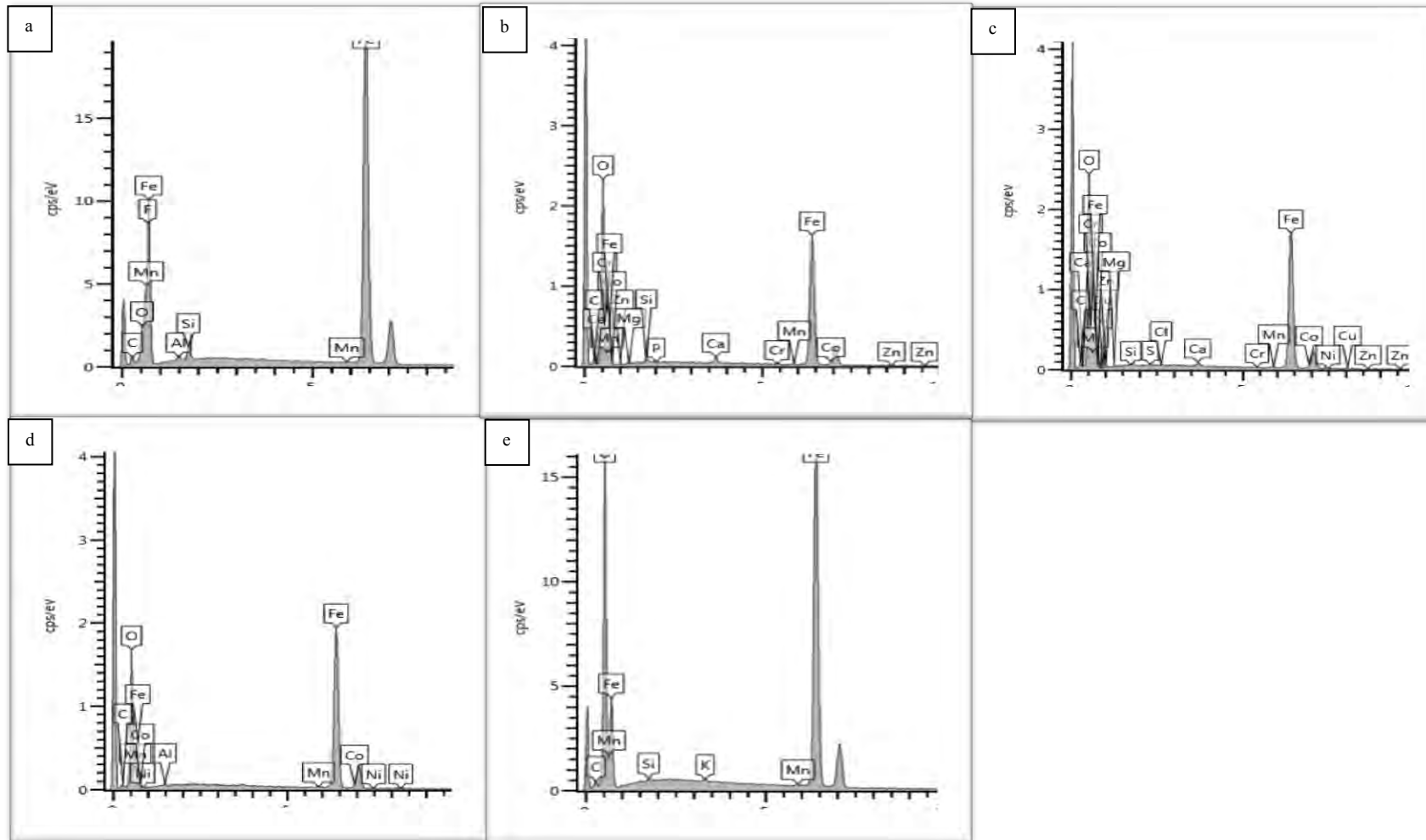


Figure A1: EDX spectra showing elemental composition of the different corrosion products on the surface of the untreated and treated mild steel coupons (Laboratory study). (a) untreated coupon, (b) Corrosion product 1, (c) Corrosion product 2, (d) Corrosion product 3 and, (e) Corrosion product 4

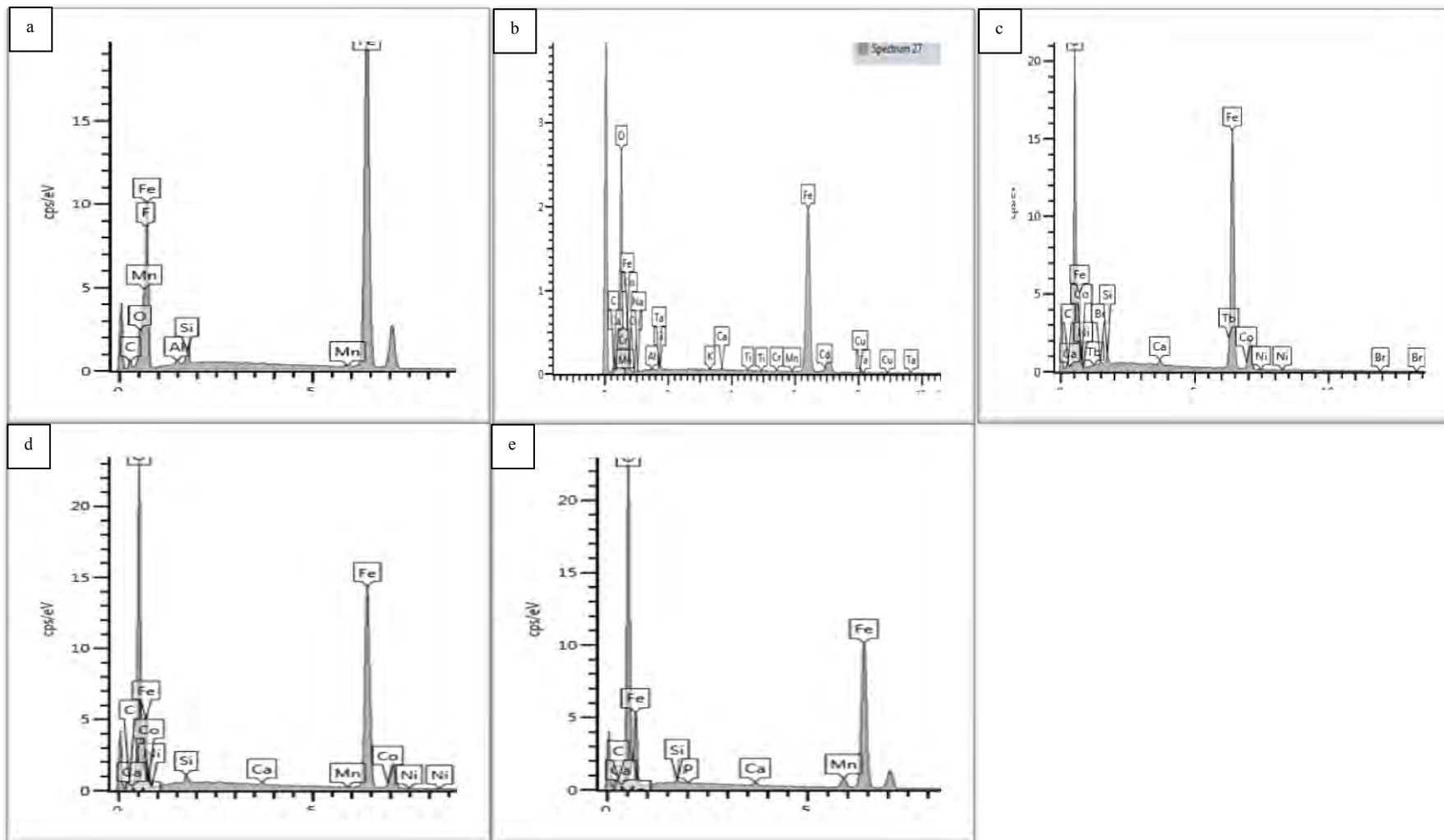


Figure A2: EDX spectra showing different elemental composition of the corrosion products on the surface of the mild steel coupons (*in situ* study). (a) untreated coupon, (b) Corrosion product 1, (c) Corrosion product 2, (d) Corrosion product 3 and, (e) Corrosion product 4

Appendix III: Bacterial population analysis: PCR Gels

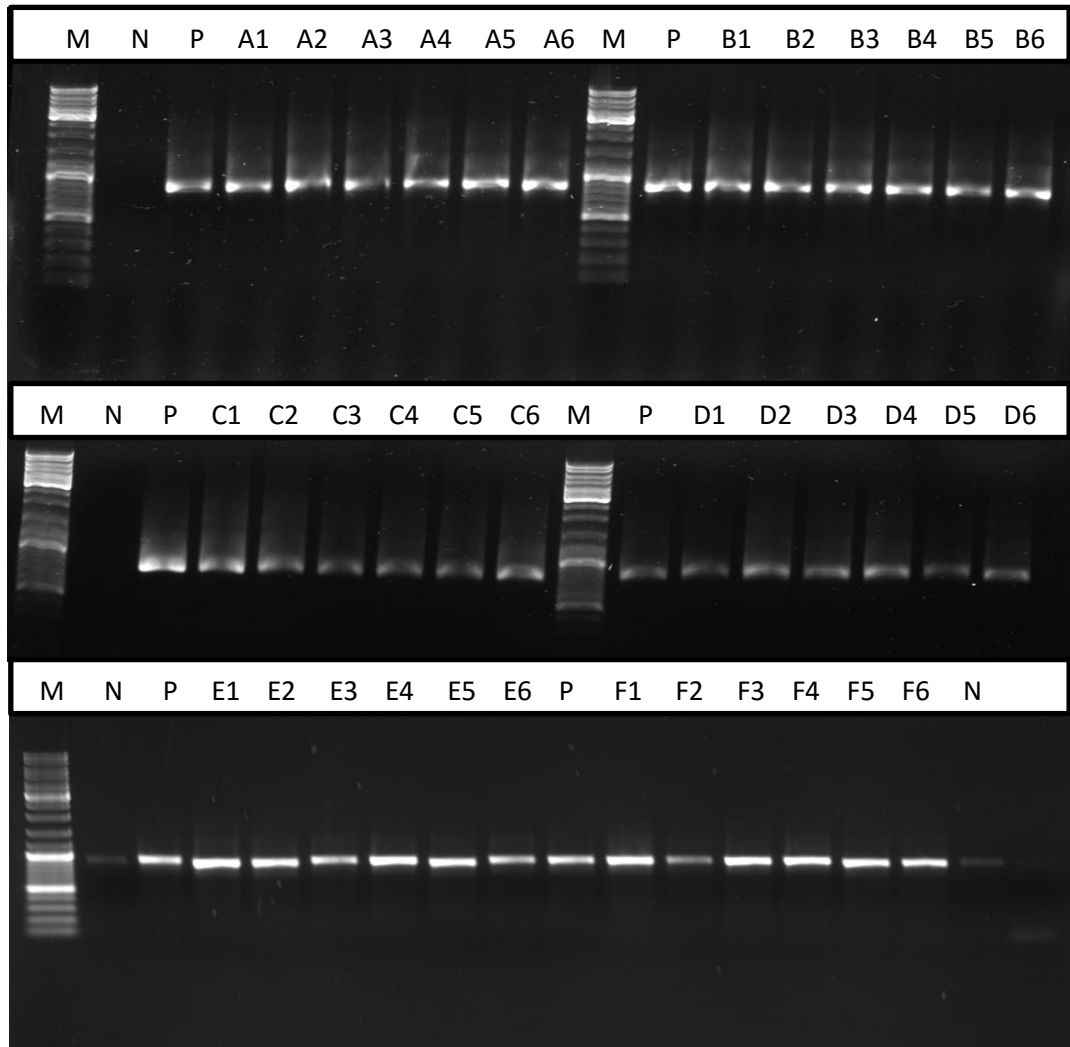


Figure A3: 16S PCR amplification products from biofilm samples formed on the surface of mild steel coupons in laboratory study. (M- molecular weight marker; N- Negative control; P- Positive control; 1- Autoclaved; 2- Non-autoclaved; 3- 5 mM nitrate; 4- 10 mM nitrate; 5- 20 mM nitrate; 6- 40 mM nitrate; A- Week 4; B- Week 8; C- Week 12; D- Week 16; E- Week 20; F- Week 24

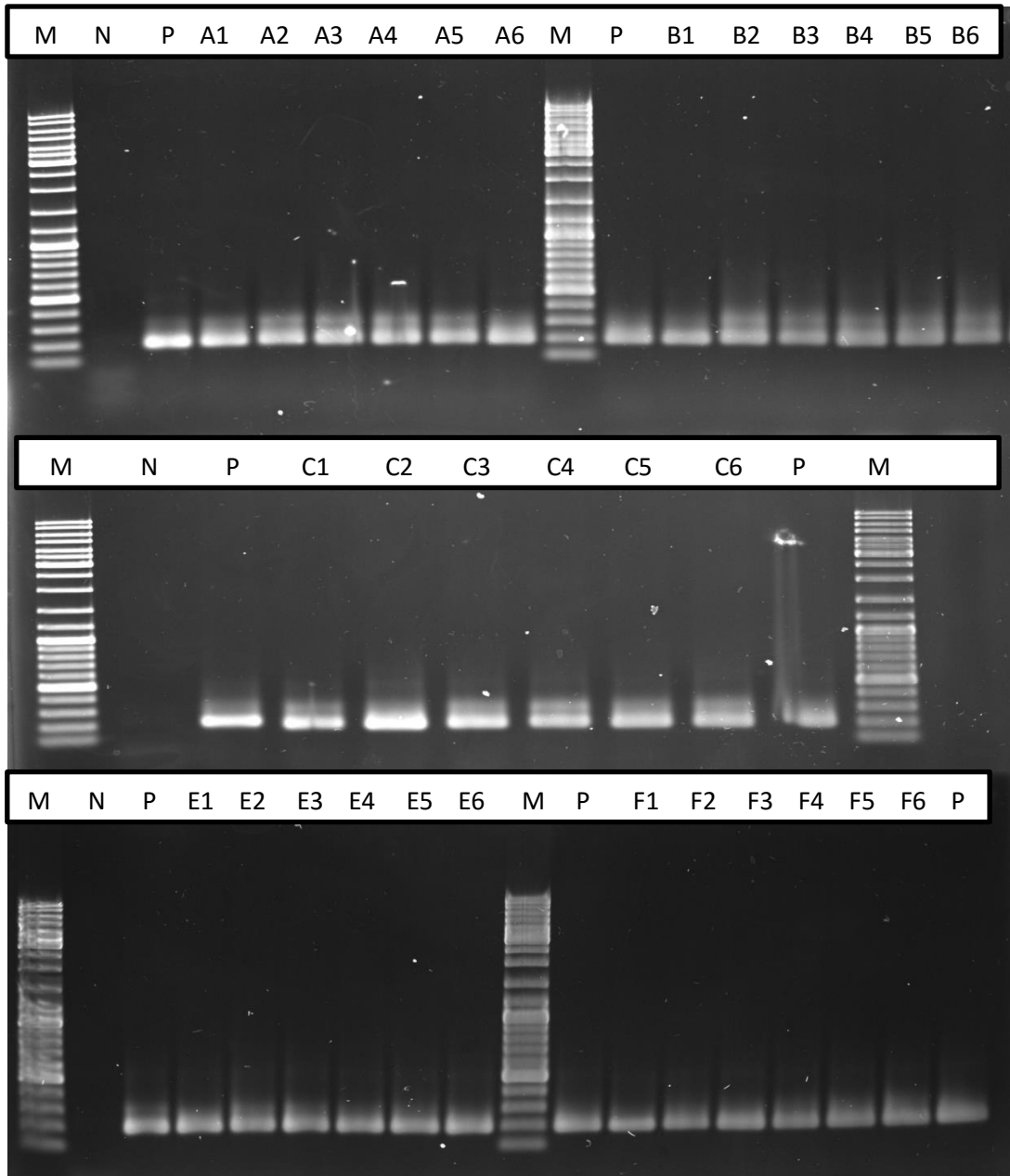


Figure A4: DGGE-PCR amplification products from biofilm samples formed on the surface of mild steel coupons in laboratory study. (M- molecular weight marker; N- Negative control; P- Positive control; 1- Autoclaved; 2- Non-autoclaved; 3- 5 mM nitrate; 4- 10 mM nitrate; 5- 20 mM nitrate; 6- 40 mM nitrate; A- Week 4; B- Week 8; D- Week 16; E- Week 20; F- Week 24

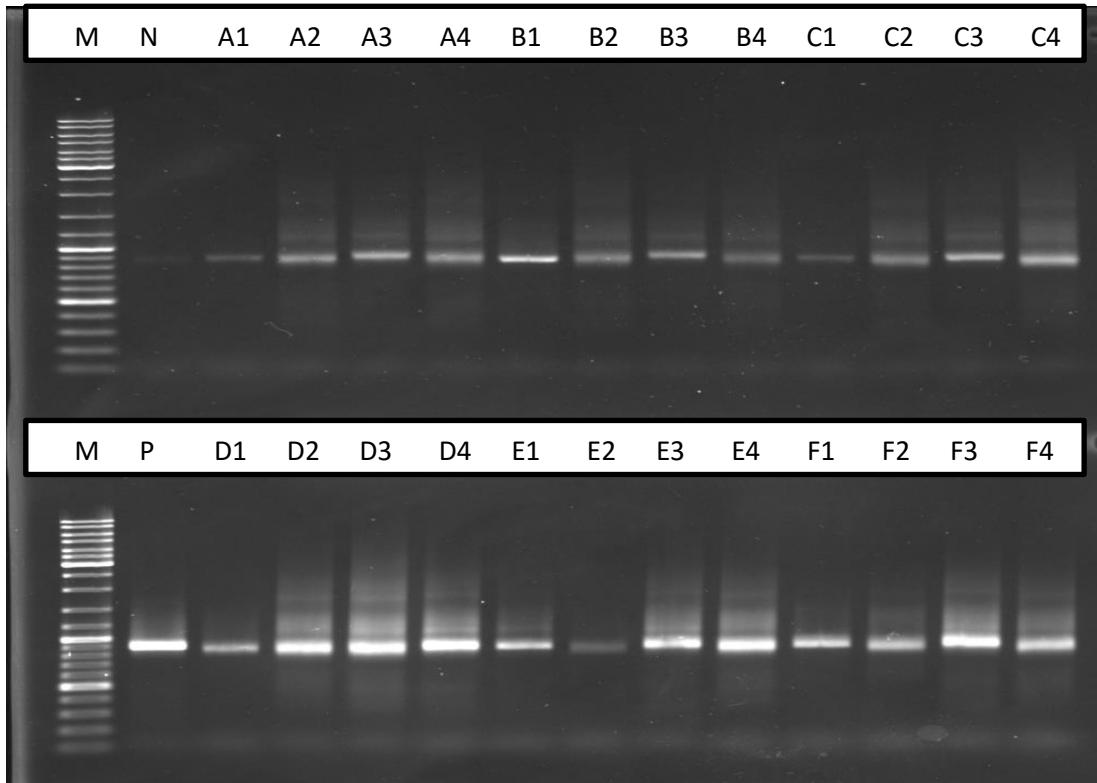


Figure A5: 16S PCR amplification products from biofilm samples formed on the surface of mild steel coupons in *in situ* study. (M- molecular weight marker; N- Negative control; P- Positive control; 1- Autoclaved; 2- Non-autoclaved; 3- Autoclaved nitrate-supplemented; 4- Non-autoclaved nitrate supplemented; A- Week 4; B- Week 8; D- Week 16; E- Week 20; F- Week 24

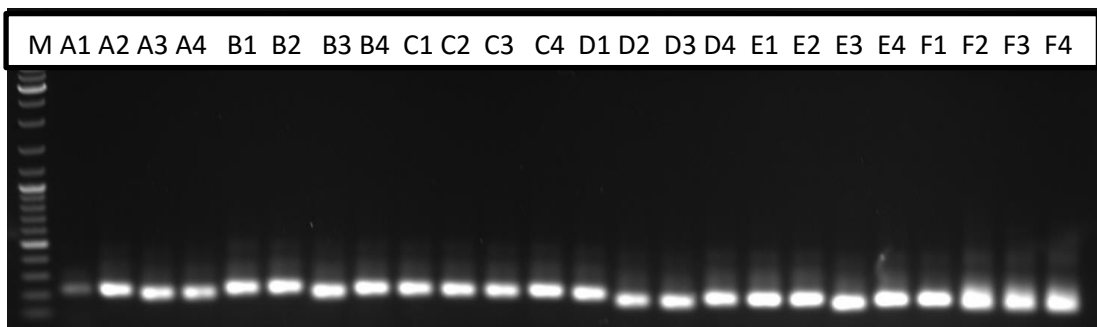


Figure A6: DGGE-PCR amplification products from biofilm samples formed on the surface of mild steel coupons in *in situ* study. (M- molecular weight marker; N- Negative control; P- Positive control; 1- Autoclaved; 2- Non-autoclaved; 3- Autoclaved nitrate-supplemented; 4- Non-autoclaved nitrate supplemented; A- Week 4; B- Week 8; D- Week 16; E- Week 20; F- Week 24

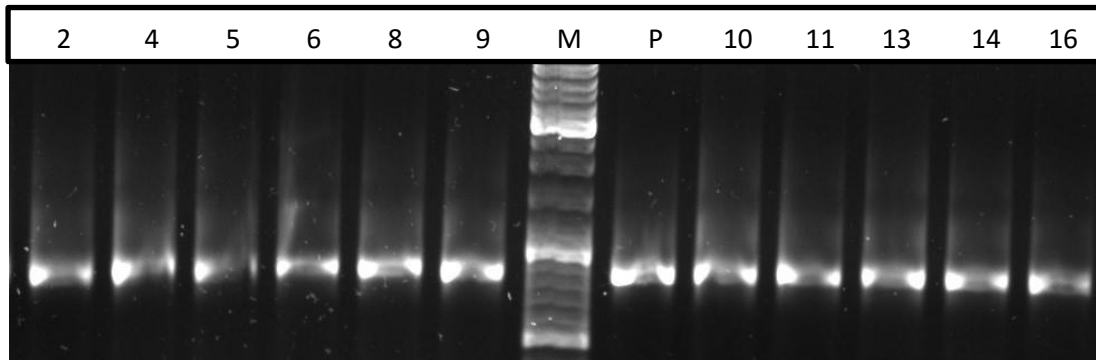


Figure A7:-PCR amplification products from biofilm samples formed on the surface of mild steel coupons treated with nitrite. (M- molecular weight marker (GeneRuler DNA Ladder Mix-ThermoScientific); P- Positive control ()); 2- Isolate 2; 4- Isolate 4; 5- Isolate 5; 6- Isolate 6; 8- Isolate 8; 9- Isolate 9; 10- Isolate 10; 11- Isolate 11; 13- Isolate 13; 14- Isolate 14; 16- Isolate 16

Appendix IV: pH measurements

Table A4: pH measurements of corrosive medium in the presence of isolated bacteria

Isolate	No nutrient				5 mM nitrite				10 mM nitrite				20 mM nitrite			
	Day				Day								Day			
	0	2	4	6	0	2	4	6					0	2	4	6
Control	6,95	7,92	8,06	8,33	6,75	8,47	10	10,14	6,89	9	9,78	9,89	6,98	8,92	10	10,22
2	6,3	6,82	8,06	8,33	6,23	10,65	11,13	11	6,21	10,65	11,13	10,65	7,05	8,46	10,78	10,9
4	6,78	7,27	8,7	8,79	6,11	8,1	8,46	9,18	6,36	8,11	8,52	10,07	6,35	8	10,5	11,98
5	6,25	7,24	8,63	8,79	6,12	8,11	8,8	9,94	6,33	8,06	7,97	8,58	7,58	7,89	10,02	10,84
6	6,24	7,05	8,62	8,06	6,18	7,9	8,96	10,78	6,33	7,92	8,12	8,97	6,99	8,91	10,65	10,98
8	6,28	7,06	8,6	8,7	6,22	7,89	8,09	8,82	6,33	6,95	8,12	8,8	6,78	8,34	9,87	10,82
9	6,37	7,26	8,49	8,06	6,24	7,98	8,27	8,96	6,3	6,9	7,98	8,53	6,47	8,55	9,81	9,781
10	6,54	7,22	8,45	8,69	6,22	7,75	8,03	8,67	6,32	6,4	8,35	8,64	6,25	8,46	10,4	10,28
11	6,89	7,17	8,55	8,43	6,23	7,25	8,02	8,58	6,31	7,63	8,04	8,81	7,55	8,51	10,28	10,92
13	7	7,29	8,36	8,41	6,26	6,36	9	9,27	6,3	5,83	8,19	9,53	6,22	9,4	10,82	9,26
14	6,47	7,16	8,31	8,33	6,26	8,43	8,36	9,75	6,32	8,25	8,02	8,8	6,51	7,98	10,98	9,29
16	6,52	7,42	8,47	8,15	6,31	8,16	7,9	9	6,38	7,54	8,72	10,87	6,17	7,65	8,98	8,99